Chapter 1 Introduction

1-1 Conducting polymers

Novel materials based on organic compounds have recently been successfully applied to electronic devices. Among these materials, conducting polymers (CP) display potential in electronic applications [1-3]. Electronically conducting polymers possess a variety of properties related to their electrochemical behaviors and are active materials whose properties can be altered as a function of their electrochemical potential. Like semiconductors, CP can thus produce novel electrical, optical and magnetic phenomena and be translated into various useful devices in optoelectronic [4-7], solar cell [8-10], sensor [11-13], and biomedical applications [14-16].

A key discovery that changed the outlook for producing highly conducting polymers was the finding in 1973 that the inorganic polymer polysulfur nitride (SN)x is highly conducting [17]. The discovery was of particular importance because they proved the possibility of generating highly conducting polymers, and stimulated the enormous amount of focus and activity necessary for the discovery of other polymeric conductors. In the years between 1971 and 1975, Shirakawa and coworkers prepared polyacetylene as organic material of conducting polymers and reached the real breakthrough in 1977 [18,19]. Following these works, there has been an explosion of activity around the characterization, synthesis and use of conducting polymers in a wide range of fields from electronics to medicine. For examples, Scheme 1-1 shows the structures of some interesting conducting polymers for organic based materials that have been developed over the past 30 years.

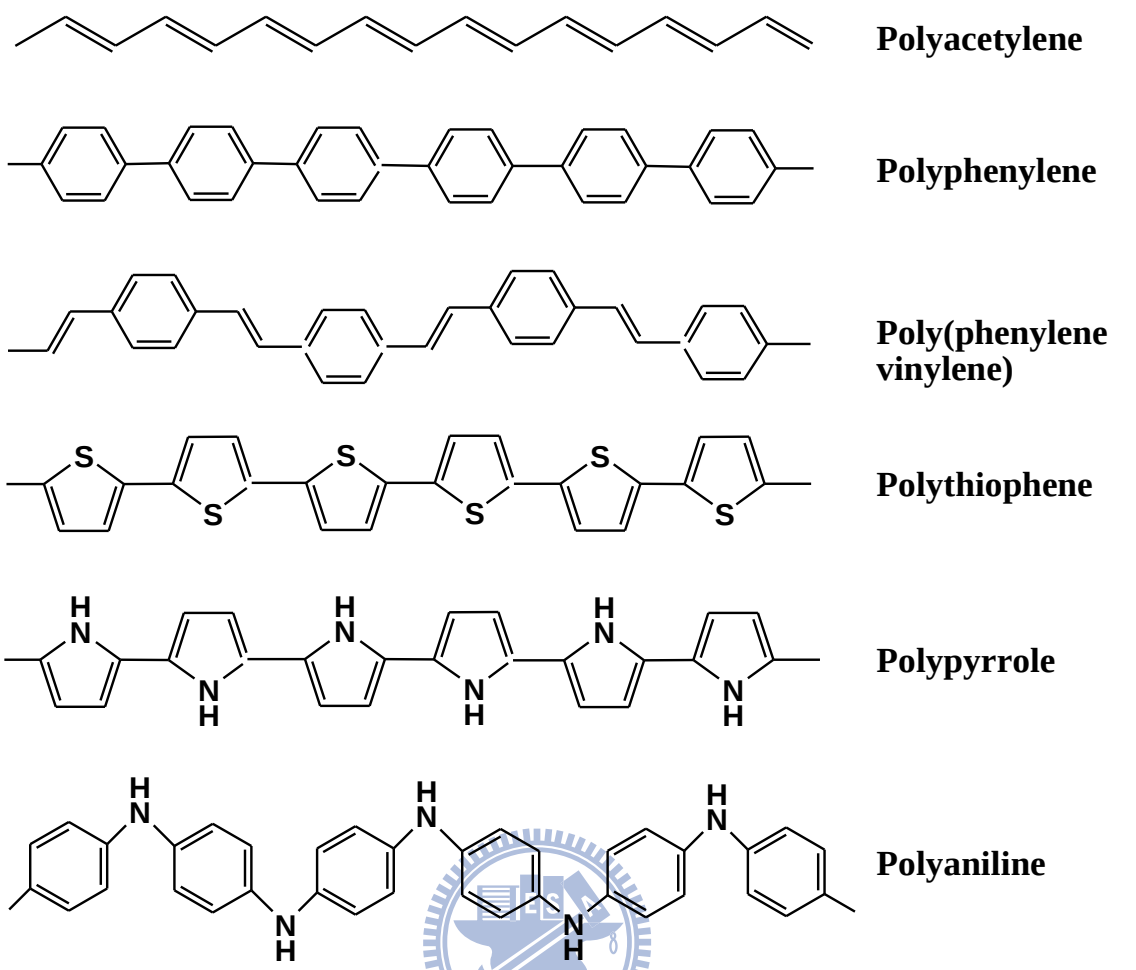

Scheme 1-1. Chemical structure of some conducting polymers

Except polyacetylene, these organic polymeric materials include polyphenylene, poly(p-phenylene vinylene)s, polythiophene, polypyrrole, and polyaniline; the conductivity of those polymers is due to conjugated π-electron systems in their structures. Therefore, all those conducting polymers are also classified as conjugated polymers and have attracted the most attention. In 2000, the importance and potential impact of conducting polymers were recognized by the world scientific community when Hideki Shirakawa, Alan J. Heeger and Alan G. MacDiarmid were awarded the Nobel Prize in Chemistry for their research in this subject [18-22].

1-2 Polysquaraines

Conjugated polymers possess intrinsic electrical conductivity. Therefore, synthesis of conjugated polymers with low optical band gaps has been employed with considerable effort recently. The band gap energy of conducting polymers varies significantly depending upon the degree of extended conjugation between consecutive repeating units and inherent electron densities of the polymer backbones. One of the approaches towards the designing of such polymers is the use of strong donor and acceptor monomers at regular arrangements in the repeating units, which has limited success in many cases. An alternate strategy is the use of organic dyes as building blocks. Squaraines are organic dyes and are thus ideal candidates for this purpose due to their unique optical properties.

Squaraines [23,24], condensation reaction of 3,4-dihydroxy-3-cyclobutene 1,2-dione (squaric acid) with electron rich aromatic and heterocyclic compounds, are a class of dyes with resonance stabilized zwitterionic structures, a classical example of these squaraines is shown in Scheme 1-2.

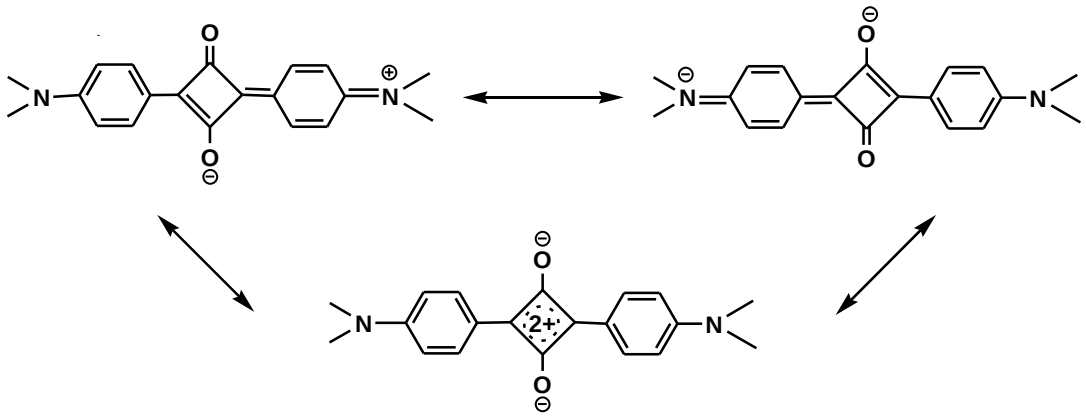

Scheme 1-2. A classical example of squaraines dyes with resonance-stabilized zwitterionic structures.

Squaraine dyes generally have donor-acceptor-donor (D-A-D) texture, which the central four member ring as electron acceptor and two electron donating group. These organic squaraine dyes exhibit sharp and absorption and emission in the visible to near-IR region [25-27]. In 1965, Triebs and Jacob reported their initial preparation squaraine dyes from reaction of the 3,4-dihydroxy-3-cyclobutene 1,2-dione with pyrrole [28], as displayed in Scheme 1-3. Later, the formation of strongly colored organic dyes have appeared and reported. These dyes are prepared by condensation between squaric acid and electron rich aromatic or heterocyclic compounds such as N,N-dialkylanilines, phenols, benzothiazoles, azulenes and pyrrole [29-32]. These class zwitterionic dyes are referred to as "squaraine" dyes, a name coined by Schmidt [33]. After these works, squaraine dyes have been developed and played an important role in the studies and designs of a whole range of the solution and solid state for photophysical and photochemical applications.

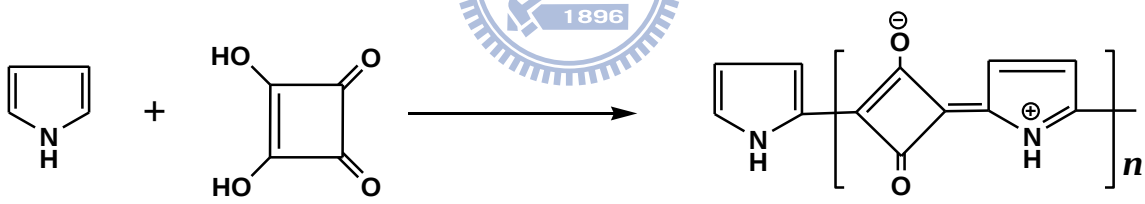

Scheme 1-3. The genesis of squaraine dyes from reaction of 3,4-dihydroxy-3-cyclobutene 1,2-dione (squaric acid) with pyrrole by Triebs and Jacob.

As the structural backbones of these squaraine dyes comprise bifunctional electron rich heterocyclic aromatic molecule such as pyrrole, carbazole, and any complex molecule possessing two suitable electron rich sites in its structure can polycondensation with squaric acid to form a polymer. In these polycondensations, squaraine dyes can thus form polysquaraines with π -conjugated structures; these polymers exhibit intrinsic

semiconducting properties and are classified as conjugated polymers or conducting polymers.

1-3 Goals of this work

Polysquaraines exhibit favorable optical properties and great flexibility for synthetic manipulation, and are suitable for the design of polymers with small optical band gaps [34-40]. The possession of unique optical properties makes polysquaraines suitable materials for several technological applications such as solar cells [41-44], xerographic sensitizers [45], optical data storage [46-48], biomedical applications and sensor [49-57]. Thus, polysquaraines remain at the forefront in many areas of development. Therefore, we selected polysquaraine as a studying material in this work.

We started the investigation of polysquaraine from the synthetic work of polycondensation of squaric acid with pyrrole derivatives. In this condensation, the intrinsic nature of pyrrole derivatives might influence the reaction and impinge on the backbone structure in polysquaraine. We thus investigated the effect of the position of the alkyl group in the pyrrole derivatives on the synthesis of polysquaraine by condensation.

In this work, we synthesized and analyzed poly(pyrrolyl)squaraines from the condensation of squaric acid with 1-octyl- and 3-octylpyrroles having the same molar mass to investigate the products from the same alkyl group linking to separate N- and C-positions. Scheme 1-4 and 1-5 show the flow charts of synthesis and analysis of polysquaraines in this work.

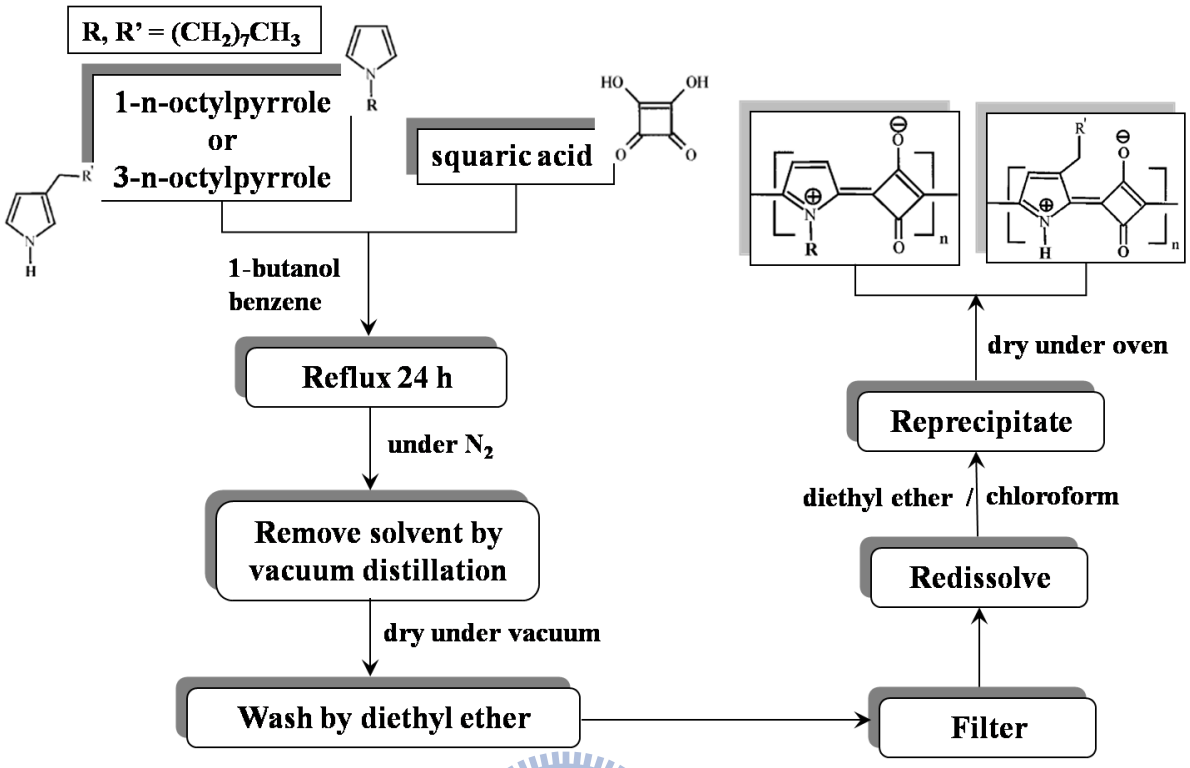

Scheme 1-4. The chart of synthesis in this work

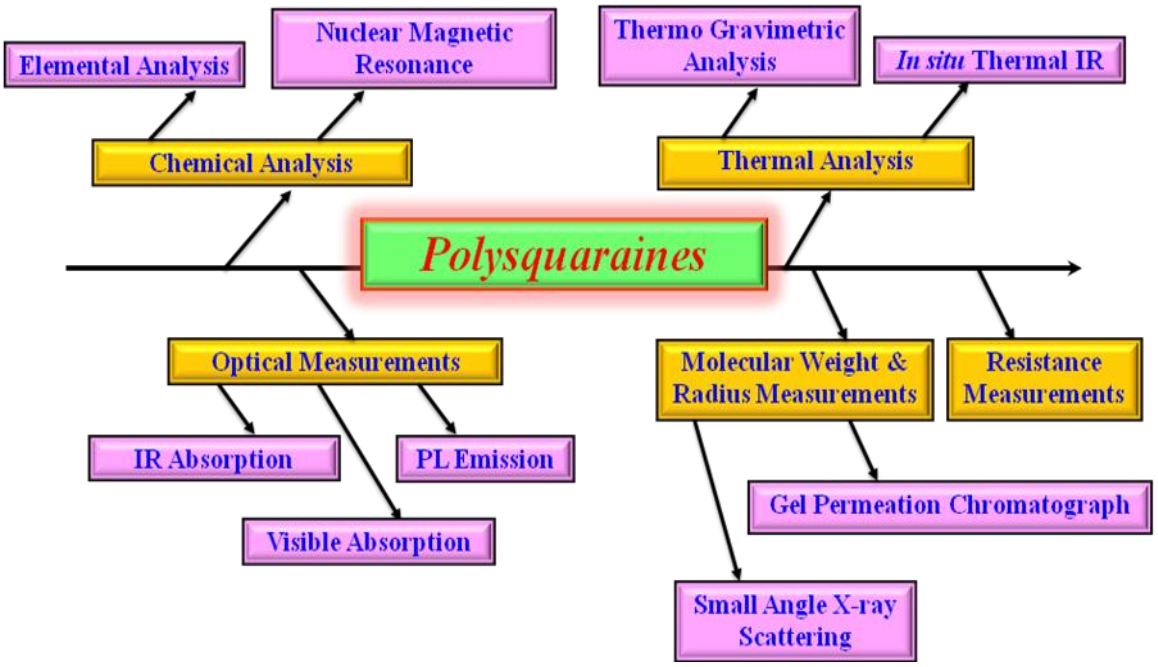

Scheme 1-5. The flow chart of analysis in this work

The optical, physical and electronic properties of conjugated polymers might be affected by a variation of the polymer conformation. Then, controlling the conformation is an important and interesting subject for applications of these conjugated polymers. Previous works have investigated the variation of the structural conformation for squaraine-based materials responding to external stimuli such as solvent concentration [58-60], solvent polarity [58,61,62], temperature [58,63], metal ions [49,64,65] and other conditions. Besides induction by these external stimuli, we tried to find other techniques that might control the conformation of polysquaraines as synthesized in this work.

Chapter 2

Effect of Alkyl Position of Pyrrole on Structures and Properties of Conjugated Polysquaraines

2-1 Introduction

As one polysquaraine, squaric acid reacts with pyrrole derivatives in condensation to form polymeric chains. In this condensation, the pyrrole derivative might react with the squaric acid with 1,2- or 1,3-addition and produce distinct backbone structures of poly(pyrrolyl)squaraines, as shown in Scheme 2-1. Previous works [66] reported that structural compositions of poly(pyrrolyl)squaraines of two types can thus be generated with formulae **I** and **II** implying the 1,2- and 1,3- reactions, respectively. Poly(pyrrolyl)squaraine containing a repeating backbone in formula **II** features a zwitterionic structure; whereas that in formula **I** adopts a covalent structure. For these polymers, the distinctive bonding character of the backbone structure affects their chemical and physical properties and thus their applications.

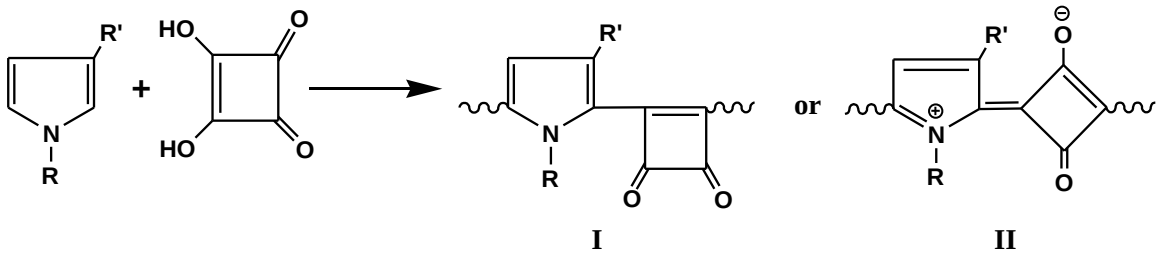

Scheme 2-1. Reaction of a pyrrole derivative with squaric acid in condensation forms repeating units in the structure of poly(pyrrolyl)squaraine of two types, of which formulae I and II imply the covalent and zwitterionic backbones; respectively. R and R' represent H or an alkyl group.

In forming the squaraine backbone with squaric acid, the intrinsic nature of pyrrole derivatives might influence the condensation and impinge on the backbone structure in polysquaraine. To improve control of the physical and chemical properties of this polymer, we investigated the effect of derivatives of the pyrrole moiety on the synthesis of polysquaraine by condensation. For this purpose, we focused on the condensation for poly(pyrrolyl)squaraines affected by the position of the alkyl group in the pyrrole derivatives. We synthesized and analyzed poly(pyrrolyl)squaraines from the condensation of squaric acid with 1-octyl- and 3-octylpyrroles having the same molar mass to investigate the products from the same alkyl group linking to separate N– and C– positions.

2-2 Experimental Section

2-2.1 Materials

Reagents 1-octylpyrrole (97.3 %), 3-octylpyrrole (99.5 %) and squaric acid (99.0 %) (all T.C.I. Co.), solvents Acetone (99.9 %), 1-butanol (99.9 %), benzene (99.8 %), cyclohexane (99.8 %), diethyl ether (99 %), ethanol (99.8 %), isopropanol (> 99.9 %), methanol (99.8 %), methylene chloride (99.8 %) and trichloromethane (99.4 %) (all Merck Co.), and drying agent anhydrous magnesium sulfate powder (J. T. Baker Co.) were obtained from the indicated suppliers.

2-2.2 Measurements

^{1}H NMR and ^{13}C NMR (700 MHz, VARIAN VNMRS-700) spectra were recorded of samples in $CDCl_3$ with TMS as an internal standard. The molar masses of the polymers were measured with a gel permeation chromatograph (GPC, Viscotek-TDA) at 25℃, using

trichloromethane as eluent and polystyrene as the standard reference; this GPC posesses multi detectors including a refractive index detector, a right angel laser light scattering detector, a low angel laser light scattering detector, a viscometer, and an UV detector.

IR absorption spectra were recorded with a spectrometer Bomem DA8 FTIR or Nicolet Magna 860 FTIR attached to the IR beamline at the National Synchrotron Radiation Research Center in Taiwan, see Figure 2-S1 in Supporting Information; a HgCdTe or DTGS detector served to span the mid-IR range 500 – 4000 cm^{-1} or 400 – 4000 cm^{-1}, respectively. The IR spectra were typically measured with resolution 0.5 cm^{-1} and 200 – 512 scans. Samples of polysquaraines were dissolved in trichloromethane. KBr discs were dipped in the samples as saturated solutions and subsequently dried in a vacuum oven to remove the solvent.

Elemental analyses (Foss Heraeus CHN-O-Rapid), thermogravimetric analyses (TGA, TA Model, N_2 atmosphere), and visible absorption spectra (Ocean Optics UV-visible spectrophotometer) were performed or measured with the indicated instruments. Photoluminescence spectra were obtained from a Jobin-Yvon Fluorolog-3 spectrophotometer.

2-2.3 Preparation of poly(1-octylpyrrole-*co*-squaric acid)

Poly(1-octylpyrrole-*co*-squaric acid) was synthesized on refluxing 1-octylpyrrole (1.1224 g, 6.26 mmol) and squaric acid (0.714 g, 6.26 mmol) in equimolar proportions in a mixture of 1-butanol (60 mL) and benzene (30 mL) under a continuous flowing N_2 atmosphere for 24 h [28,29 66-68]. The dark blue solutions obtained were filtered, and the filtrates were concentrated with vacuum distillation and poured into diethyl ether. The

crude products were collected on filtration and washed with diethyl ether, before being redissolved in trichloromethane to yield solutions that were filtered again; the filtrates were evaporated to dryness in an open fume cupboard to eliminate the $HCCl_3$. The precipitates were finally washed again with diethyl ether and dried in a vacuum chamber near 295 K for two days.

In this condensation, water contamination might interfere and affect the product generated. We carefully treated water contamination problem in several ways. (1) The solvents were dried with $MgSO_4$. (2) The highly pure N_2 was dried further on passing over silica gel. (3) The reaction vessels were fully passivated with copious amounts of dry N_2 at least 30 min before reagents were admitted. (4) The reaction system was purged a further 30 min a heater was initiated. (5) The reaction mixture was stirred and refluxed with azeotropic solvents at 120 °C; under these conditions, water was removed by the flowing nitrogen. To verify the thorough removal of water, we attached a water trap to the condenser and obtained no liquid water.

The dark blue product of poly(1-octylpyrrole-*co*-squaric acid) was obtained with the yield 53 %. ^{1}H NMR ($CDCl_3$): δ = 0.9 (br s, 3H, CH_3), 1.23 (br s, 10H, CH_2), 1.58 (br s, 2H, CH_2), 3.63 (br s, 2H, CH_2), 4.6-4.8 (br s, 2H), 6.4-6.8 (br s, aromatic), see Figure 2-S2 in Supporting Information.

Elemental analysis for $(C_{16}H_{19}NO_2 \cdot H_2O)_n$ $(275.188)_n$: Calcd. C 69.78, N 5.09, H 7.69; Found C 71.20, N 5.10, H 8.42. IR (KBr) : 2956 (as s, CH_3), 2923 (as s, CH_2), 2871 (s, CH_3), 2850 (s, CH_2), 1736 (s, C=O), 1622 (s, C–O), 1482 (ring modes), 1463 (as b, CH_3), 1422 (scissor, CH_2), 1357 (umbrella b, CH_3), 1082 (b, CH), 755 (b, CH), 721 cm^{-1} (r,

CH_2). Visible: λ_{max}/nm (methanol) 539.4, (ethanol) 542.3, (isopropanol) 542.6, (1-butanol) 545.8.

2-2.4 Preparation of poly(3-octylpyrrole-*co*-squaric acid)

Poly(3-octylpyrrole-*co*-squaric acid) was prepared from reaction of 3-octylpyrrole (1.1224 g, 6.26 mmol) and squaric acid (0.714 g, 6.26 mmol) according to the same process used to prepare poly(1-octylpyrrole-*co*-squaric acid) [29,66-68]; in which the product was obtained with the yield 66 %.

^{1}H NMR ($CDCl_3$): δ = 0.84 (s, 3H, CH_3), 1.23 (d, 10H, CH_2) 1.63 (t, 2H, CH_2), 2.51(s, 2H, CH_2), 6.38 (br s, 1H, aromatic) , 10.43 (br s, 1H, NH), see Figure 2-S3 in Supporting Information; ^{13}C NMR ($CDCl_3$): δ = 14.09, 22.67, 26.63, 27.39, 29.23, 29.28, 29.36, 29.51, 29.69, 30.47, 31.50, 31.79, 31.88, 115.19, 115.45, 125.87, 132.43, 133.12, 143.05, 174.76, 177.13, see Figure 2-S4 in Supporting Information.

Elemental analysis for $(C_{16}H_{19}NO_2)_n$ $(257.3)_n$: Calcd. C 74.68, N 5.44, H 7.44; Found C 74.37, N 5.3, H 8.79. IR (KBr): 3350 (s, NH), 3157 (s, CH), 2955 (as s, CH_3), 2922 (as s, CH_2), 2871 (s, CH_3), 2851 (s, CH_2), 1742 (s, C=O), 1600 (s, C–O), 1557 (b, NH), 1539 (b, NH), 1491 (ring modes), 1465 (as b, CH_3), 1429 (scissor, CH_2), 1373 (umbrella b, CH_3), 1112 (b, CH), 936 (b, CH), 882 (b, CH), 775 (b, CH), 726 cm^{-1} (r, CH_2). Visible λ_{max} / nm (methanol) 538.2, (ethanol) 540, (isopropanol) 541.4, (1-butanol) 542.2.

2-3 Results and Discussion

Squaric acid might react with a pyrrole derivative by 1,2- or 1,3-addition to form poly(pyrrolyl)squaraines of two types, designated as formulae **I** and **II**. Condensation of these two reagents might thus generate poly(pyrrolyl)squaraine possessing both repeating units of formulae **I** and **II** in the polymer chain. The general condensation of squaric acid with 1-octylpyrrole and 3-octylpyrrole is expressed in Scheme 2-2; the end products poly(1-octylpyrrole-*co*-squaric acid) and poly(3-octylpyrrole-*co*-squaric acid) are denoted with formulae **III** and **IV**, respectively.

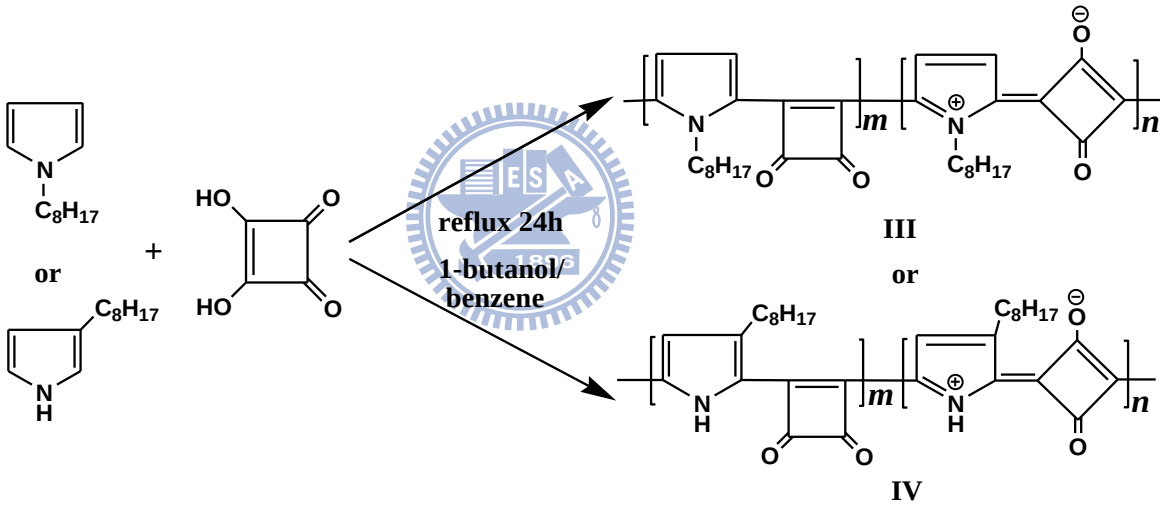

Scheme 2-2. In the general condensation of squaric acid with 1-octylpyrrole and 3-octylpyrrole, the end-product poly(pyrrolyl)squaraines are represented with formulae **III** and **IV**, respectively.

These poly(pyrrolyl)squaraines might contain *m* repeating units with a covalent backbone and *n* repeating units with a zwitterionic backbone in their structures; poly(1-octylpyrrole-*co*-squaric acid) and poly(3-octylpyrrole-*co*-squaric acid) as we synthesized

are named poly(1-octylpyrrolyl)squaraine, abbreviated **P1,** and poly(3-octylpyrrolyl)squaraine, **P3**, respectively.

2-3.1 Molecular weight of polysquaraines as synthesized

The molar masses of as synthesized **P1** and **P3** were determined with the GPC. The values of M_n for **P1** and **P3** are 23 and 21 kDa, and that of M_w for **P1** and **P3** are 45 and 38 kDa, respectively. The polydispersity index (M_w/M_n) of **P1** (1.96) is thus greater than that of **P3** (1.81). The dissimilarity of polydispersity for these two polymers hints of a variation of their structures.

2-3.2 Structure analysis based on IR absorption

Infrared spectra serve to distinguish the chemical characteristics of polymers through their sensitivity to functional groups. Polysquaraines feature strong absorption in the mid-IR range, in which occurs useful information to characterize the structural composition of these polymers. Distinct IR absorption spectra of **P1** and **P3** in the spectral range 400 – 4000 cm^{-1} are shown in Figure 2-1. Including weak absorption features, the lines in IR spectra of **P1** and **P3** number 27 and 32, respectively. For the analysis of these features, we recorded IR spectra also of the three monomers, as depicted in Figure 2-2.

IR spectra of the **P1** and **P3** are divided into two regions. The left region, from 2700 to 3400 cm^{-1}, contains strong absorptions attributed to C–H and N–H stretching modes. The intense lines observed between 2800 and 3000 cm^{-1} are assigned to C–H stretching modes of the octyl moiety in both polymers. Unlike the octyl group linked to –N atom in **P1**, **P3** has its octyl group linked to a –C atom and shows a signal of the –NH group according to a –NH stretching mode near 3300 cm^{-1} in Figure 2-1(b).

The right parts of the spectra, from 400 to 1750 cm^{-1}, serve as 'fingerprints' of other functional groups and modes. The lines associated with carbonyl (–CO) functional groups in the intrinsic structural backbone of the polymer are typically discernible in the spectra. The covalent and zwitterionic –CO functional groups in polysquaraines have characteristic absorptions near 1750 cm^{-1} and 1600 cm^{-1} [69-74], respectively; these values are smaller than the corresponding value 1815 cm^{-1} of squaric acid.

As carbonyl moieties of these two kinds are thus distinguished directly in the IR spectra, we derive information about these dissimilar components in polymers on the basis of these lines. For instance, Figure 2-1 (b) shows a strong absorption at 1600 cm^{-1} and a weak one at 1742 cm^{-1}; the intensity of the latter attributed to covalent carbonyl is about 3 % as that of the former associated with zwitterionic carbonyl. This result demonstrates that **P3** possesses mostly zwitterionic repeating units in the polymer chain, so that it's repeating units represented as *n* in Scheme 2-2 are about 97 %. Even with the same procedures for the polycondensation, a variation of backbone structures might happen from batch to batch. To test this uncertainty, we prepared polysquaraines **P3** for four batches, **P3-1**, **P3-2**, **P3-3**, and **P3-4**. The IR absorption spectra of **P3-1**, **P3-2**, **P3-3**, and **P3-4** are compared in Figure 2-3; the shapes of these spectra are similar. The percentages of zwitterionic and covalent carbonyl backbones in polymer chains for these **P3** polysquaraines are listed in Table 2-1. All these **P3** polysquaraines possess mostly zwitterionic structures larger than 96 %.

For a similar analysis applied to the **P1**, the ratio of the intensity for the line attributed to zwitterionic carbonyl about 1622 cm^{-1} to that for the covalent one near 1736 cm^{-1} is approximately 2:1, as shown in Figure 2-1(a); hence **P1** includes 1/3 covalent units in its structure [75-80]. Also, we prepared polysquaraines **P1** for four batches, **P1-1**, **P1-2**, **P1-3**, and **P1-4**; the IR absorption spectra of these products are compared in Figure 2-4. With

the same argument, we analyzed the backbone structures of theses polymers. By this means, the percentages of zwitterionic and covalent carbonyl backbones in polymeric chains for these **P1** polysquaraines are also listed in Table 2-1. Approximately, the zwitterionic carbonyls to the covalent ones in polymeric chains of these **P1** polysquaraines follow the same ratio 2:1.

2-3.3 Position of the alkyl group in the reagent of the pyrrole derivative affects the structural construction

The condensation product from a reaction of squaric acid and a pyrrole derivative might retain two basic structural units in the polymer chain, as shown in Scheme 2-1. The condensation via 1,2- or 1,3-addition is discussed elsewhere and the polymerization reaction is still under investigation. The reaction and its mechanism might be subject to interference from water contamination in the polymerization and affect the product generated [66]; perhaps the 1,2-addition occurs significantly only in reactions performed in solvent systems from which the produced water is not removed. For the purpose of application as a CP, the poly(pyrrolyl)squaraine has a desired structure predominantly 1,3-squarate. We thus eliminated water as a contamination problem according to several methods described in the experimental section. By this means, we obtained product **P3** from reagent 3-octylpyrrole possessing mostly zwitterionic repeating units (>97 %), but polymer **P1** from the reagent 1-octylpyrrole was produced with a backbone ratio 2:1 of the zwitterionic repeating units to the covalent ones.

What is the source of this discrepancy in the ratio of structural components for **P1** and **P3**? As we used the same experimental procedures to synthesize the polymers, we conclude that water contamination is not the only factor directing the polymerization. Of

the reagents to produce these two polymers, 1-octylpyrrole for **P1** and 3-octylpyrrole for **P3**, both pyrrole derivatives have the same molecular moiety, octyl, but linked at separate positions in pyrrole. As explained above, **P3** from the alkyl group linked to the –C atom in pyrrole comprises mostly a zwitterionic structure, whereas **P1** from the alkyl group linked to the –N atom possesses one third covalent units in polymer chain. We conclude that the position of the alkyl group in the reagent of the pyrrole derivative affects the structural construction in the condensation of poly(pyrrolyl)squaraine.

Regarding Schemes 2-1 and 2-2, the condensation of the pyrrole derivative with squaric acid might adopt 1,2- or 1,3- addition to form the covalent and zwitterionic backbones, respectively. For the route of 1,3-addition, the electron cloud of the double bond between positions 2 and 3 in the pyrrole derivative donates to the bond linking to the squaric acid, in which the double bond is eventually formed. The electron donation of the alkyl group in position 3 might thus promote 1,3-addition. 3-Octylpyrrole, that thus possesses an octyl group in the 3 position, can hence contribute to 1,3-addition to yield the most zwitterionic backbones, whereas 1-octylpyrrole that has an H atom in the 3 position engages in both additions in a weighted ratio.

2-3.4 Solvent effect in visible absorption spectra

As the polysquaraines have π -conjugated structures that produce intense absorption of visible light, visible absorption spectra serve also to characterize these polymers. We measured the visible absorption spectra of poly(pyrrolyl)squaraines as synthesized in solvents of two classes – hydrogen-bonding (HB) solvents and non-hydrogen-bonding (NHB) solvents, as shown in Figures 2-5 and 2-6, respectively.

The poly(1-octylpyrrolyl)squaraine and poly(3-octylpyrrolyl)squaraines as synthesized exhibit distinct features in their visible absorption spectra. **P3** has a single and narrow visible absorption centered about 538-550 nm depending on the solvent, as displayed in Figures 2-5 (b) and 2-6 (b), producing a red color in solution, whereas **P1** has a line with maximum absorption at 539-553 nm and a broad shoulder near 600 nm, as depicted in Figures 2-5 (a) and 2-6 (a), appearing blue in solution.

As discussed above, because **P3** possesses mostly zwitterionic repeating units in its structure, the backbones tend to be identical and to bestow on its visible absorption only one narrow band, with maxima in various solvents listed in Table 2-2, whereas **P1** contains two backbones in its polymer chain, so producing a more complicated absorption in its visible spectra. Through comparison with the narrow absorption for zwitterionic **P3**, we assign the corresponding narrow band of **P1**, of which the maxima are also listed in Table 2-2, which we attribute to its zwitterionic moiety; the shoulder is due to its covalent part.

The wavelengths of the maximum visible absorptions of the polymers as synthesized varied with the solvent, possibly related to its polarity. The relative permittivity ε_r that is a measure of a solvent to separate charge and to orient a dipole is a useful parameter to describe the polarity of the solvent. Relations of the visible absorption maxima of **P1** and **P3** versus relative permittivity of HB solvents are displayed in Figure 2-7. As the wavenumbers of maximum absorption exhibit a linear shift with relative permittivity in the HB solvents [81,82], the visible absorption spectra of both polymers as synthesized exhibit significant negative solvatochromism [83-87]; i.e., the absorption exhibits a bathochromic effect with decreasing polarity in alcoholic solvents. The slopes of these relations for **P3** and **P1** are almost the same; the zwitterionic structures in these two polymers are hence similar, but for the same solvent the wave length of maximum

absorption of **P3** is blue-shifted relative to **P1**; this phenomenon reflects the fact that the mass ratio of the zwitterionic moiety in **P3** is greater than that in **P1**.

2-3.5 Solvent effect in photoluminescence spectra

Polysquaraines possess π molecular orbitals delocalized along the polymer chain; therefore, it is expected that these polymers have high photoluminescence quantum yields. Figure 2-8 shows the photoluminescence spectra of **P1** and **P3** in four HB-solvents. In solvents of methanol, ethanol, isopropanol, and 1-butanol, the maximum emission bands of **P1** were observed at 552.2, 555.3, 555.4, and 556.0 nm, respectively; the peaks shift within 4 nm. Whereas, those bands of **P3** were recorded at 559.5, 563.7, 567.4, and 568.0 nm, respectively; the positions of maximum peaks differ in the wavelength range 8.5 nm.

Similar to the visible absorptions in HB-solvents, the emission bands of **P1** and **P3** undergo hypsochromic shifts with increasing solvent polarity. Relations of the emission maxima of **P1** and **P3** versus relative permittivity of HB solvents are displayed in Figure 2-9. As the wavenumbers of maximum emission display a linear shift with relative permittivity in the HB solvents, the photoluminescence spectra of both polymers also possess significant negative solvatochromism.

Due to the similar zwitterionic structures in these two polymers, the slopes of these relations for **P3** and **P1** are also the same, as shown in Figure 2-9. Compare to the absorptions in the same solvent, the Stokes shifts of **P1** and **P3** are in the ranges 12.2 – 13.0 cm^{-1} and 21.3 – 26.0 cm^{-1}, respectively; the values for **P3** are greater than those for **P1**. This occurrence also reveals the phenomenon that the mass ratio of the zwitterionic moiety in **P3** is greater than that in **P1**.

2-3.6 Thermal stabilities of polysquaraines as synthesized

For various applications the thermal stability of these polysquaraines is a matter of concern. As displayed in Figure 2-10, the TGA curves of **P1** and **P3** under N_2 were recorded at heating rate 15 ℃/ min. Both polymers exhibited no loss of mass at temperature below 155 ℃; when temperatures went up to 200.0 ℃, the mass loss of **P1** and **P3** were 1.2 % and 0.8 %, respectively.

If we define the temperature at which mass loss is 5 % as ***Td***, we obtain values 259.8 ℃ for **P1** and 270.1 ℃ for **P3**. For a temperature below 304 ℃, the extent of mass loss of **P1** is slightly greater than for **P3**, but above 304℃, the mass loss of **P3** increases more rapidly; this result indicates that the thermal degradation of **P3** under the latter condition is more pronounced than that of **P1**. In the chain of polysquaraine, the covalent backbone is expected to be more stable than the zwitterionic one. As **P1** comprises more covalent moieties than **P3**, **P1** hence tends to resist thermal degradation above 304 ℃.

Further evidence of thermal stability for these two polymers was obtained from thermal tests monitored with IR spectra. We dipped polymers on the low-E plates and heated the plates *in situ* for IR measurements in the reflection mode, see Figure 2-S5 in Supporting Information. IR spectra of polysquaraines as synthesized in the spectral range 650 – 4000 cm^{-1} at various temperatures are shown in Figure 2-11 and 2-12.

The IR reflection spectra remained constant below 155 ℃ for both polymers, but varied slightly at 180 ℃ at which the mass losses were 0.5 % and 0.2 % for **P1** and **P3**, respectively. The line at 1600 cm^{-1} attributed to the zwitterionic carbonyl of **P3** was present at 236 ℃, but vanished by 266 ℃ in Figure 2-12, whereas the line at 1736 cm^{-1}

attributed to the covalent carbonyl of **P1** was observable at 287 ℃ in Figure 2-11. This test is consistent with the thermal stability of the covalent backbone exceeding that of the zwitterionic one in the structure of polysquaraine.

2-4 Summary

Poly(1-octylpyrrolyl)squaraine and poly(3-octylpyrrolyl)squaraine were synthesized from squaric acid with 1-octylpyrrole and 3-octylpyrrole under identical conditions of condensation. Visible absorption spectra, photoluminescence spectra, TGA curves, and IR spectra were recorded to characterize the structures of these polymers as synthesized; the measured optical and thermal properties are consistent with backbone structures. The polysquaraine from 3-octylpyrrole possesses mostly zwitterionic repeating units (>97 %), but the polymer from 1-octylpyrrole consists of zwitterionic and covalent repeating units in a ratio 2:1. Observations from the visible absorption and photoluminescence spectra in varied solvents, TGA curves, and thermal IR measurements for these two polymers reconciled to their structures. This result indicates that the position of the alkyl group in the pyrrole derivative affects the conformation in the condensation of poly(pyrrolyl)squaraine. These polysquaraines are stable below temperature 155 ℃ and their visible absorption and photoluminescence properties in hydrogen-bonding solvents exhibit negative solvatochromism.

2-5 Figures and Tables

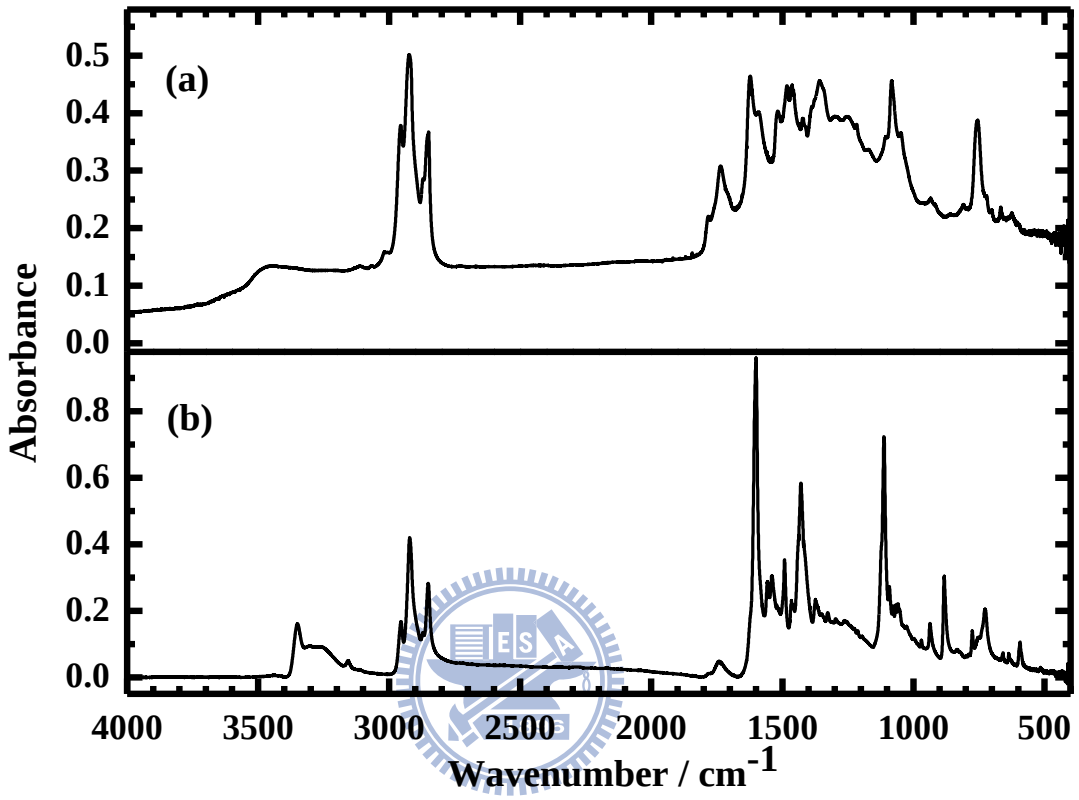

Figure 2-1. IR absorption spectra of polysquaraines as synthesized, in the spectral range 400 – 4000 cm^{-1}: (a) **P1**; (b) **P3** .

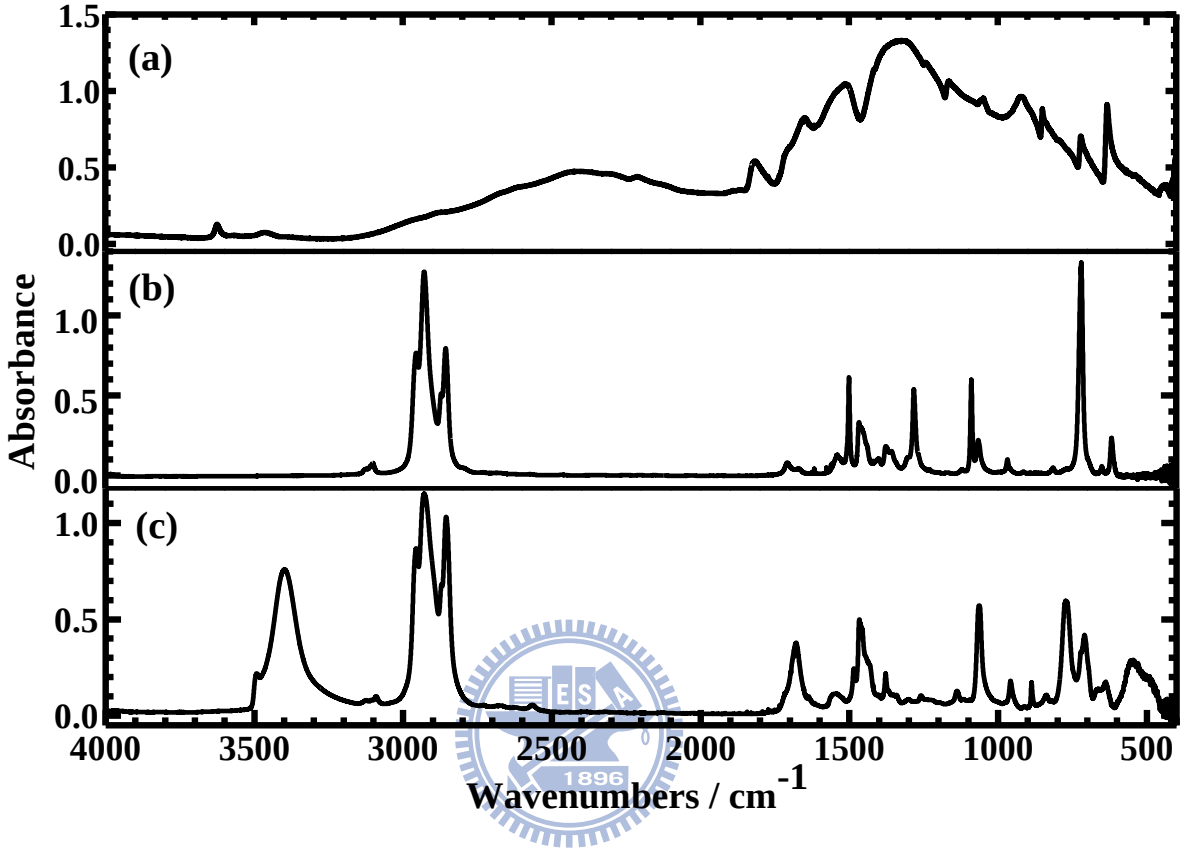

Figure 2-2. IR absorption spectra of monomers in the spectral range 400 – 4000 cm^{-1} (a) squaric acid; (b) 1-octylpyrrole; and (c) 3-octylpyrrole.

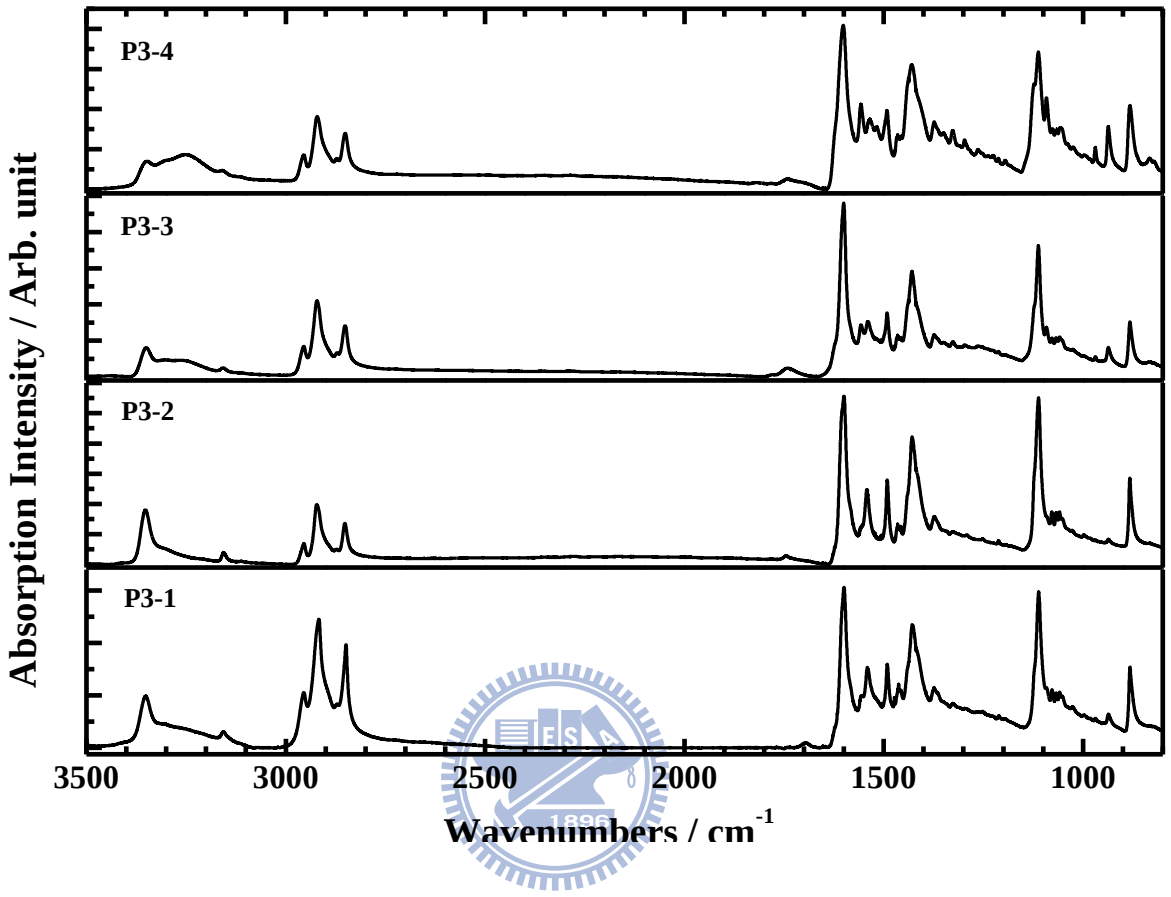

Figure 2-3. IR absorption spectra of polysquaraines **P3** as synthesized for four batches.

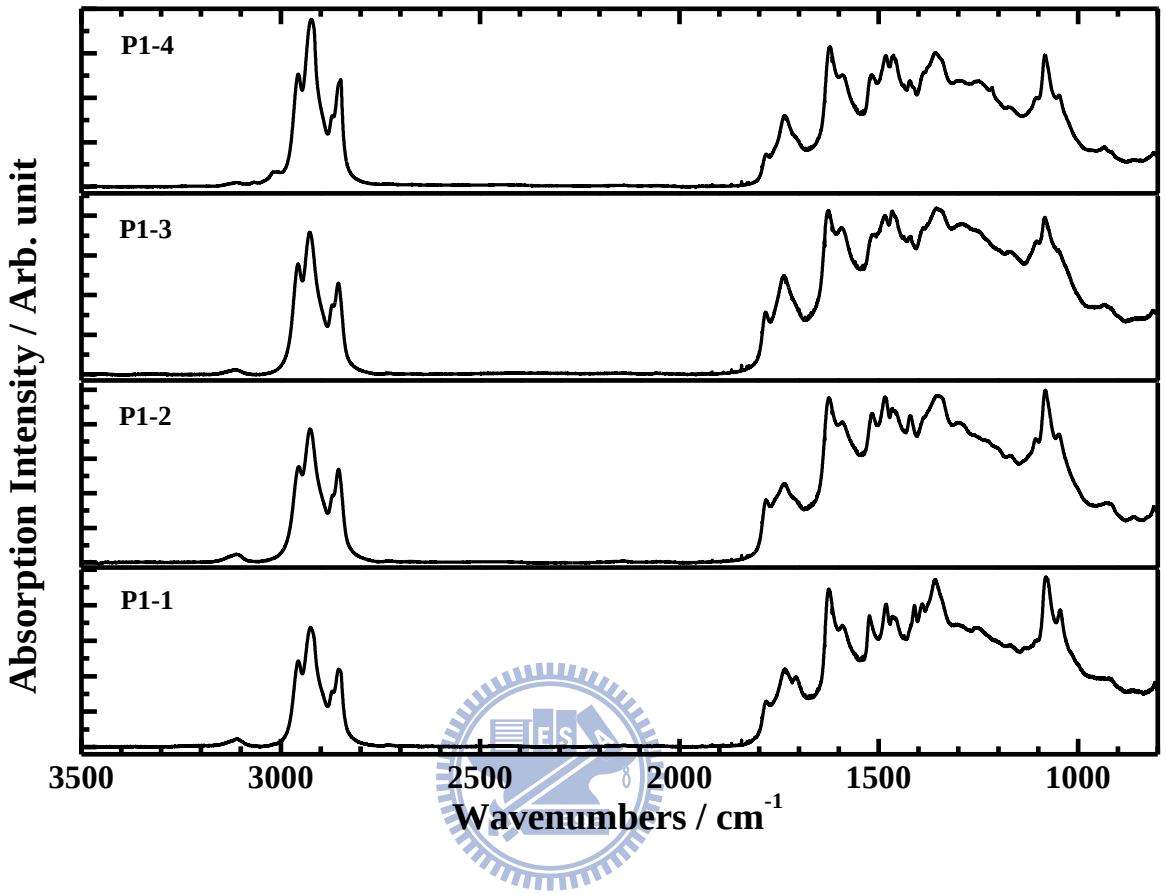

Figure 2-4. IR absorption spectra of polysquaraines **P1** as synthesized for four batches.

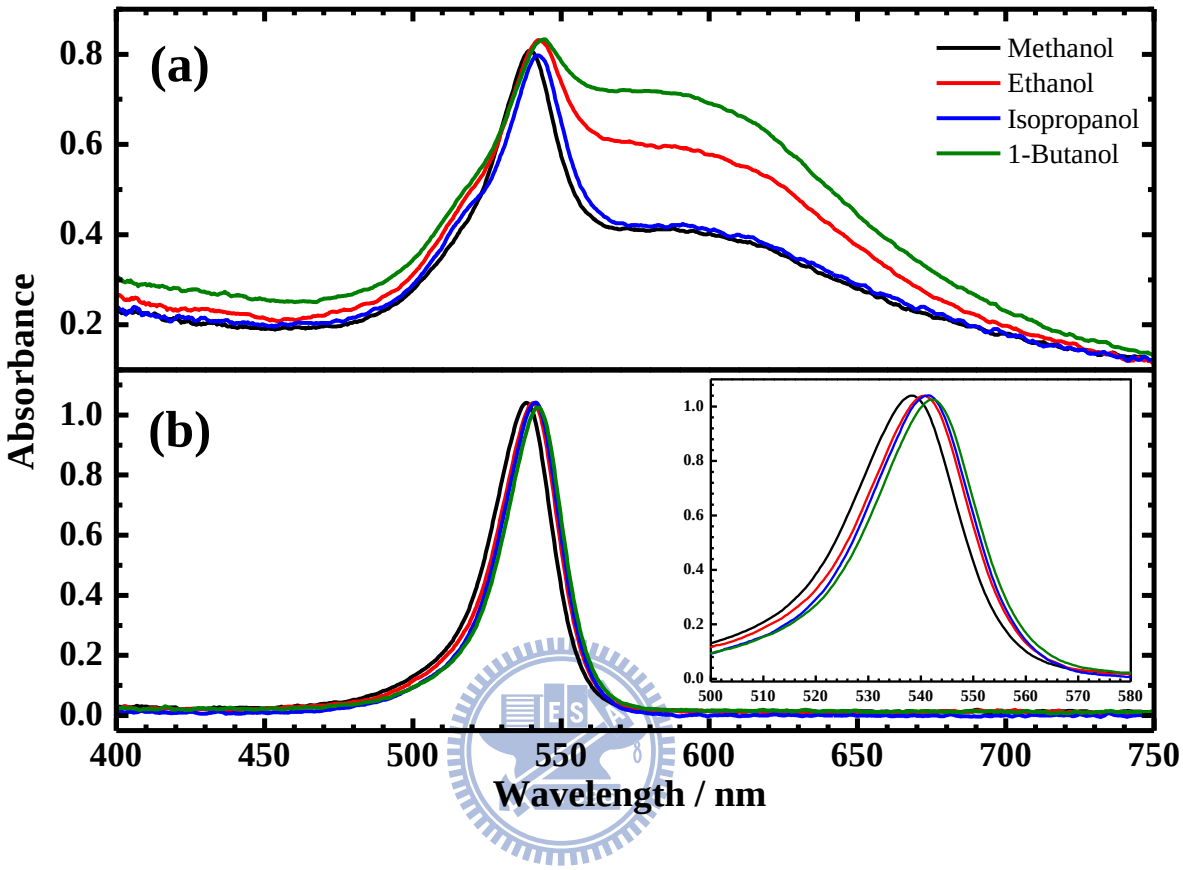

Figure 2-5. Visible absorption spectra of poly(pyrrolyl)squaraines, as synthesized, in hydrogen-bonding solvents: (a) **P1**; (b) **P3**

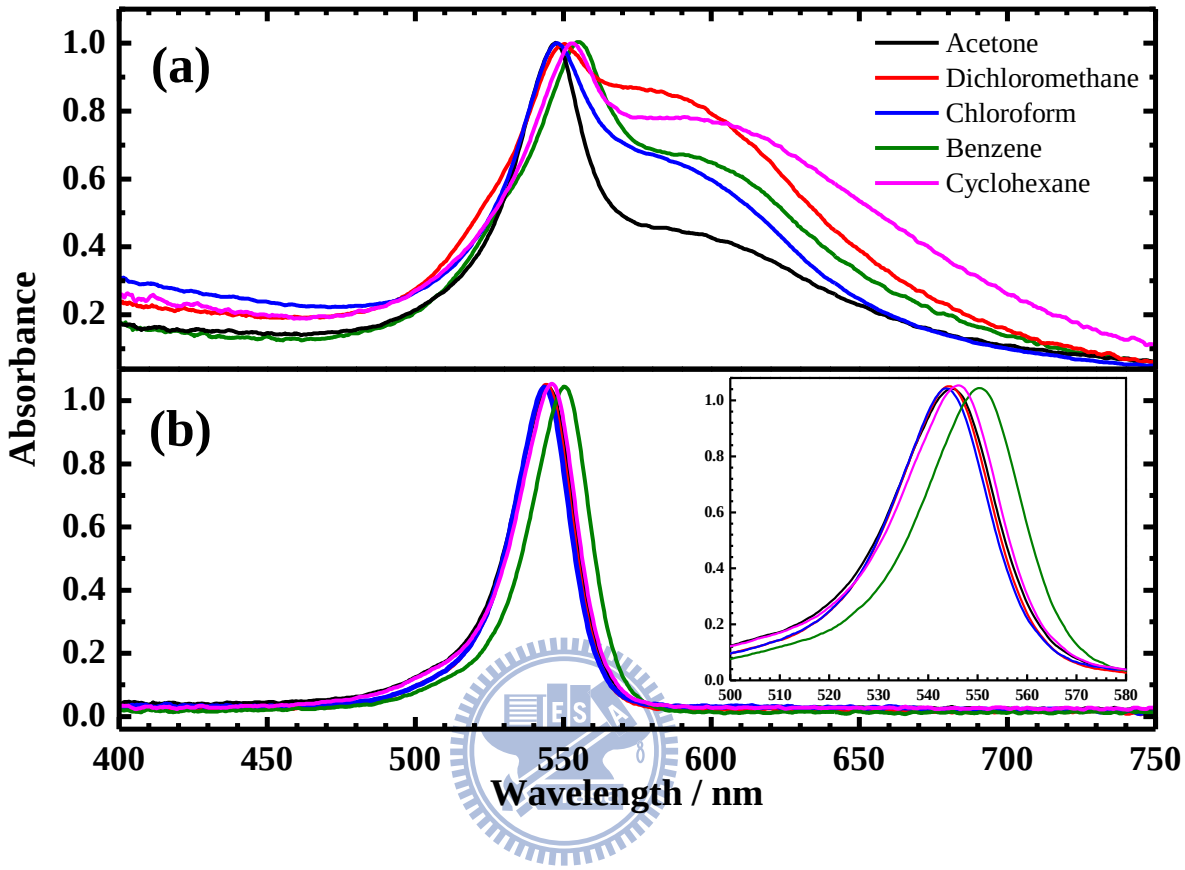

Figure 2-6. Visible absorption spectra of poly(pyrrolyl)squaraines, as synthesized, in non-hydrogen-bonding solvents: (a) **P1**; (b) **P3**.

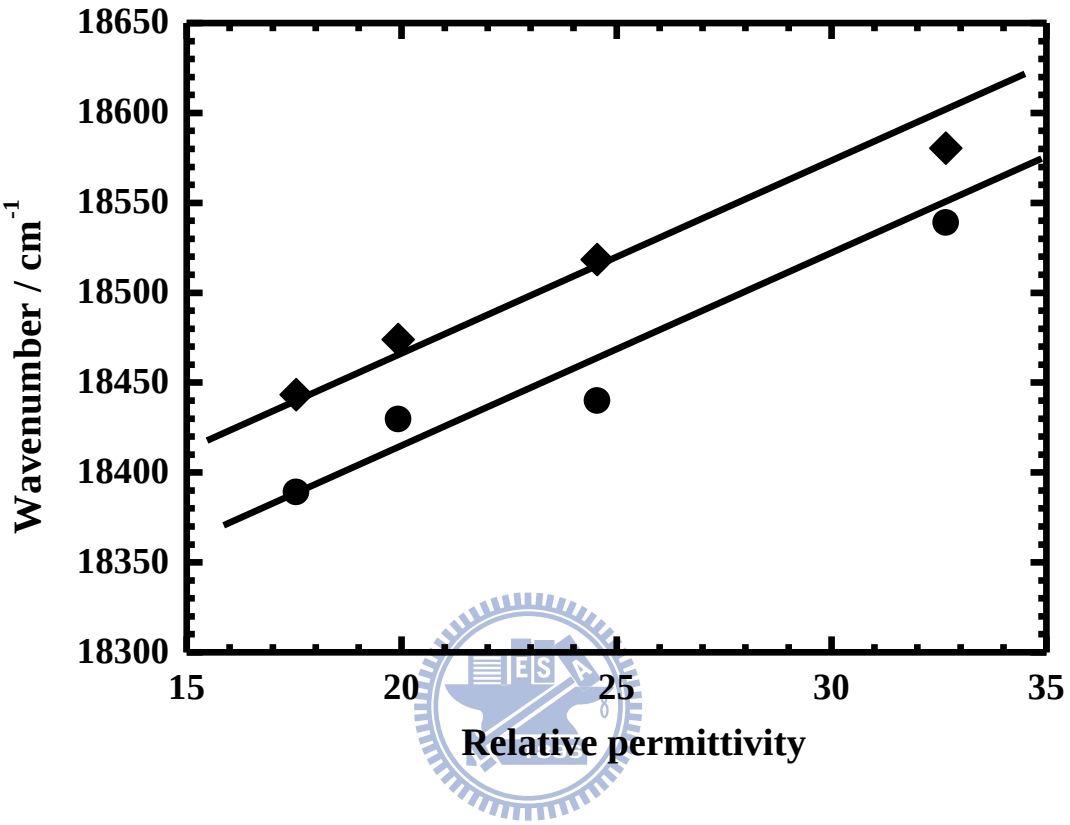

Figure 2-7. Wavenumber of absorption maxima of **P1** (solid circle) and **P3** (solid diamond), as synthesized, versus relative permittivity of methanol, ethanol, isopropanol and 1-butanol.

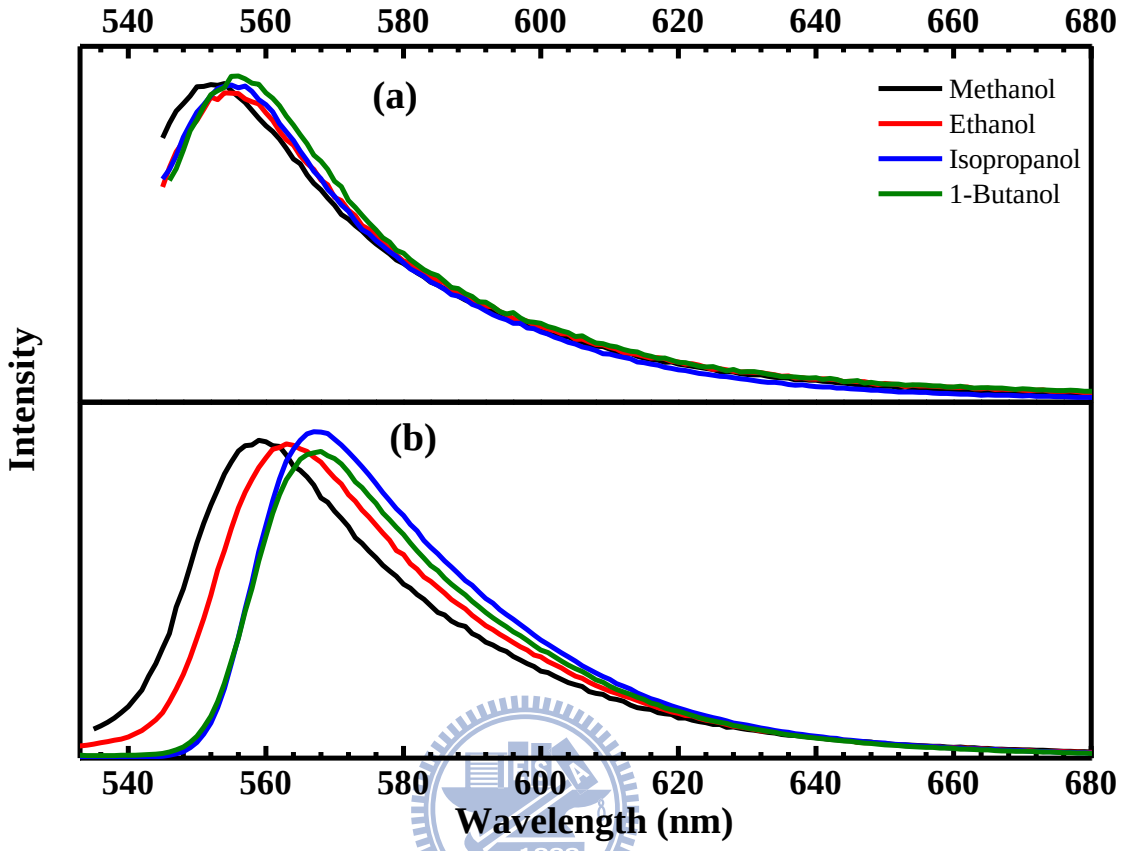

Figure 2-8. Photoluminescence spectra of poly(pyrrolyl)squaraines, as synthesized, in hydrogen-bonding solvents: (a) **P1** excited at 540 nm; (b) **P3** excited at 530 nm.

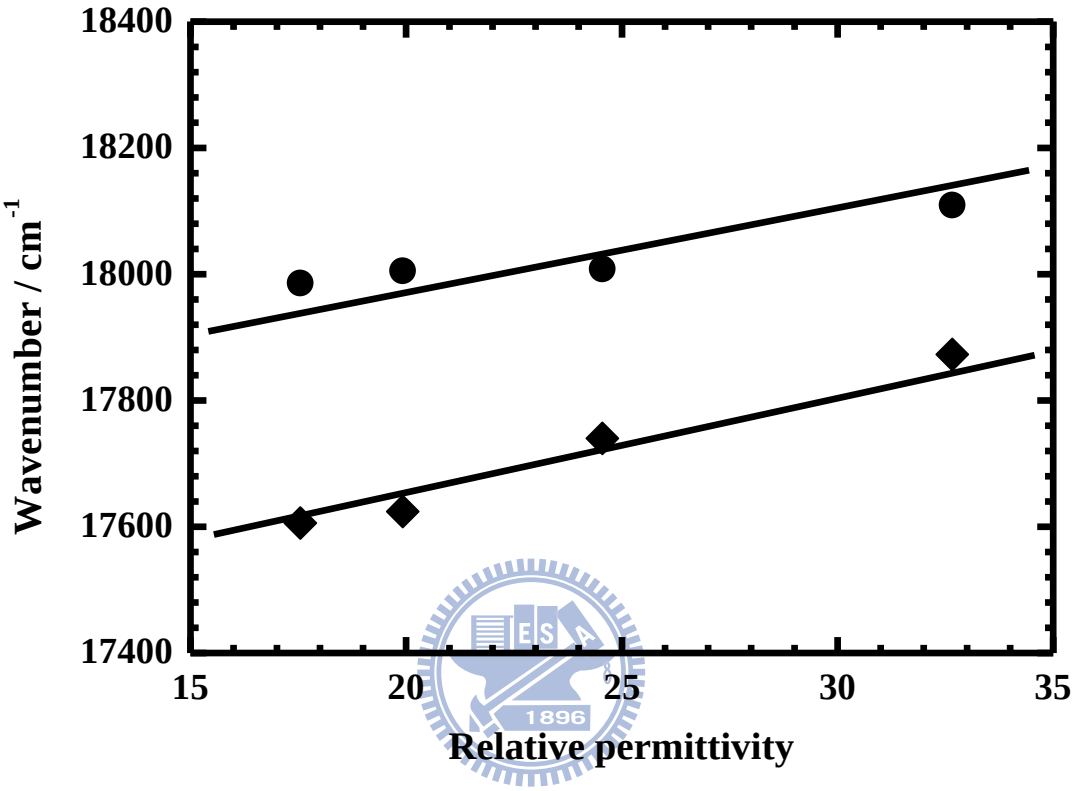

Figure 2-9. Wavenumber of emission maxima of **P1** (solid circle) and **P3** (solid diamond), as synthesized, versus relative permittivity of methanol, ethanol, isopropanol and 1-butanol.

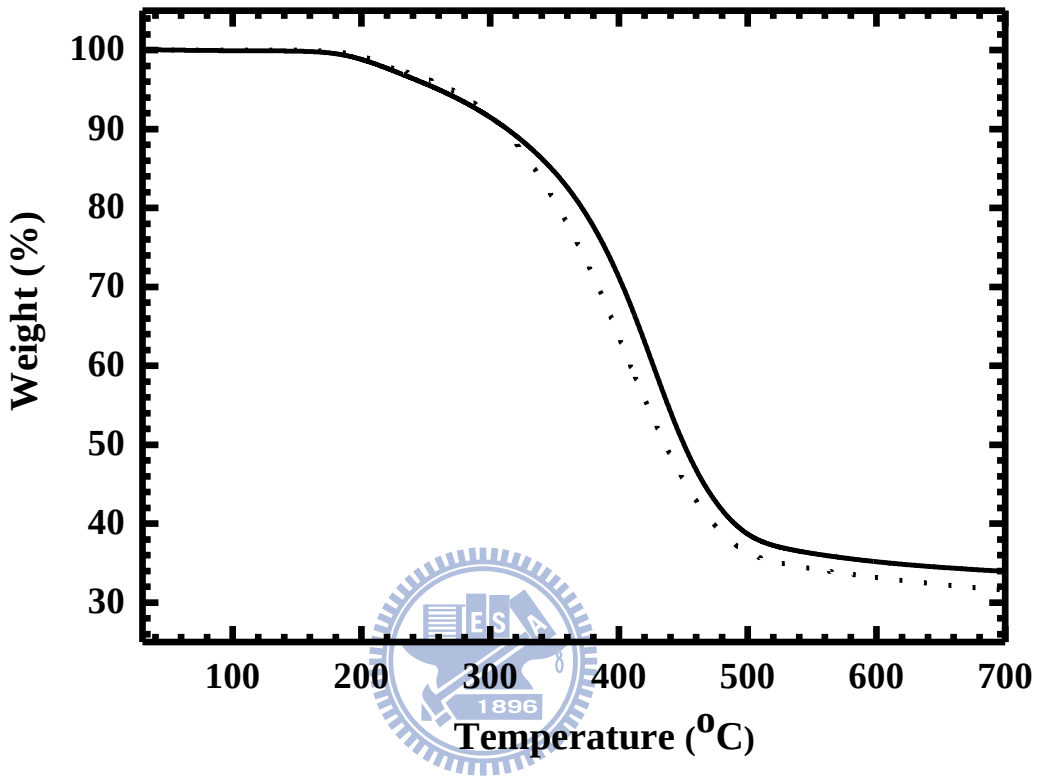

Figure 2-10. Thermal gravimetric analysis (TGA) curves of **P1** (solid line) and **P3** (dotted line) as synthesized.

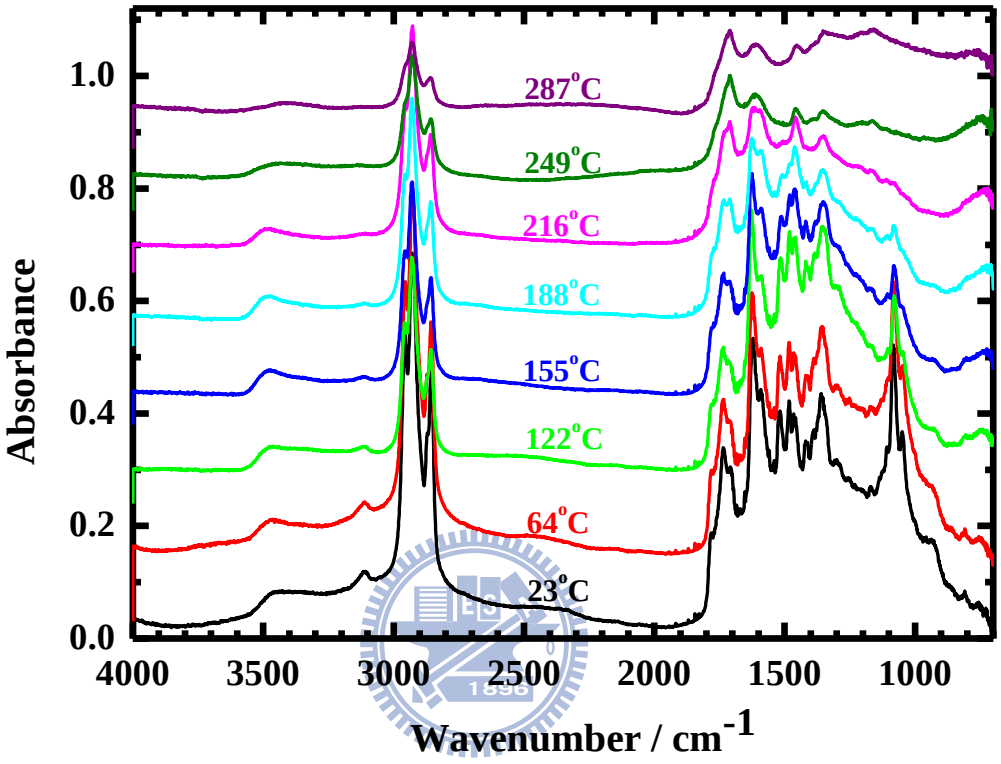

Figure 2-11. IR absorption spectra of **P1** at various temperatures as indicated.

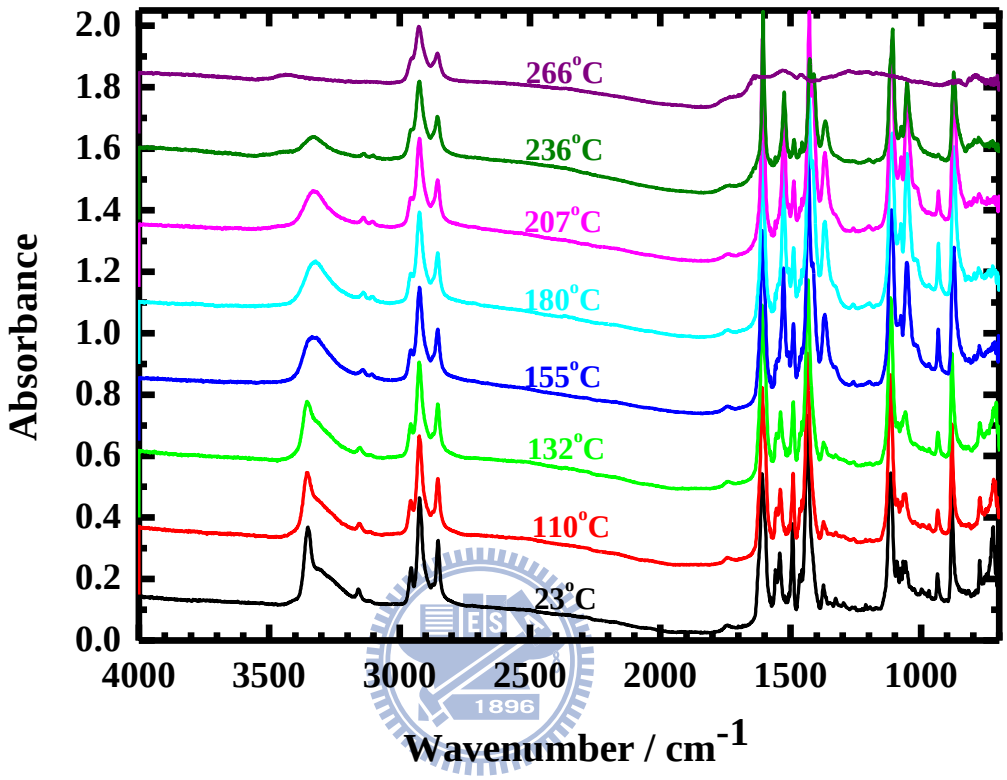

Figure 2-12. IR absorption spectra of **P3** at various temperatures as indicated.

Table 2-1. Wavenumbers (cm^{-1}), intensities, and ratios of covalent and zwitterionic carbonyl of poly(1-octylpyrroyl)squaraines **P1** and poly(3-octylpyrroyl)squaraines **P3** as synthesized.

Batch No.	ν_{C-O} (cm^{-1}) Covalent Part, *m*	Intensity	ν_{C-O} (cm^{-1}) Zwitterionic Part, *n*	Intensity	Ratio Covalent : Zwitterionic
P1-1	1736.0	0.111	1625.0	0.222	1 : 2.0
P1-2	1737.5	0.228	1625.0	0.477	1 : 2.1
P1-3	1737.5	0.248	1626.5	0.413	1 : 1.6
P1-4	1736.0	0.160	1622.0	0.314	1 : 1.9
P3-1	1700.0	0.019	1600.0	0.612	3 : 97
P3-2	1745.0	0.038	1600.0	1.110	3 : 97
P3-3	1742.0	0.039	1600.0	0.961	4 : 96
P3-4	1741.5	0.030	1601.5	0.817	4 : 96

Table 2-2. Wavelength/nm of maximum visible absorption of **P1** and **P3,** as synthesized, in various solvents

solvent	relative permittivity	P1	P3
H_3COH	32.66	539.4	538.2
C_2H_5OH	24.55	542.3	540.0
i-C_3H_7OH	19.92	542.6	541.4
C_4H_9OH	17.55	543.8	542.2
$(CH_3)_2CO$	20.56	547.4	544.8
H_2CCl_2	8.93	550.1	544.3
$HCCl_3$	4.89	547.9	543.6
C_6H_6	2.27	550.0	550.3
C_6H_{12}	2.02	553.3	546.2

2-6 Supporting Information

2-6.1 The IR beamline BL14A1 at the National Synchrotron Radiation Research Center

The IR beamline BL14A1 located in National Synchrotron Radiation Research Center (NSRRC) has been opened since September 2005. The end-station of infrared microspectroscopy (IMS) beamline is a technology of combination of the state-of-the-art FT-IR spectroscopy, optical microscope with all-reflecting optics, and synchrotron infrared radiation generated from bending magnet edges in a 1.5 GeV electron storage ring. This IMS beamline based on synchrotron source provides considerable brightness advantages over conventional IR sources.

The optical layout of IR beamline BL14A1 is shown in Figure 1-S1.

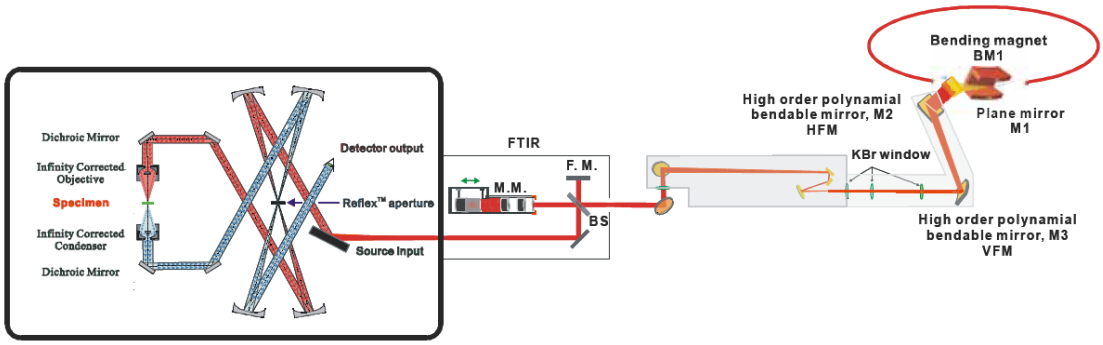

Figure 2-S1. The optical layout of IR beamline BL14A1

The technical data of IR beamline BL14A1 are listed in the following table.

Operational (general use)	Yes
%Time available (general use)	75%
Experiments	FT-IR, ATR-FT-IR and Infrared Microspectroscopy
Source	Bending Magnet
Ring Current (mA)	300 mA
Average Beam Lifetime	Infinite Under NSRRC Top Up Conditions
Energy Range	4000-650 cm^{-1}
Spectral Resolution	0.125 cm^{-1}
Spot Size	FWHM: 10 μm (H) x13 μm (V)
Optics	Bendable Horizontal Focusing Mirror, Bendable Vertical Focusing Mirror, Parabolic Collimating Mirror
Acceptance Angle (mrad)	70 mrad(H) x 30 mrad(V)
Flux (photons/sec)	2×10^{12}
Wavelength Min (μm)	2.5
Wavelength Max (μm)	15.4
Mirrors	Au Coated
Detector	LN Cooled MCT/A
Biohazard	Contact in Advance
Software	OMNIC 7.3 and Atlμs
Hardware	Nicolet Magna 860 Spectrometer and Spectra Tech Continμm IR Microscope
Backup Devices	USB2.0 Portable Disk

2-6.2 ^{1}H NMR spectrum of P1

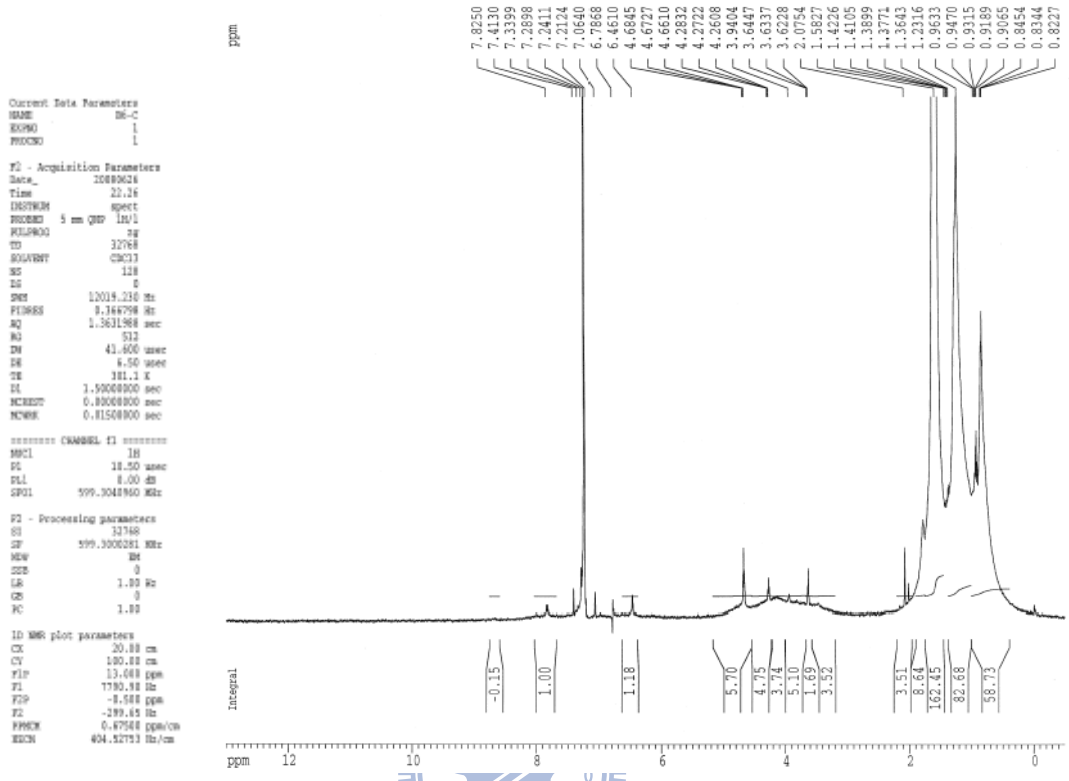

Figure 2-S2. ^{1}H NMR spectrum of **P1.**

δ= 0.9 (br s, 3H, CH_3), 1.23 (br s, 10H, CH_2), 1.58 (br s, 2H, CH_2), 3.63(br s, 2H, CH_2), 4.6-4.8 (br s, 2H), 6.4-6.8 (br s, aromatic)

2-6.3 ^{1}H NMR spectrum of P3

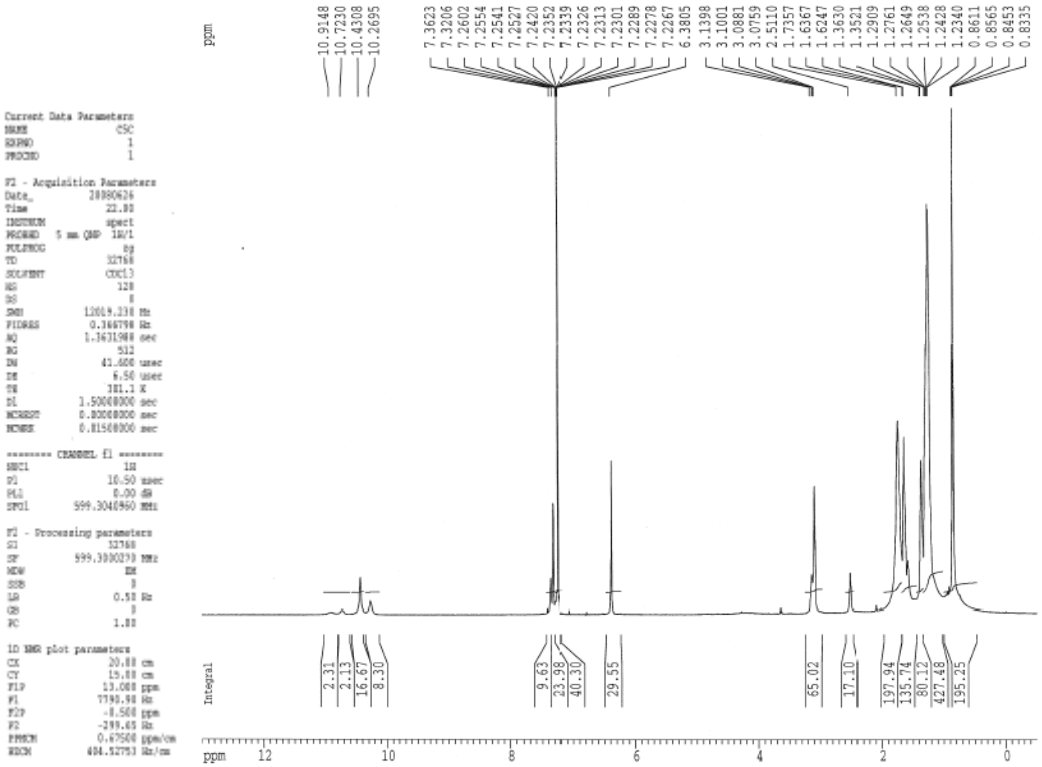

Figure 2-S3. ^{1}H NMR spectrum of **P3.**

δ= 0.84 (s, 3H, CH_3), 1.23 (d, 10H, CH_2) 1.63 (t, 2H, CH_2), 2.51(s, 2H, CH_2), 6.38 (br s, 1H, aromatic) , 10.43 (br s, 1H, NH)

2-6.4 ^{13}C NMR spectrum of P3

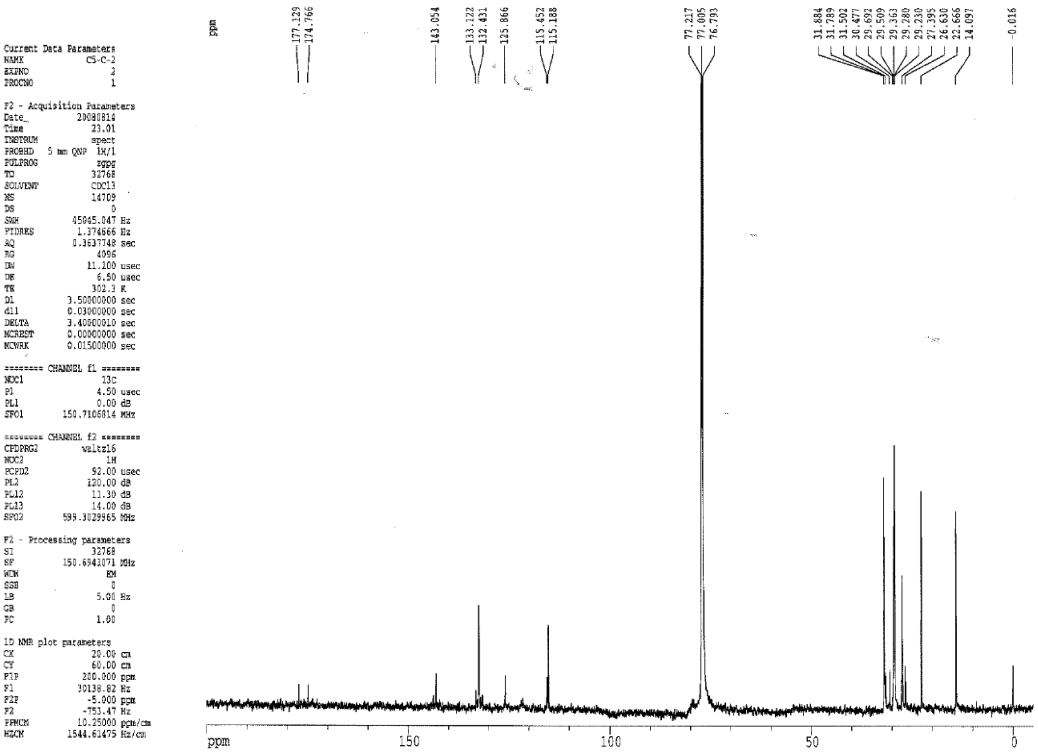

Figure 2-S4. ^{13}C NMR spectrum of **P3.**

δ= 14.09, 22.67, 26.63, 27.39, 29.23, 29.28, 29.36, 29.51, 29.69, 30.47, 31.50, 31.79, 31.88, 115.19, 115.45, 125.87, 132.43, 133.12, 143.05, 174.76, 177.13

2-6.5 Sample plate for *in situ* IR measurement

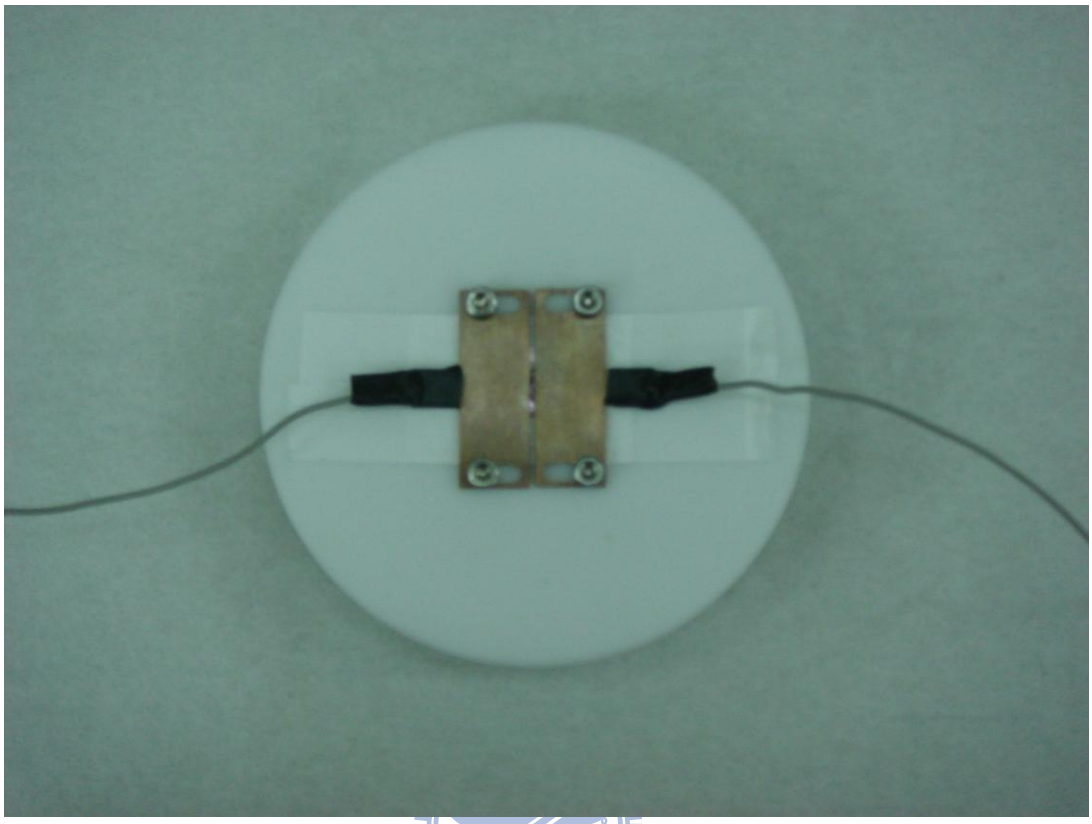

Figure 2-S5. The picture of the sample plate for *in situ* IR measurement

Chapter 3

Reversible Isomerization of a Zwitterionic Polysquaraine Induced by a Metal Surface

3-1 Introduction

Polymers with extended π-electron conjugation that have unique intrinsic conductivity are classified as conjugated polymers or conducting polymers (CP) [1-3,88]; these compounds exhibit novel electrical, optical and magnetic phenomena that can serve optoelectronic [89,90], solar cell [91-93], sensor and biomedical applications [94-96] in various devices. The polymeric nature of a CP enables great structural flexibility; CP thus attracts attention and remains at the forefront in many areas of development. One of the most significant interests in developing a CP is that its optical, physical and electronic properties are affected strongly by a variation of the polymer conformation [97-100]. Development of a CP requires an understanding of its detailed structure and its variation under various manipulations. This topic has hence become a focus of research from both scientific and practical points of view.

Polysquaraines are zwitterionic dyes containing squaraines and π-conjugated polymers that are characterized by intense red absorption [25-27]; these compounds are suitable for the design of conducting polymers with small optical band gaps [34-40]. This possession of unique properties has made polysquaraines provide great sensitivity and optimal performance in such applications as communication and biosensors, etc. [46,48,51,101,102].

The optical, physical and electronic properties of CP are affected strongly by a variation of the polymer conformation because of excitonic interaction among the constituent chromophores. To optimize the performance, controlling the conformation is a critical issue for applications based on these materials. Preceding authors have investigated the variation of the structural conformation for squaraine-based materials through external stimuli by solvent concentration [58-60], solvent polarity [58,61,62], temperature [58,63], metal ions [49,64,65] and other conditions. Besides induction by these external stimuli, other techniques might control the conformation of polysquaraine.

A condensation of squaric acid with electron-donating aromatic compounds produces squaraines [28,30,103]. In one such reaction, squaric acid reacts with a pyrrole derivatives to form poly(pyrrolyl)squaraines [76], having either covalent or zwitterionic backbones, so differing in the chain of the polymer. The intrinsic molecular structure of polysquaraine is expected to influence strongly its stability and opto-electronic properties; for instance, as the positive moiety containing a N atom in the zwitterionic polysquaraine can bind to either a H atom or an alkyl group (R), this subtle local variation of molecular structure likely affects its chemical and physical properties.

Here we demonstrate that, besides induction by metal ions, the structure of poly(3-octylpyrrole)squaraine having a zwitterionic repeating unit is variable when its solution in trichloromethane makes contact with the surface of an active metal. A possible structural alteration of this CP is thus a reversible isomerization from a linear conformer to a folded one induced with an active metal surface. This observation has no precedent; our findings provide an impetus for further investigation of the structural modification of similar CP and the structural dynamics of their polymer chains in solution.

3-2 Experimental Section

3-2.1 Materials

Reagents 1-octylpyrrole (97.3 %), 3-octylpyrrole (99.5 %) and squaric acid (99.0 %) (all from T.C.I.), lithium perchlorate (99.99 %), sodium perchlorate (98+ %), cesium perchlorate (99.999 %), magnesium perchlorate (99.0 %), and barium perchlorate (99.999 %) (all from Sigma-Aldrich), copper perchlorate hexahydrate (98 %), calcium perchlorate tetrahydrate (98 %) (Acros), solvents 1-butanol (99.9 %), benzene (99.8 %), diethyl ether (99 %), ethanol (99.8 %) and trichloromethane (99.4 %) (all from Merck) were obtained from the indicated suppliers.

Plates of iron (0.1 mm, 99.994 %), aluminum (0.25 mm, 99.997 %), silver (0.1 mm, 99.998 %), cobalt (0.1 mm, 99.995 %), nickel (0.5 mm, 99.994 %), tin (1.0 mm, 99.9985 %), lead (1.0 mm, 99.9995 %), zinc (2.0 mm, 99.999 %), gold (0.1 mm, 99.9975 %), rhenium (0.025 mm, 99.97 %), tantalum (0.127 mm, 99.95 %), molybdenum (0.5 mm, 99.0+ %) and copper gauze (100 mesh, diameter 0.11mm) (all from Alfa Aesar), of copper (0.5 mm, 99.98 %), rhodium (0.025 mm, 99.9 %), tungsten (0.127 mm, 99.9+ %), platinum (0.127 mm, 99.99 %) and palladium (0.25 mm, 99.98 %) (all from Sigma-Aldrich) were obtained from the indicated suppliers.

3-2.2 Preparation of poly(octylpyrrole)squaraine

To synthesize poly(octylpyrrole-co-squaric acid), 1-octylpyrrole or 3-octylpyrrole (1.1224 g, 6.26 mmol) and squaric acid (0.714 g, 6.26 mmol) in equimolar proportions were refluxed in a mixture of 1-butanol (60 mL) and benzene (30 mL) under continuously

flowing N_2 for 24 h [66,104]. The general condensation of squaric acid with 1-octylpyrrole and 3-octylpyrrole is displayed in Scheme 3-1.

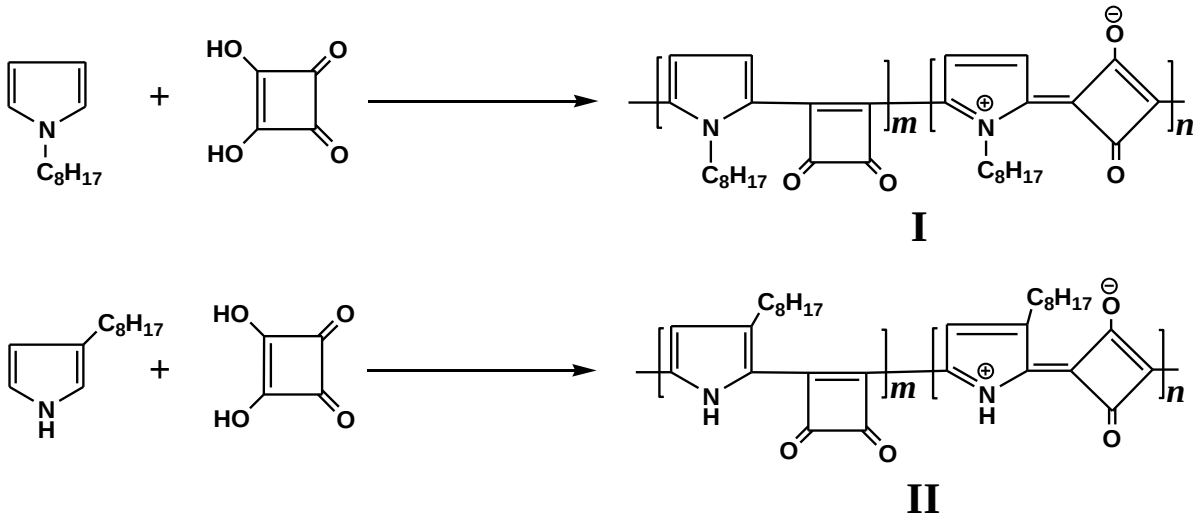

Scheme 3-1. In the general condensation of squaric acid with 1-octylpyrrole and 3-octylpyrrole, the product poly(pyrrolyl)squaraines containing m repeating units of covalent backbone and n repeating units of zwitterionic backbone are represented with formulae **I** and **II**, respectively.

After the obtained solutions were filtered, the filtrates were concentrated through vacuum distillation and poured into diethyl ether. The crude products were collected on filtration and washed with diethyl ether, before being redissolved in trichloromethane to yield solutions that were filtered again; the filtrates were evaporated to dryness in an open fume cupboard to eliminate $HCCl_3$. The precipitates were finally washed again with diethyl ether and dried in a vacuum chamber near 295 K for two days.

According to our syntheses, the end products poly(1-octylpyrrole-co-squaric acid) and poly(3-octylpyrrole-co-squaric acid) are named poly(1-octylpyrrolyl)squaraine, denoted **P1**, and poly(3-octylpyrrolyl)squaraine, denoted **P3**, respectively.

3-2.3 Characterization

P1 and **P3** were characterized with elemental analysis, thermogravimetric analysis, gel-permeation chromatography, and ^{1}H NMR, ^{13}C NMR, UV/visible absorption, infrared absorption and photoluminescence spectra. By these means, we deduced that product **P1** from reagent 1-octylpyrrole possesses backbone ratio 1:2 of covalent repeating units to zwitterionic ones, whereas polymer **P3** from reagent 3-octylpyrrole was produced with mostly zwitterionic repeating units (>97 %), as shown in Scheme 3-2. The detailed characterization of **P1** and **P3** can be found in Chapter 2 [104]. The molecular masses according to *M*n are 23 kDa for **P1** and 21 kDa for **P3**, and according to *M*w are 45 kDa for **P1** and 38 kDa for **P3**.

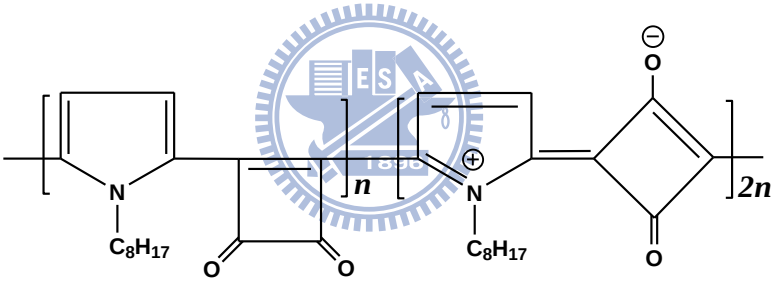

P1

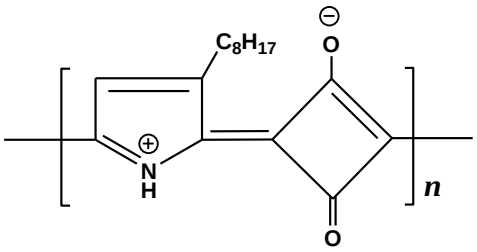

P3

Scheme 3-2. The molecular structures of **P1** and **P3**; **P1** consists of repeating units of covalent and zwitterionic structural backbone in a ratio 1:2, whereas **P3** possesses mostly zwitterionic repeating units (>97 %).

3-2.4 Measurements

Visible absorption spectra were recorded with a UV-visible spectrophotometer (Ocean Optics). IR absorption spectra were recorded with an interferometric spectrometer (Nicolet Magna 860 FTIR) attached to the IR beamline at National Synchrotron Radiation Research Center (NSRRC); a HgCdTe detector rendered the mid IR range 500 – 4000 cm^{-1} or a DTGS detector for 400 – 4000 cm^{-1}. The resistance of the polymer solution was measured by the AC impedance method using electrochemical workstations (PARATAT 2263).

Small-angle X-ray scattering (SAXS) curves were recorded with the 15-keV beam (ca. 0.2x0.2 mm) from beam line 23A at NSRRC [105]; the technical data of this beamline can be found in Supporting Information 3-6.1 and the optical layout is depicted in Figure 3-S1of Supporting Information. The target polymers were dissolved in trichloromethane then injected into a stainless-steel or copper cell (diameter 5 mm, thickness 2.2 mm), with Kapton windows for incident X-rays; the drawing and the photo of the liquid cell are displayed in Figure 3-S2 and Figure 3-S3, respectively, of Supporting Information.

3-3 Results and Discussion

The target polysquaraines were synthesized from squaric acid with 1-octylpyrrole and 3-octylpyrrole under condensation conditions [104]. The general condensations of squaric acid with 1-octylpyrrole and 3-octylpyrrole are expressed in Scheme 3-1. The end products of poly(pyrrolyl)squaraines for poly(1-octylpyrrole-co-squaric acid) and poly(3-octylpyrrole-co-squaric acid) are denoted with formulae **I** and **II**, respectively.

Polysquaraines are described as having π-conjugated structures that typically possess intense absorption in the visible range. Figure 3-1 displays the visible spectra of poly(pyrrolyl)squaraines in trichloromethane; poly(1-octylpyrrolyl)squaraine (**P1**) and poly(3-octylpyrrolyl)squaraine (**P3**) exhibit distinct features in their visible spectra.

The visible absorption of zwitterionic **P3** in trichloromethane exhibited a single and narrow absorption band centred at 543.6 nm, producing a magenta color in solution, whereas **P1** has a line with maximum absorption at 547.9 nm and a broad shoulder near 600 nm, resembling navy blue in solution.

As reported in the Chapter 2 [104], because **P3** as synthesized possesses mostly zwitterionic repeating units in its structure, the backbones tend to be identical and to bestow on its visible absorption only one narrow band, whereas **P1** contains backbones of two types in its polymer chain, so producing a more complicated absorption in its visible spectrum. Through comparison with the narrow absorption for zwitterionic **P3**, we deduce the corresponding narrow band of **P1** to imply its zwitterionic moiety; the shoulder is due to its covalent part.

3-3.1 Visible absorption spectra of P1 and P3 in trichloromethane solution inserted with metals

In most electronic devices, connection to a metal surface or contact through opto-electronic materials is generally unavoidable. Because metals used in devices are typically rigid, these materials, including conducting polymers, tend to be considered stable when they bond to a metal or are in contact with its surface. The physical and chemical properties of CP are poorly explored and understood; an assumption of a CP being inactive towards a metal should be verified before we accept it as common knowledge.

The strengths and shapes of the visible absorption features of **P1** and **P3** in a silica cell remained constant for over seven days; these polymers hence appear to be stable in trichloromethane solution. With a polymer solution as blank for comparison, we inserted metal plates or gauzes into the silica cells and monitored the visible absorption of the polymer solutions as a function of time. For polymer **P1** in the silica cell, the strength and shape of the absorption spectra remained constant no matter which metal was inserted in the solution; we conclude that solution of polymer **P1** is insensitive to contact with metals.

When metal plates were inserted into solutions of polymer **P3**, the absorption spectra of solutions varied depending on the metal. For metals Al, Co, Ni, Mo, Pd, Sn, Ta, W, Re, Au and stainless steel, we observed no change of the visible absorption spectra for solutions of polymer **P3**, as displayed in Figure 3-2. These results thus resembled those for polymer **P1**; zwitterionic polysquaraine **P3** in trichloromethane is hence unaffected on contact with those metals.

In contrast, when metal plates of Ag, Cu, Fe, Zn, Rh, Pt and Pb were inserted into solutions of polymer **P3** in trichloromethane, the visible absorption spectra of the solutions

altered markedly. For example with an Ag plate (surface area 907 mm^2), after 40 h the intensity of the band at 543.6 nm decreased about 10 % and the intensity near 500 nm increased perceptibly, as displayed in Figure 3-3. Polymer **P3** in trichloromethane solution is hence unstable to contact with those metals, but the rates and extents of alteration of visible absorption of the solution varied, depending on the particular metal. For metals Ag, Rh (see Figure 3-4), Pb (see Figure 3-S4 in Supporting Information), Zn (see Figure 3-S5 in Supporting Information), and Pt (see Figure 3-S6 in Supporting Information) the visible spectra altered slightly over a protracted period.

For the solution of polymer **P3** at 295 K in contact with a Fe plate in a silica cell, the absorption altered more markedly, as shown in Figure 3-5. The stature of the band at 543.6 nm decreased about 66 % after inserted Fe plates with surface area 1720 mm^2 into solution for 47 h; a new band at 513.8 nm rised discernibly.

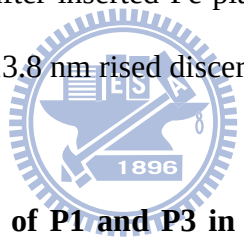

3-3.2 Visible absorption spectra of P1 and P3 in trichloromethane solution inserted with copper

When we inserted a Cu plate into a solution of poly(3-octylpyrrole)squaraine, the visible absorption spectra of these polymer solutions altered more profoundly. Figure 3-6 illustrates the temporal variation of visible absorption spectra for the case of a Cu plate (surface area 382 mm^2) at 295 K; over 40 h the original spectral feature with maximum absorption at 543.6 nm gradually decreased, and became replaced with another broad feature with a maximum at 513.8 nm. All these spectra retain an isosbestic point at 525.8 nm. The inset photograph in Figure 3-6 displays the distinct color change from pale magenta before insertion of the copper plate to pale orange afterward.

For these active metals, the relative rates of variation of the spectra of poly(3-octylpyrrole)squaraine solution are derived from the decrease of absorbance at 543.6 nm during the same periods. The corresponding rates relative to that for copper are listed in Table 3-1. Among these active metals, copper is most active, and iron second: the rate for iron is about 0.37 that for copper. Relative to the rate for copper, the rates for other metals are Rh 0.21, Ag 0.09, Pt 0.08, Zn 0.06, and Pb 0.03. Although copper and iron are metals commonly used in electronic devices, nobody expects that these two metals would effect a color change of this kind for a CP.

Figure 3-6 demonstrates the existence of an isosbestic point in the temporal variation of the absorption spectra of the solution of polymer **P3** into which was inserted a copper plate. This effect implies two species to be present in the varying system; one species is characterized with its absorption at 543.6 nm and the other at 513.8 nm. As no obvious driving force is present to induce a chemical reaction in this system, and consistent with the reversibility of whatever transformation, two distinct chemical species are unlikely to exist there. An alternative possibility is that the same chemical species exists in two structures, or isomers, in that solution; in that case the color change would reflect a conformational isomerization of this polysquaraine induced by a copper surface.

3-3.3 The relationship of color change vs. metal surface area and temperature

Induced by active metals in solution, the color of poly(3-octylpyrrole)squaraine solution might change; among these active metals, copper is most active. To study what could cause this variation, we thus selected copper as the testing metal. First, we investigated the relationship of this color change vs. surface area of metal.

The rates of decreasing intensity at 543.6 nm and increasing intensity at 513.8 nm for **P3** polymer solutions depend on the area of exposed surface of coppers, increasing with increasing area. For copper plates with surface areas 860, 1720 and 1960 mm^2, the color changes were completed in 11, 6 and 4 h, respectively. Figure 3-7 depicts the decrease of absorbance at 543.6 nm in 1 h vs. area of copper surface at 295 K: the relation is linear. The rate of color modification for this zwitterionic polysquaraine **P3** induced by a copper surface thus increases with its increasing area.

For an active metal in contact with the polymer solution, the rate of decreasing absorbance at 543.6 nm and increasing absorbance at 513.8 nm depended also on the temperature, increasing with increasing temperature. Figure 3-8 depicts how the absorbance decreased at 543.6 nm for 1 h vs. temperature after copper plates (surface area 1720 mm^2) were inserted into solutions of **P3**. The plot of ln k vs. T^{-1} in range 283–323 K is linear, consistent with a barrier of activation for the process accompanying the absorption line shifting from 543.6 nm to 513.8 nm. The activation energy, denoted Ea and derived from the Arrhenius equation, ln k = ln A - Ea/RT (R = gas constant) for the assumed isomerization of polymer **P3** in trichloromethane solution induced by copper is thus (18.9±0.7) kJ mol^{-1}.

3-3.4 Reversibility of the color change induced by metal

A notable feature of the transformation of visible absorption of this zwitterionic polymer with metals is its reversibility. After the absorption at 543.6 nm became replaced with the feature at 513.8 nm induced by metals, the reverse shift from 513.8 nm to 543.6 nm occurred on removal of the metals from the solution.

Figure 3-9 shows this phenomenon; on removal of the copper plates from the solution after insertion for 11 h, the absorption at 513.8 nm of the polymer solution with the Cu plates became replaced with the band at 543.6 nm. The temporal variation of these spectra preserves the same isosbestic point at 525.8 nm. This reversibility of absorption behavior implies that the polymer, without the metal in contact with its solution, reverted to its original conformation.

The rate of the reverse transformation of **P3** on removal of a metal from the solution depends also on temperature, increasing with increasing temperature. The completion of the reverse transformation required 24 h at 323 K but more than 102 h at 295 K. Figure 3-10 depicts the dependence of absorbance at 513.8 nm for 1 h on temperature after the inserted copper plates were removed from the **P3** solutions. The linear relation in terms of ln k vs. T^{-1} in the range 303 – 328 K implies activation energy (38±6) kJ mol^{-1} of the reverse isomerization.

3-3.5 Mechanism for switchable conformation

This observation of a reversible optical effect of the zwitterionic polysquaraine induced by metal plates is unprecedented. How can one explain this phenomenon for a carrier induced only by its solution in contact with a metal surface? To account for this phenomenon accompanying a structural isomerization, we propose the transformation for the zwitterionic polymer in solution to occur in three sequential steps: diffusion to and adsorption on a metal surface, folding of the structure, and desorption and diffusion from the metal, as schematically displayed in Figure 3-11.

According to this mechanism, the backbone structure of this free zwitterionic polymer in solution is originally present in a linear form. When a metal plate is inserted

into the solution, the polymer molecule diffuses to the metal surface and becomes adsorbed, process (a). As the zwitterionic moieties of the polymer affix to the metal surface, the molecule becomes strongly anchored on the surface through the interaction of its charged regions with the metal. Although anchored on the metal surface at some points, other portions of the polymer chain are free to move in the solution and to swing back and forth in motion until the polymer folds, process (b). This closure decreases the force of the anchor attachment to the metal surface; as a result, the folded polymer desorbs from the metal surface, process (c). The folded polymer retains its modified conformation in solution and thus exhibits its altered optical property on removal of the metal plate. In absence of the interaction with a metal surface, the free folded polymer eventually acquires energy on collisions and reverses its closure by becoming linear again.

Although not definitive, this mechanism of isomerization explains the observation of the optical reversible phenomena for the zwitterionic polysquaraine on interaction with a metal. From a thermodynamic point of view, the free zwitterionic polymer in solution tends to maximize its entropy and thus exists in an almost linear form [63,106-108]. When the zwitterionic polymer makes contact with the surface of the active metal, the zwitterionic moiety attaches to the metallic surface to resemble becoming anchored on the metal surface. If the adsorption on the metallic surface occurs in this step, the rate of transformation should depend on the extent of the metal surface. Figure 3-7 shows that the rate of transformation for **P3** induced by copper is proportional to the area of the copper surface; also, the fitting line of the relationship intercepts at the point of the origin. That the structural modification of the polymer is directly associated with the area of the metal surface supports adsorption as the first step.

The adsorbed polymer might desorb from the surface from random movements or collisions and maintain its linear conformation in solution, but, while the zwitterionic polymer is anchored at one end on the metal surface, the other terminus of the polymer chain remains free to move in the solution. The polymer chain would swing back and forth and might fold its structure. If an energy term for the folded conformation compensates the entropy term, this conformation might be stable and exist in solution for a protracted period. The zwitterionic poly(3-octylpyrrole)squaraine has alternately negatively charged -O- and positively charged $-NH^+$ moieties that might interact in the folded conformation. The closure might cause the -O- and the $-NH^+$ moieties to attract each other and to bind together through hydrogen bonds. Scheme 3-3 illustrates the proposal molecular structures of the reversible isomerization of poly(3-octylpyrrole)squaraine induced by an active metal; the internal hydrogen bonds are schematically depicted in the folded conformation.

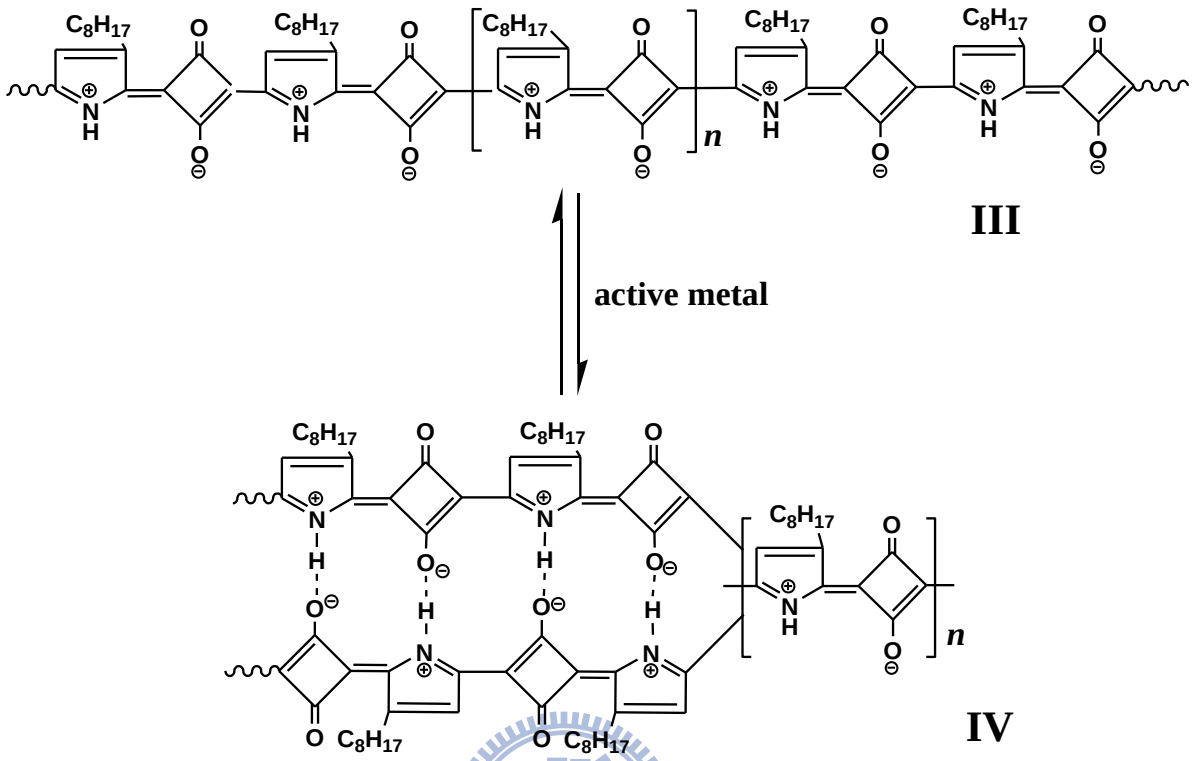

Scheme 3-3. Reversible structural transformation of poly(3-octylpyrrole)squaraine induced by an active metal depicted in molecular structures; formulae **III** and **IV** represent the linear and folded conformers, respectively.

3-3.6 Evidence of folding structure from IR absorption spectra

According to Scheme 3-3, we perceive that internal hydrogen bonds might be formed in the folded structure of poly(3-octylpyrrole)squaraine. Such a formation of hydrogen bonds might play a key role in this closure. Information about the structure of this polysquaraine in solution might be derived from infrared spectra. As shown in Figure 3-12, although trichloromethane absorbs strongly in the mid IR region, so interfering with measurements of dissolved samples, it is still possible to obtain useful IR absorption spectra of liquid samples by careful subtraction of the absorption by the solvent. Figure 3-

13 presents the IR net absorbance of poly(3-octylpyrrole)squaraine between solutions without, in 3-13 (A), or with, in 3-13 (B), contact with a Cu plate, relative to the solvent.

Apart from artefacts produced by imperfect subtraction of trichloromethane in both spectra, the significant feature located at 1602 cm^{-1} belongs to the functional group of the zwitterionic carbonyl of this polysquaraine sample [75,78,80,104]. A notable difference between these two spectra is a line at 3364 cm^{-1} that appears only in Figure 3-13 (B), and that is assigned to an OH stretching mode of a intra-hydrogen bond [109]. As discussed above, the carrier sample of poly(3-octylpyrrole)squaraine in trichloromethane is postulated to exist as a linear form (formula **III**) that contains no OH functional group, consistent with its absence from Figure 3-13 (A), whereas in the presence of the copper plate this polysquaraine sample has a folded structure (formula **IV**); the negatively charged -O- then binds to positively charged $-NH^+$ to form a internal hydrogen bond, revealed through its OH stretching mode at 3364 cm^{-1} in Figure 3-13 (B). The evidence from the IR spectra is thus consistent with a folded conformation of this polysquaraine sample induced by active metal surfaces, as demonstrated in Scheme 3-3.

To retain its maximum entropy in solution, the free zwitterionic polymer is thus configured as a flexible linear chain. For the zwitterionic polymer to convert to a folded conformation, energy must be released to compensate the entropy term. In this folding, poly(3-octylpyrrole)squaraine possesses $–NH^+$ groups that can bind to its –O- ends. In this way internal hydrogen bonds O–H form in the folded conformation and stabilize the folded structure for this polymer. If the structure has no contribution from such an energy factor, the polymer would not fold its chain.

To clarify this point, we compared the behaviors of poly(1-octylpyrrole)squaraine in the same experimental conditions. The similar structure of poly(1-octylpyrrole)squaraine possesses its octyl group bound to –N (position 1) instead of –C (position 3); with such an alkyl location, it contains charged $-^{+}NC_8H_{17}$ groups, not $-NH^{+}$ groups , as shown in formula **I**. No intra-hydrogen bond can form even when the charged $-^{+}NC_8H_{17}$ group is able to approach the charged –O- group. In this case, no hydrogen bond can form to stabilize the closure of the structure; poly(1-octylpyrrole)squaraine can thus adopt no folded structure. As the visible absorption of poly(1-octylpyrrole)squaraine solution in contact with a metal remained constant under our experimental conditions, poly(1-octylpyrrole)squaraine preserves its linear conformation in solution. This constancy of the poly(1-octylpyrrole)squaraine in solution is consistent with the folded model.

3-3.7 Evidence from small-angle X-ray scattering experiments

Experiments of small-angle X-ray scattering provide further evidence supporting the isomerization of the target polymer in solution induced on contact with an active metal. For SAXS measurements of poly(3-octylpyrrole)squaraine in trichloromethane solution, we used stainless-steel and copper cells. As the SAXS curve remained constant for this cell, stainless steel is an inactive metal for the isomerization of this polymer in solution. In contrast, the SAXS profiles of solution for poly(3-octylpyrrole)squaraine in a copper cell varied with time, as shown in Figure 3-14.

The SAXS curve of the polymer solution in the copper cell at the initial stage, displayed as a solid line, was similar to that in the stainless steel cell; it gradually altered and eventually became the dotted curve in Figure 3-14. The radius of gyration (*Rg*) of the polymer is determined from the plot of ln I(*q*) versus q^2 in the range of small *q*; the value

of *Rg* thus extracted from the slope ($-Rg^2/3$) of this plot [110,111], as shown in the insert of Figure 3-14, was (21±2) nm and (16±2) nm in the copper cell at the initial and final stages, respectively. The result is consistent with two conformers existing in solution and with our folded model.

3-3.8 Possible mechanisms for isomerization

Summarizing the above, we observed reversible changes in visible absorption, IR absorption and SAXS spectra of poly(3-octylpyrrole)squaraine in solution in contact with particular metals; we postulate that the effects reflect conformational isomerization of this conducting polymer induced by metals. Is there another possible mechanism to cause the changes in these spectra of poly(3-octylpyrrole)squaraine on exposure to metal plates in solution? One mechanism that might explain these spectral changes is the chemical oxidation of the polymer chains by either dissolved metal ions or oxidation of the polymer chains by dissolved oxygen at the metal surfaces.

Zwitterionic organic dyes act as ligands and react with metal ions to form stable complexes, resulting in altered optical properties. As synthesized, poly(3-octylpyrrole)squaraine reacts thus with metal ions; the color of its solution alters concurrently. To test the role of metal ions, we added cations to similar polymer solution.

On reaction of our poly(3-octylpyrrole)squaraine, as synthesized, with Cu^{2+} cation in trichloromethane solution, the absorption maximum gradually shifted with time from 543.6 nm to 524.0 nm; the intensity of the former band correspondingly decreased, as shown in Figure 3-15. For this reaction we prepared a saturated solution of Cu^{2+} in $HCCl_3$ over $Cu(ClO_4)\cdot 6H_2O$. The curves of these spectra intersect at 531.2 nm, an isosbestic point.

Thus either poly(3-octylpyrrole)squaraine reacted with Cu^{2+} ion in trichloromethane or the metal ion altered the structure of this zwitterionic polymer, in either case to shift the absorption band of poly(3-octylpyrrole)squaraine. Scheme 3-4 illustrates the proposed transformation of the molecular structure of poly(3-octylpyrrole)squaraine caused by Cu^{2+}; the linear backbone of this polymer represented as formula **III** converts to a folded complex with Cu^{2+} ion as formula **V**. In such modification of conformation caused by a cation, the metal ion plays a key role.

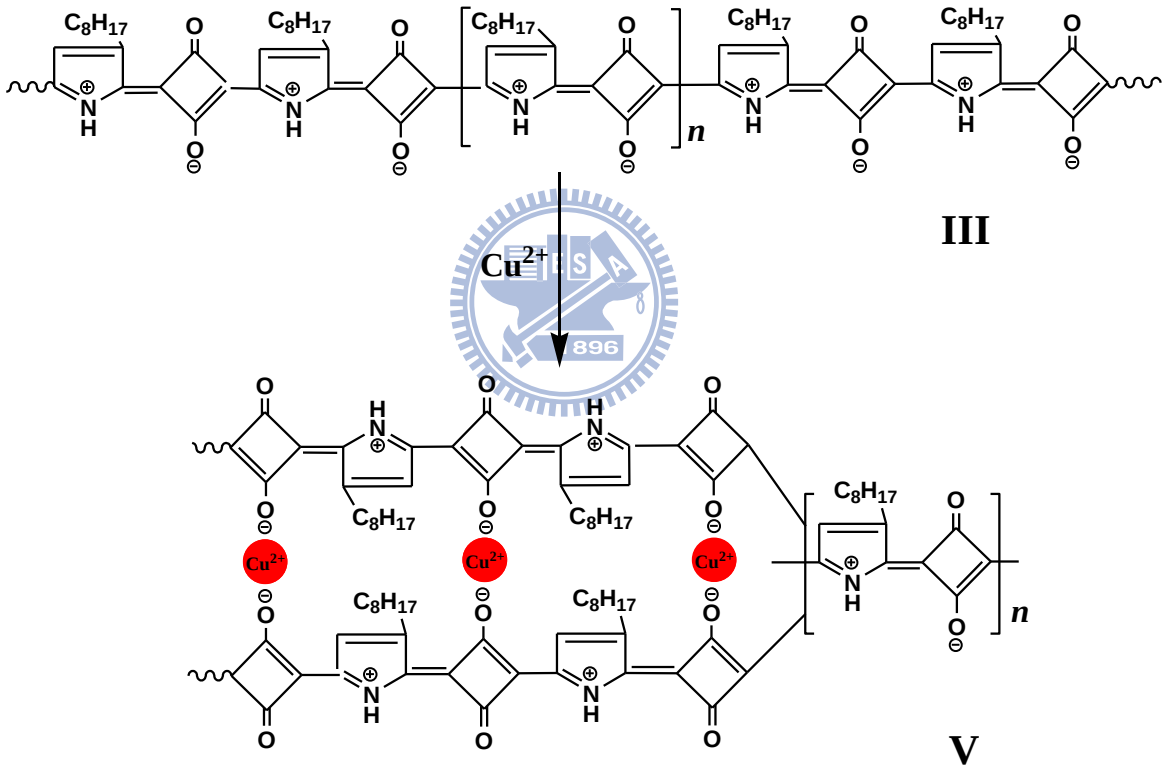

Scheme 3-4. Structural transformation of poly(3-octylpyrrole)squaraine induced by Cu^{2+} depicted in molecular structures.

To compare with other cations, we also added Na^{+}, Cs^{+}, Mg^{2+}, Ba^{2+} and Ca^{2+} into the trichloromethane solution containing the target polymer. In these experiments, there

was no spectral change on adding these metal cations except Ca^{2+}, Figure 3-16 shows temporal variation of the visible absorption spectrum of poly(3-octylpyrrole)squaraine in trichloromethane to which was added the Ca^{2+} in trichloromethane. The stature of the line at 543.6 nm decreased about 40 % after for 126 h and the intensity near 500 nm increased discernibly. In the case of Ca^{2+}, the isosbestic point is located about 525 nm, significantly distinct from that with Cu^{2+} at 531.2 nm.

As mentioned above, the zwitterionic polymers react with metal ions to form stable complexes, resulting in altered optical properties. The extension of the optical change depends not only on the metal ions but also on their solubilities in solvents; for example, the solubility of calcium perchlorate tetrahydrate might be less soluble than copper perchlorate hexahydrate in trichloromethane. This phenomenon of a color change for a polysquaraine induced by a metal ion implies a prospective practical technical application as a sensor.

Scrutiny of Figures 3-6 and 3-15 indicates that, although the spectral changes are similar, they are not the same. The wavelength of the line caused by the copper ion is 523.9 nm, whereas that influenced by the copper plate is 513.8 nm; the difference is about 10 nm. Moreover, the isosbestic point on adding the copper ion is at 531.2 nm, but that on inserting the copper plate is at 525.8 nm; the difference is about 5.4 nm. These discrepancies suffice to indicate that copper ion is not the factor driving the transformation of this zwitterionic polymer solution induced by metallic surfaces.

Copper is unlikely to dissolve into ionic from copper sheet in trichloromethane. Moreover, after dissolved cations cause a structural modification of this CP, it is difficult to remove those cations from the solution; for this reason the transformation is irreversible so that altered structure does not revert to the original conformation. In contrast, with the metal plates, simply withdrawing the plate from the solution of the polymer suffices to

initiate reversion of the polymer to its original form. These two structural transformations of this zwitterionic polymer differ intrinsically: with the metal plate in heterogeneous contact with the solution of the polymer, the phenomenon involving the structure of the polymer is reversible, whereas with metal ions homogeneously present in the solution phase the change is irreversible. According to this test, we exclude the possibility of a conformational change of this CP induced by a metal being due to a metal ion that is dissolved from the metal.

In addition, although this polysquaraine solution exhibited a similar variation of the conformation induced by both cations and some active metal plates, but this zwitterionic polymer folds its structure in two distinct ways. While the polysquaraine reacts with a cation and folds its structure, the negative charge of –O- binds to the cation; in this case, no OH group is be formed in the complex. The difference IR absorption spectrum of poly(3-octylpyrrole)squaraine with added Cu^{2+} cations in trichloromethane is shown in Figure 3-17; compared to Figure 3-13 (B), this IR absorption spectrum possessed no such OH band. The evidence from the IR spectra thus further confirms the distinct conformational changes of this polysquaraine sample induced by cations and by the surfaces of active metals.

An analogous argument of reversible and irreversible processes applies also to oxidation of the polymer from oxygen dissolved at the metal surfaces: a conformational change caused by such oxidation would be irreversible. Without adding a reductant, the oxidation product would not be reduced to its original form. The intrinsic irreversibility of an oxidation mechanism is inconsistent with the reversible observation and must be excluded.

3-3.9 Activation energies of isomerization

As mentioned above, the linear conformation of the target polymer is stable in solution; without perturbation, it does not transform spontaneously to the folded structure. The barrier for transformation from the linear zwitterionic polysquaraine to the folded conformer is large in the free solution. Induced by active metals, this CP performs the folding isomerization in solution, in which an active metal behaves as a catalyst for the conformational transformation.

With the copper catalyst, the activation energy of the structural change from the linear to the folded conformer for poly(3-octylpyrrole)squaraine is decreased to (18.9±0.7) kJ mol^{-1}; the value is sufficiently small that isomerization proceeds near 295 K, but the folded conformer of poly(3-octylpyrrole)squaraine is unstable in the free solution and eventually opens its conformation; the activation energy of this structural opening for poly(3-octylpyrrole)squaraine is (38±6) kJ mol^{-1}.

According to our proposed model, these activation energies are associated with intramolecular hydrogen bonds N—H---O. The typical bond strength of an intra-hydrogen bond N—H---O is about 8 kJ mol^{-1} [112-115]. By comparison with the activation energy of the unfolding, perhaps five hydrogen bonds N—H---O are formed in the folded conformer.

3-3.10 Photoluminescent spectra of linear and folded conformers

The conformation of the zwitterionic polysquaraine is thus reversible, back and forth, depending on the presence or absence of an active metal. We thus reversibly control the conformation of this CP with this simple heterogeneous process without altering the

chemical environment in solution, whereas adding metal ions to the polymer solution causes an irreversible change of the chemical environment and the structure for this CP.

The isomerization of this polysquaraine induced with a metal surface modified the optical properties, not only the visible absorption spectra described above but also the emission spectra. Figure 3-18 displays photoluminescent spectra (PL) of this polymer in trichloromethane; the emission maximum shifted from 562 nm to 557 nm accompanying the conformational change induced with the copper plate.

The quantum yield of this polysquaraine with the linear structural conformation reduced to 47% as that of folded one. Regarding the PL yields for comparison, we used 2,3-benzanthracene as an external standard under the same optical conditions. Based on the PL intensity of 2,3-benzanthracene at 478 nm, in Figure 3-19, the relative quantum yields of the linear and folded target polymers are 2.23 and 1.07, respectively.

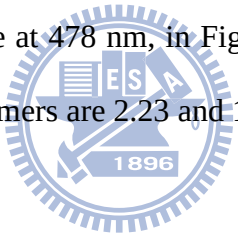

3-3.11 Conductivity of linear and folded conformers

The optical, physical and electronic properties affected by a variation of the polymer conformation are quite interesting for applications. For example, the conductivities of altered conformational structures for target polymer in solution might be different.

Figure 3-20 displays the impedance plots of linear and folded conformers of this CP. The conductivity σ of the polymer in solution was calculated from the measured resistance (R_p), the area (S 1.227 cm^2) and length (L 0.44 cm) of the liquid cell using the equation $\sigma = L/SR_p$; in which, the R_p of the polymer solution was determined from the intercept of the line of the impedance curve at the high frequency end. By this means, the conductivities of

the linear and folded conformers were obtained to be 3.27×10^{-7} and 1.56×10^{-7} s/cm, respectively; the value of the linear conformer is twice to that of the folded one.

3-3.12 Manipulation of the durations of forward and reverse isomerizations

The observation of this reversible structural modification accompanying the optical alterations for the zwitterionic polysquaraine induced by active metal surface is unprecedented; it represents a new chemical and physical process. This optical-switching property of a CP induced by active metals has prospective applications. Our findings provide an impetus for the investigation of the structural modification of similar CP and the structural dynamics of their polymer chains in solution.

If the response periods of the transformations can be further decreased with improved technique, an optical switch might be achievable in the liquid state. The durations of forward and reverse reactions for this isomerization might be subject to manipulation.

As shown in Figure 3-6, the forward isomerization of the target polymer in trichloromethane was completed longer than 40 h by inserted a copper plate (surface area 382 mm^2) at 295 K. For the forward transformation, increasing the surface area of metal and temperature decreases the duration of reaction. By increasing the surface area, we thus can reduce the forward reaction time. Figure 3-21 shows that the forward isomerization completed in 6 h with surface area 1720 mm^2 of copper plates at 296 K.

The reaction time of forward isomerization could even be reduced by using gauzes. For example, with Cu gauze (100 mesh, diameter 0.11 mm and mass 2.133 g) in a cell of liquid volume 3 mL and optical path of length 1.0 cm, the change was completed in 60 min

at 296 K, as displayed in Figure 3-22. Increasing the temperature could reduce the forward time further, with the same Cu gauze (100 mesh, diameter 0.11 mm and mass 2.133 g) in a cell of liquid volume 3 mL, the change was completed in less than 30 min at 323 K.

For the reverse transformation in the free solution, increasing the temperature decreases the duration of unfolding. As shown in Figure 3-9, the backward isomerization time was over 22 h at 323 K. Thus, the reverse transformation in the free solution is slow. Strikingly, ultrasonic agitation to perturb the folded polymer solution also decreases the duration profoundly: we found that only 25 min was required to accomplish the reversal with ultrasonic agitation, as shown in Figure 3-23.

We believe the response periods of the transformations might be further decreased with improved technique. This reversible behavior accompanying color changes hence endows materials of this type with a great prospective capability for display applications or information storage, and might lead to the development of other significant applications. For example, by means of this mechanism, an optical switch might be achievable in the liquid state.

This reversible phenomenon encourages the discovery of further knowledge about the interactions of polymers with metallic surfaces, and about the dynamics and energetics of conformational changes of polymers. We expect our findings to motivate the investigation of conformational modifications of other CP and applications of this phenomenon. Applying these polymer solutions onto substrates might enable these CP to retain their specific structures in the solid after removal of solvent. The properties and applications of these switchable films or materials remain uncharted territory. These CP might be developed as shape-memory polymers [116-118]. Further work is required.

3-4 Summary

Visible and infrared absorption spectra and small-angle X-ray scattering curves of poly(3-octylpyrrole)squaraine, having a zwitterionic repeating unit, in trichloromethane solution altered on contact of the solution with the surface of an active metal. These observed spectral variations are deduced to indicate that the conformation of this CP becomes modified on contact with an active metallic surface.

Spectral evidence unambiguously confirms the reversible isomerization of poly(3-octylpyrrole)squaraine induced by an active metallic surface; the structure of this polysquaraine might be switchable from a linear conformer to a folded one back and forth depending on the presence or absence of an active metal. Induced by the copper surface, the activation energy of the forward isomerization is (18.9±0.7) kJ mol^{-1}, whereas the activation energy of the reverse process to regenerate the linear conformer is (38±6) kJ mol^{-1}; this result might indicate that about five intramolecular hydrogen bonds form in the folded conformer of poly(3-octylpyrrole)squaraine.

Observation of the reversibility of the postulated change of conformation associated with a metallic surface for this zwitterionic polymer provides an impetus to investigate both this structural modification of other CP and applications of this phenomenon.

3-5 Figures and Tables

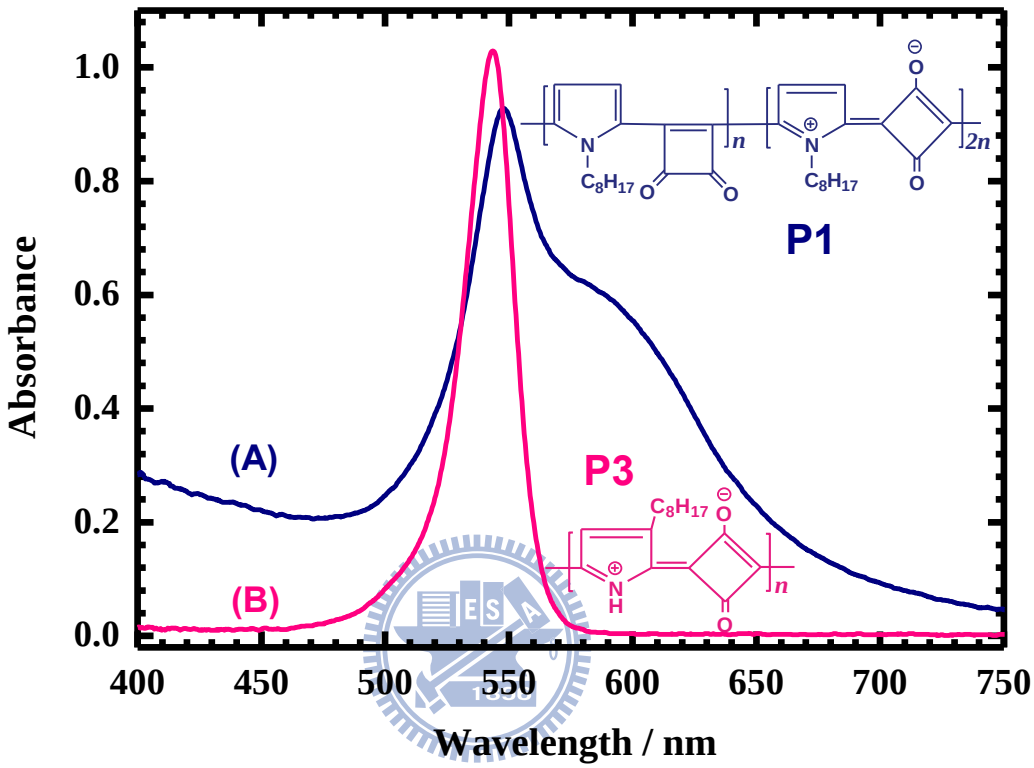

Figure 3-1. Visible absorption spectra of poly(pyrrolyl)squaraines in trichloromethane solution (concentration 3.5 mg/L) and a silica cell (length 1 cm of optical path) at 295 K: (A) poly(1-octylpyrrolyl)squaraine (**P1**); (B) poly(3-octylpyrrolyl)squaraine (**P3**). The insets show the molecular structures of **P1** and **P3**; **P1** consists of repeating units of covalent and zwitterionic structural backbone in a ratio 1:2, whereas **P3** possesses mostly zwitterionic repeating units (>97 %).

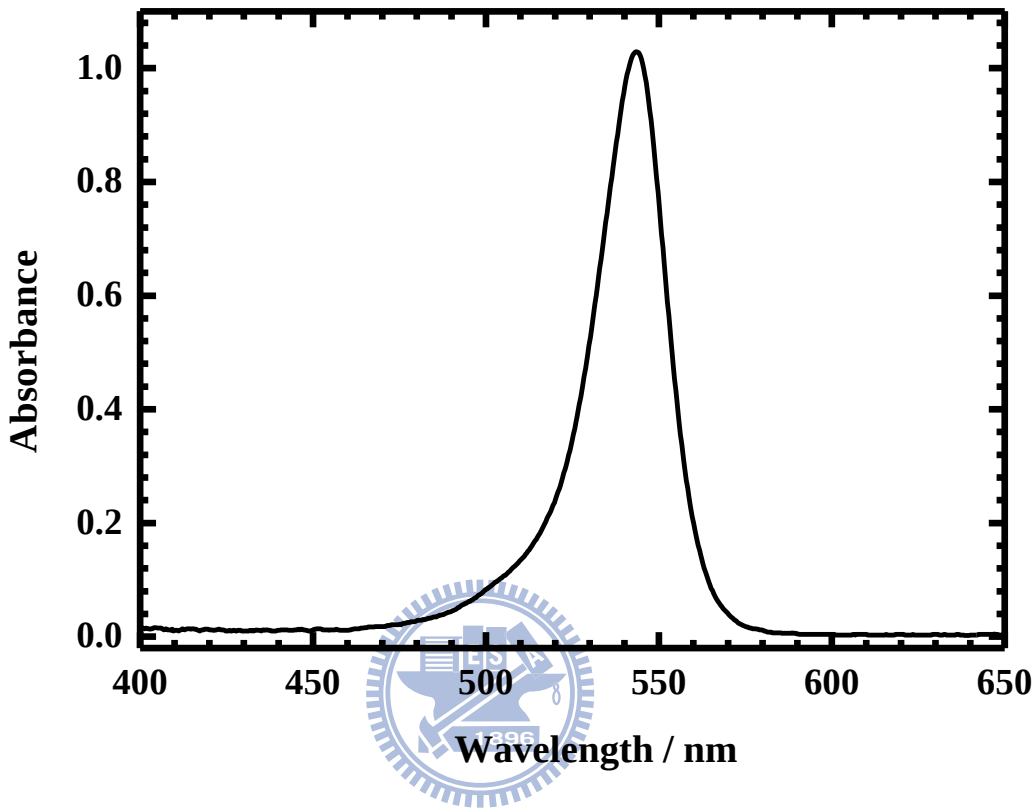

Figure 3-2. Visible absorption spectrum of poly(3-pyrrolyl)squaraines in trichloromethane solution (concentration 3.5 mg/L) and a silica cell (length 1 cm of optical path) at 295 K has no change inserted with metals Al, Co, Ni, Mo, Pd, Sn, Ta, W, Re, Au and stainless steel.

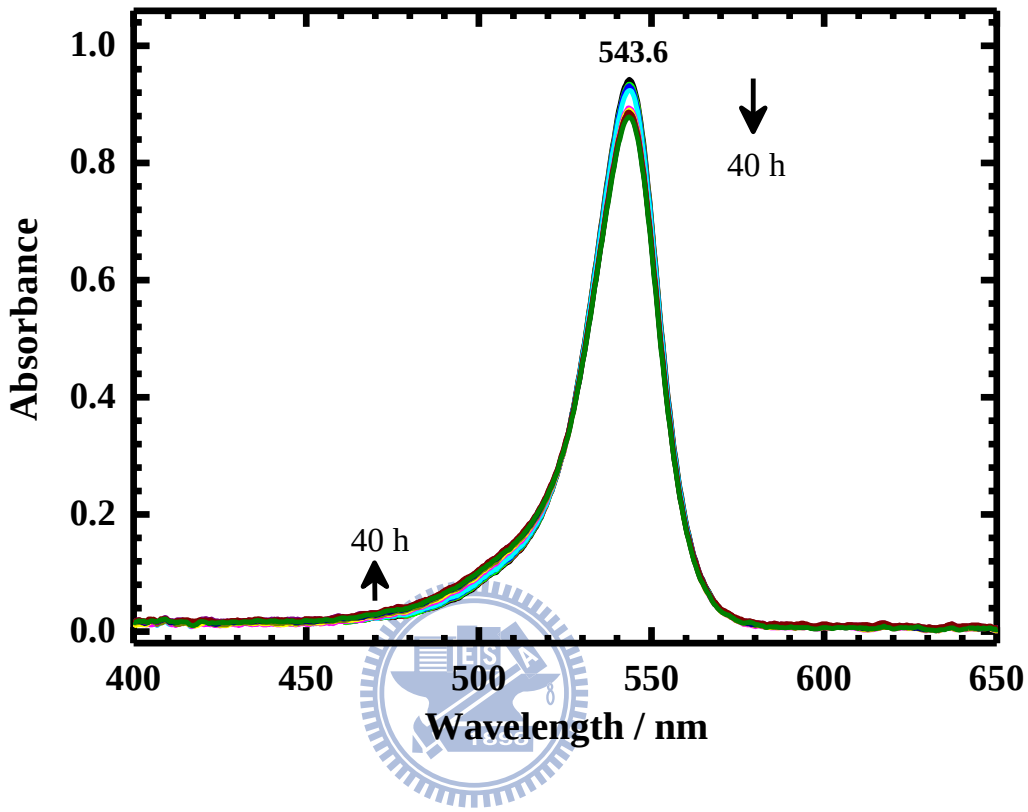

Figure 3-3. Temporal variation over 40 h of visible absorption spectra of poly(3-octylpyrrole)squaraine (3.5 mg/L) in trichloromethane solution (3.0 mL) in a silica cell (optical path 1 cm) into which was inserted a Ag plate (surface area 907 mm^2) at 295 K.

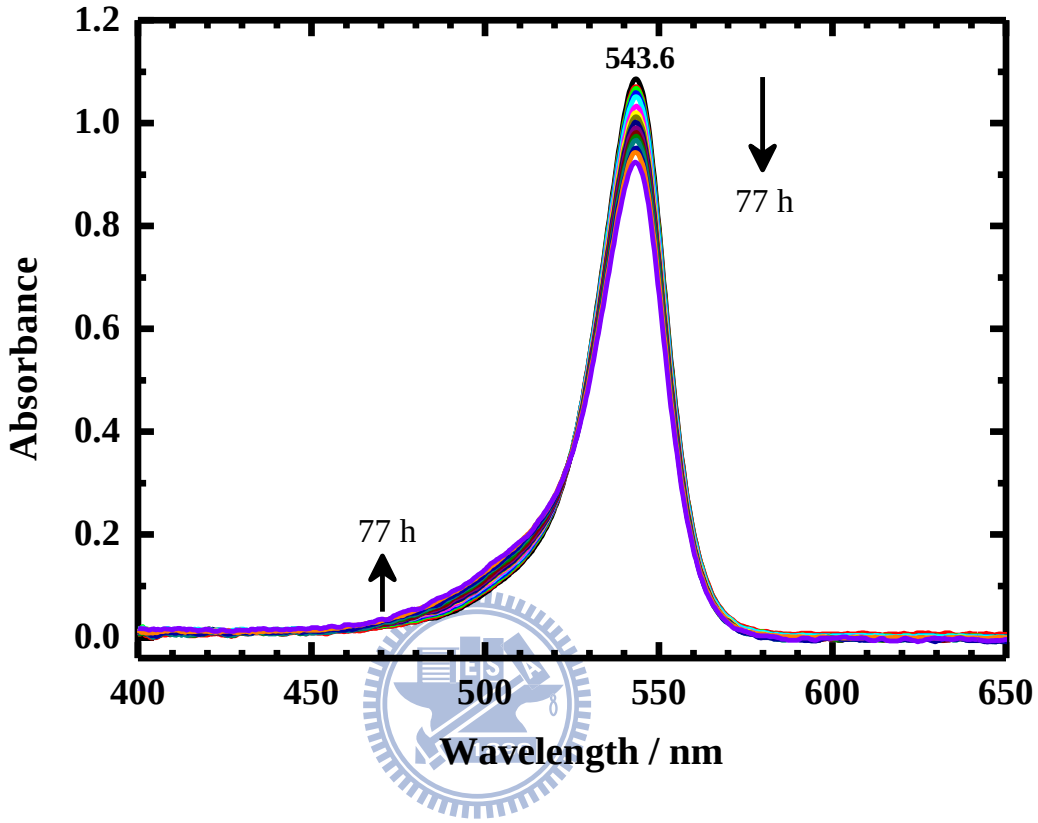

Figure 3-4. Temporal variation over 77 h of visible absorption spectra of poly(3-octylpyrrole)squaraine (3.5 mg/L) in trichloromethane solution (3.0 mL) in a silica cell (optical path 1 cm) into which was inserted a Rh plate (surface area 372 mm^2) at 295 K.

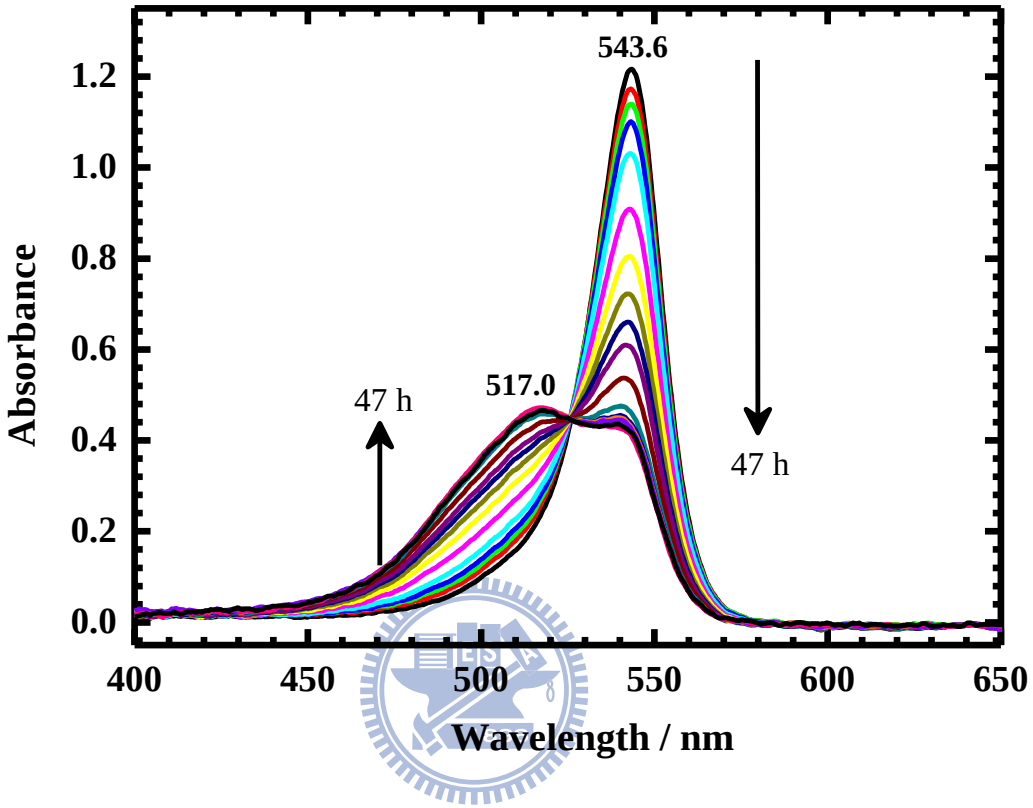

Figure 3-5. Temporal variation over 47 h of visible absorption spectra of poly(3-octylpyrrole)squaraine (3.5 mg/L) in trichloromethane solution (3.0 mL) in a silica cell (optical path 1 cm) into which was inserted Fe plates (surface area 1720 mm^2) at 295 K.

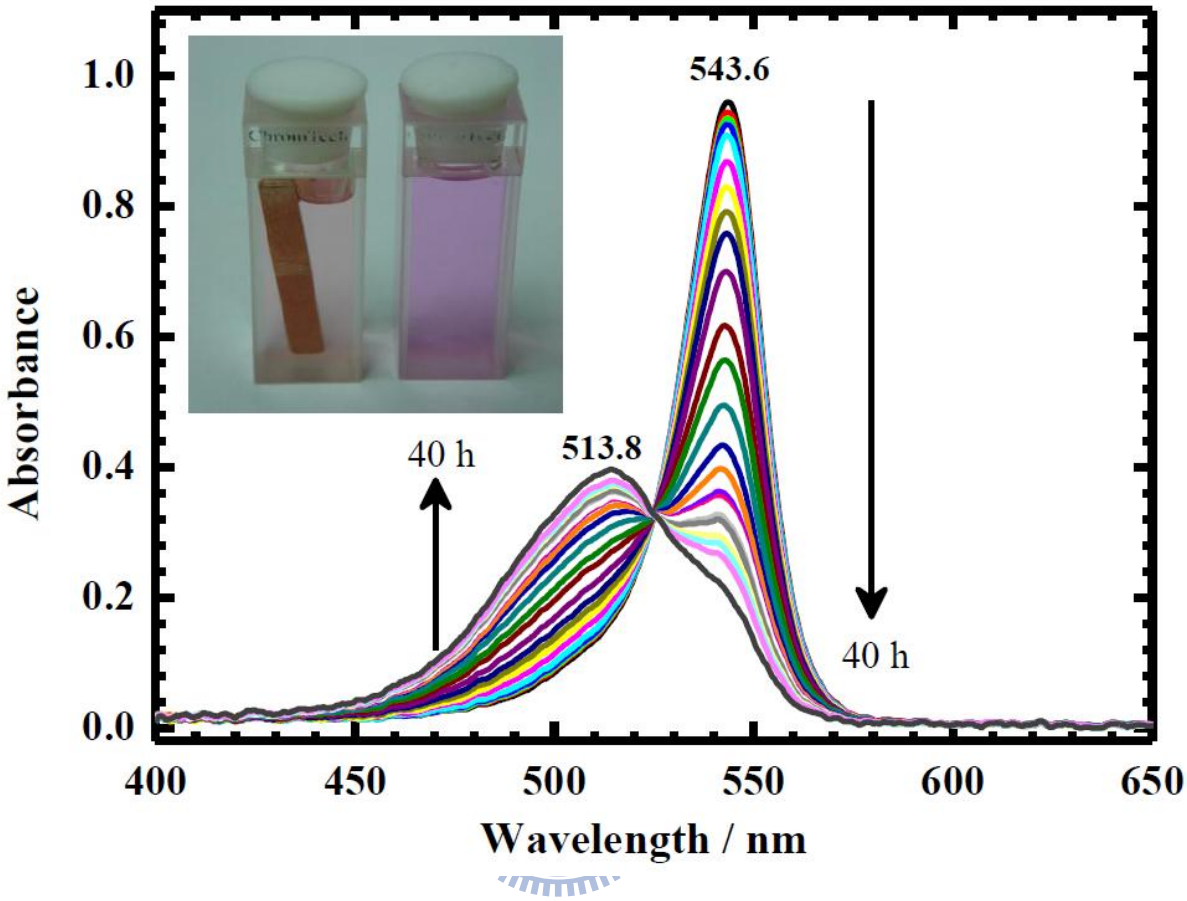

Figure 3-6. Temporal variation over 40 h of absorption spectra of poly(3-octylpyrrole)squaraine (3.5 mg/L) in trichloromethane solution (3.0 mL) in a silica cell (optical path 1 cm) into which was inserted a copper plate (surface area 382 mm^2) at 295 K. Inset photograph: visible color change of poly(3-octylpyrrole)squaraine in trichloromethane solution: (right side) no metal plate, (left side) after 40 h with a Cu plate.

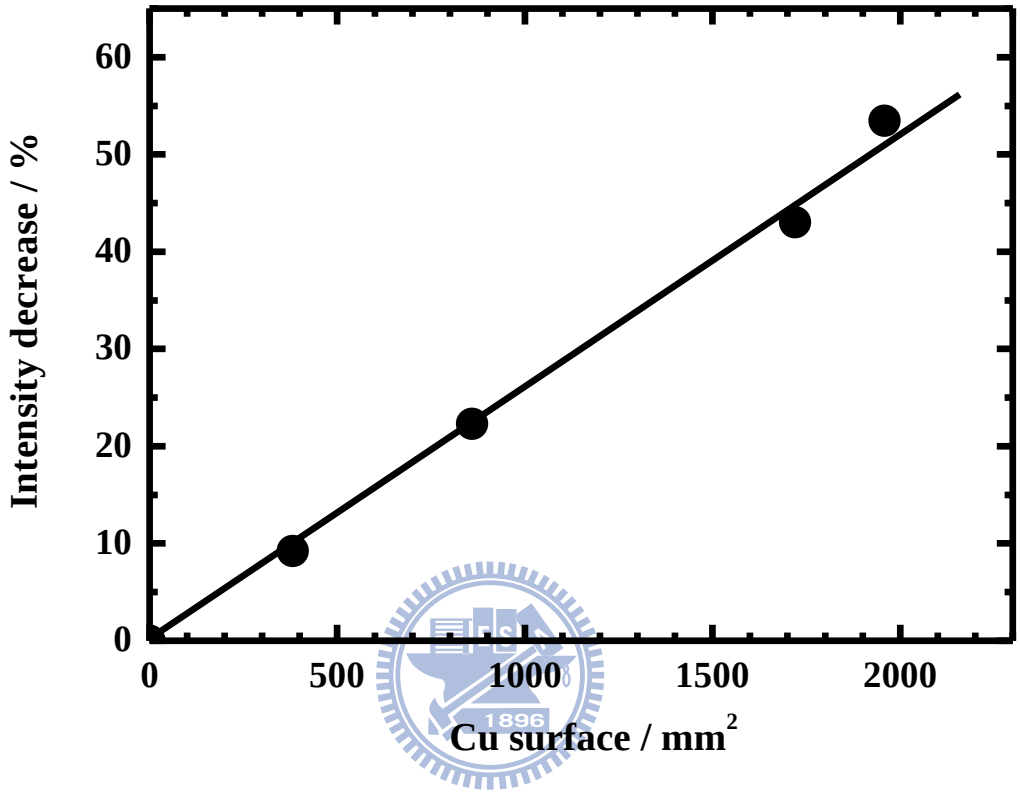

Figure 3-7. For poly(3-octylpyrrole)squaraine in trichloromethane solution, the decrease of absorbance at 543.6 nm in 1 h vs. area of copper surface at 295 K.

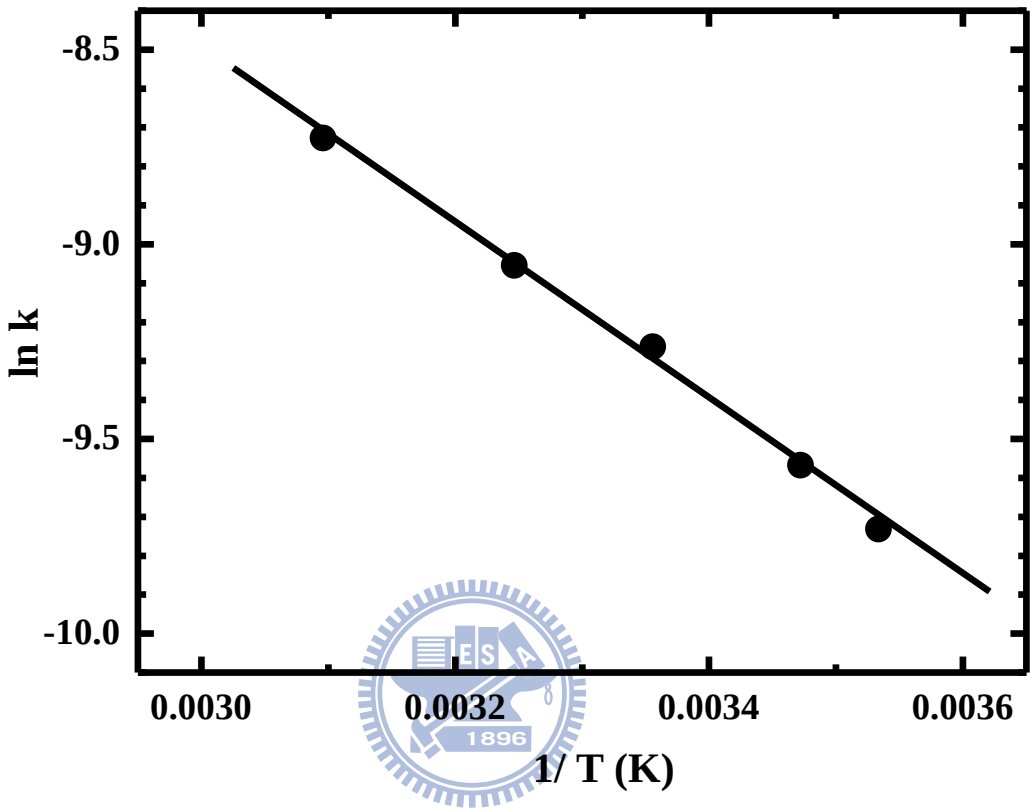

Figure 3-8. Absorbance decrease at 543.6 nm in 1 h vs. temperature; copper plates (surface area 1720 mm^2) were inserted into trichloromethane solutions of poly(3-octylpyrrole)squaraine.

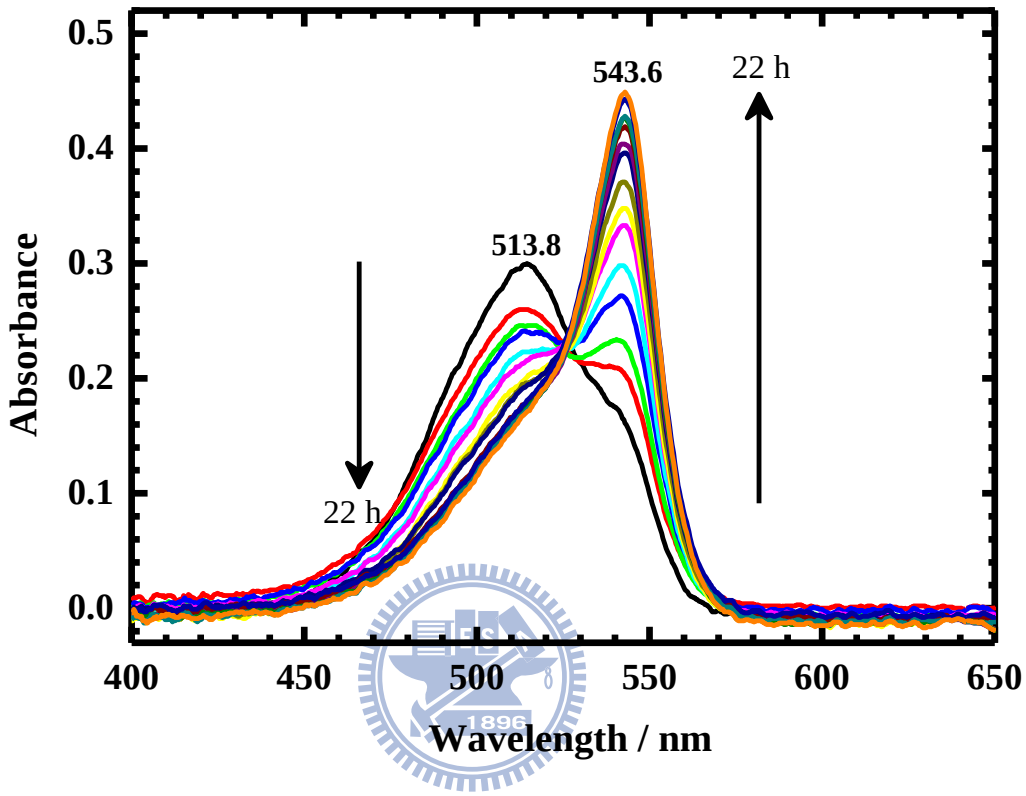

Figure 3-9. Temporal variation of absorption spectra of poly(3-octylpyrrole)squaraine in trichloromethane at 323 K after removal of the copper plate following its insertion for 11 h: scans were made at hourly intervals from 0 to 12 h, then at 15, 19 and 22 h.

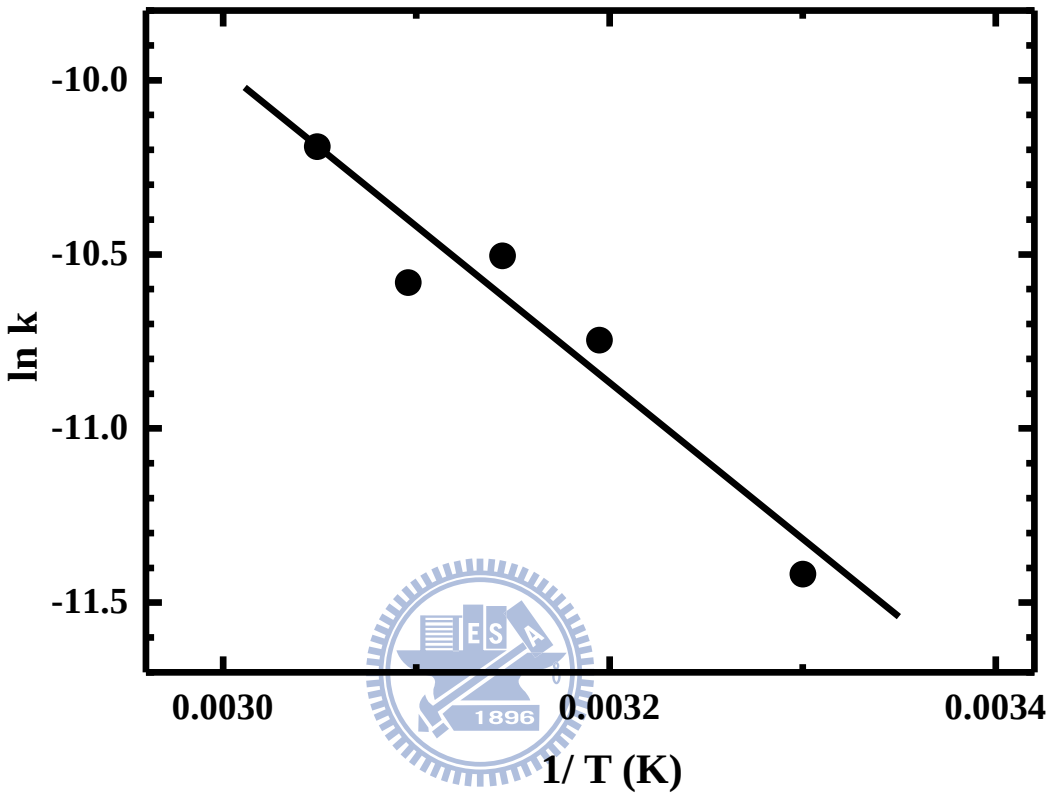

Figure 3-10. Absorbance decrease at 513.8 nm in 1 h vs. temperature after removal of inserted copper plates from **P3** solutions.

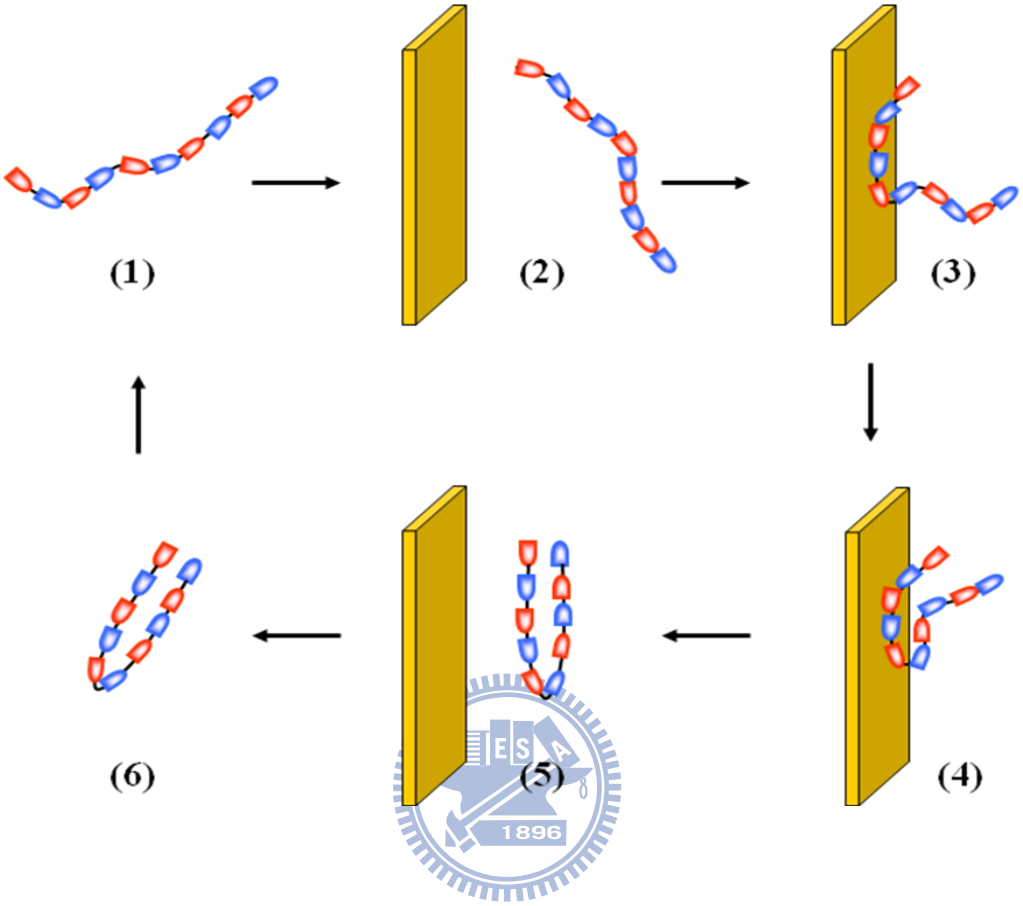

Figure 3-11. Schematic illustration of the isomerization of a zwitterionic polymer induced with a plate of an active metal; the colored segments represent separate charged moieties of the polymer.

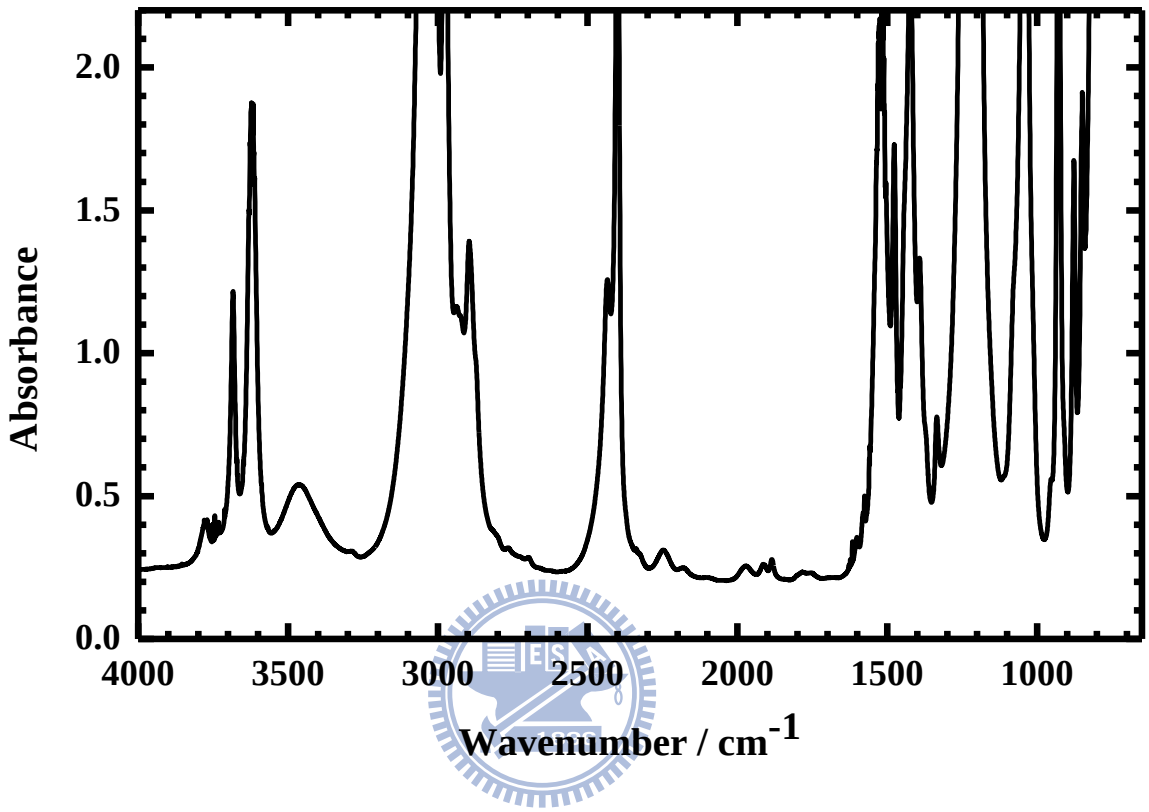

Figure 3-12. IR absorption spectrum of trichloromethane with optical path 1 mm.

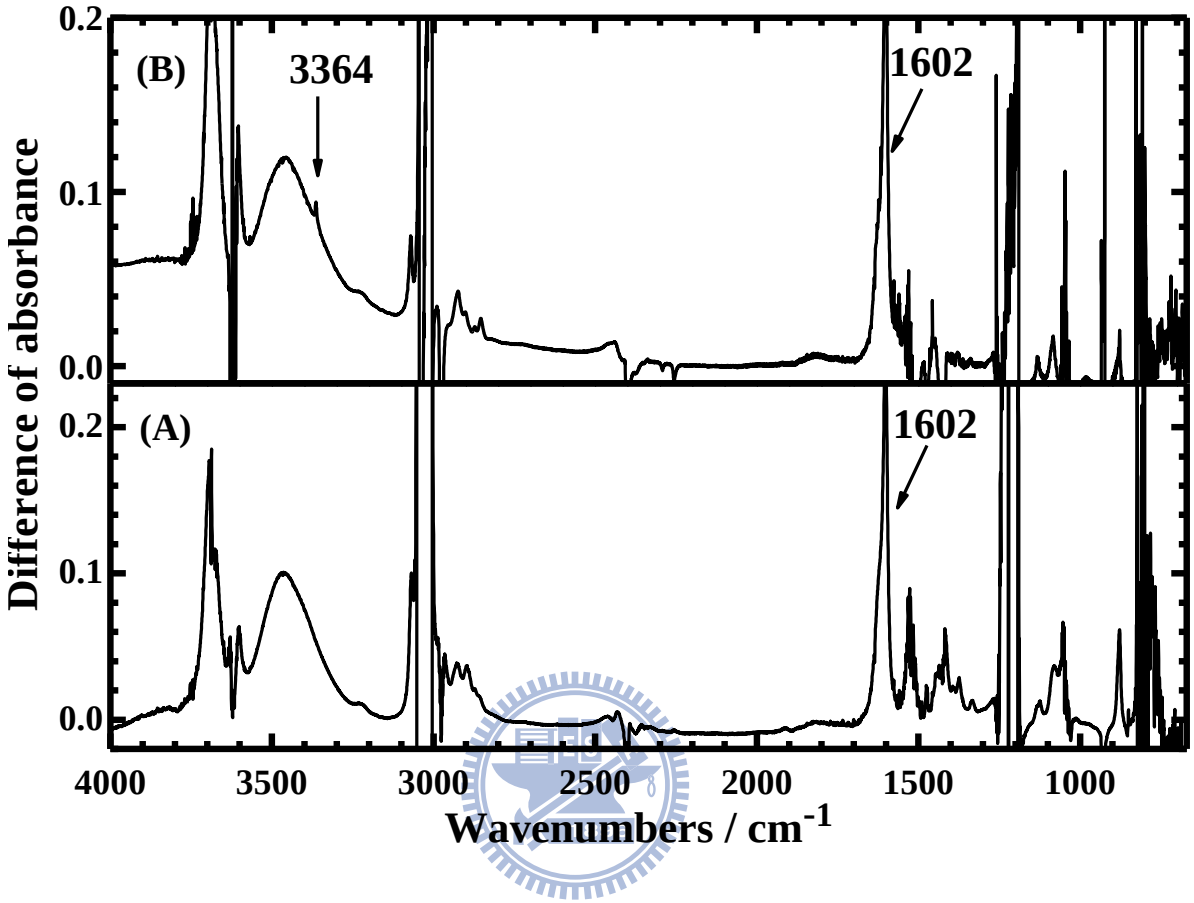

Figure 3-13. Difference IR absorption spectra in trichloromethane solution with optical path 1 mm relative to pure solvent: (A) poly(3-octylpyrrole)squaraine in trichloromethane solution, (B) the same solution into which a Cu plate is inserted.

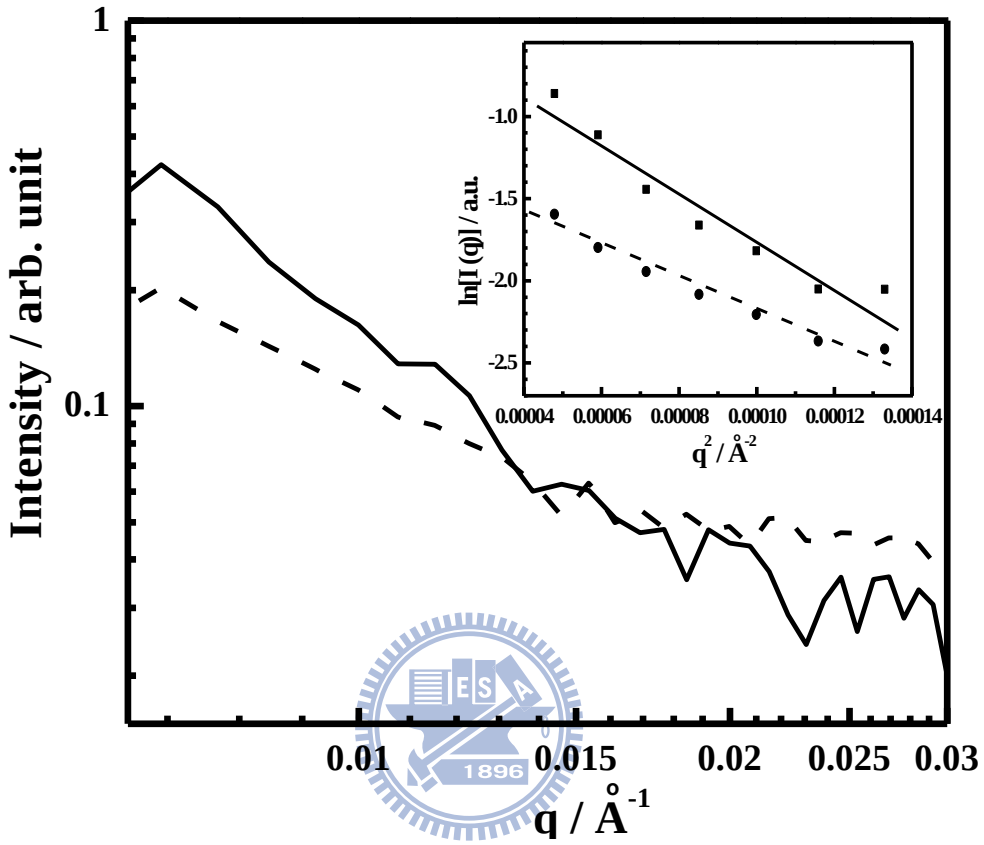

Figure 3-14. SAXS profiles of poly(3-octylpyrrole)squaraine in trichloromethane solution in a copper cell at initial (solid line) and final (dotted line) stages. The inset depicts relations of ln I(q) versus q^2 for small q at initial (solid line) and final (dotted line) stages.

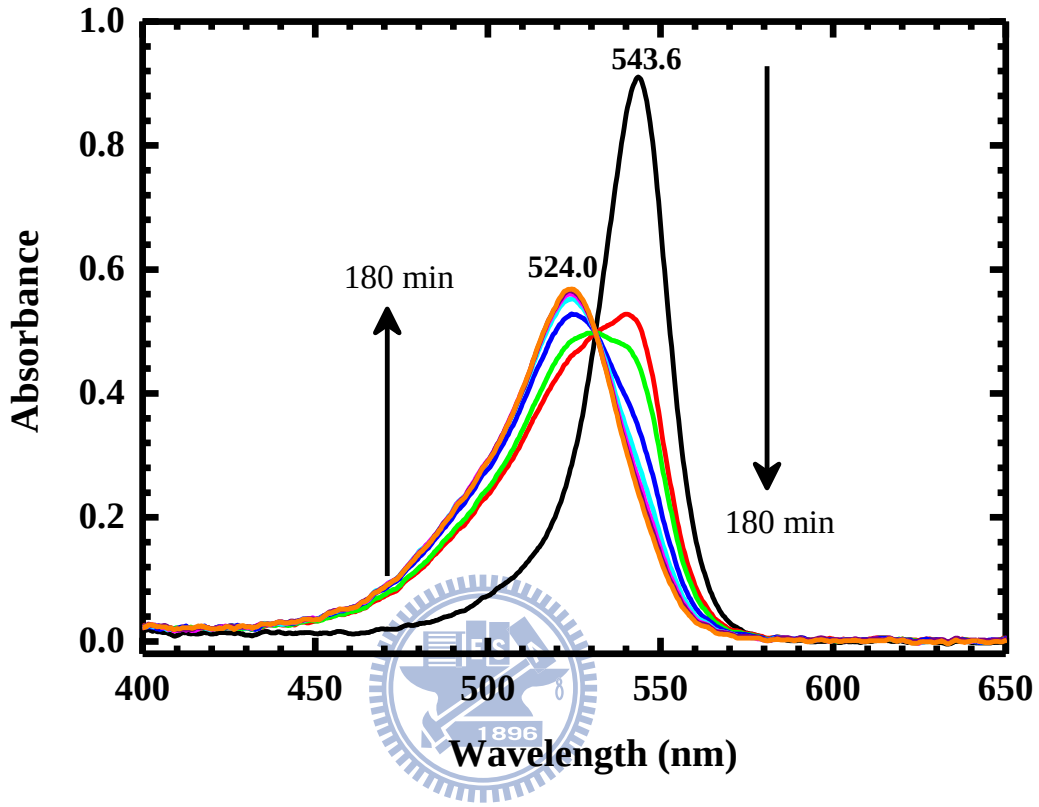

Figure 3-15. Temporal variation of visible absorption spectra of poly(3-octylpyrrole)squaraine in trichloromethane (3 mL) in a quartz cell (length 1 cm of optical path) to which was added a saturated solution (10 μL) of Cu^{2+} in trichloromethane: before addition (black curve), and after 2, 5, 10, 30, 60, 120, 180 (orange curve) min. For this reaction we prepared a saturated solution of Cu^{2+} in trichloromethane over $Cu(ClO_4)_2 \cdot 6H_2O$.

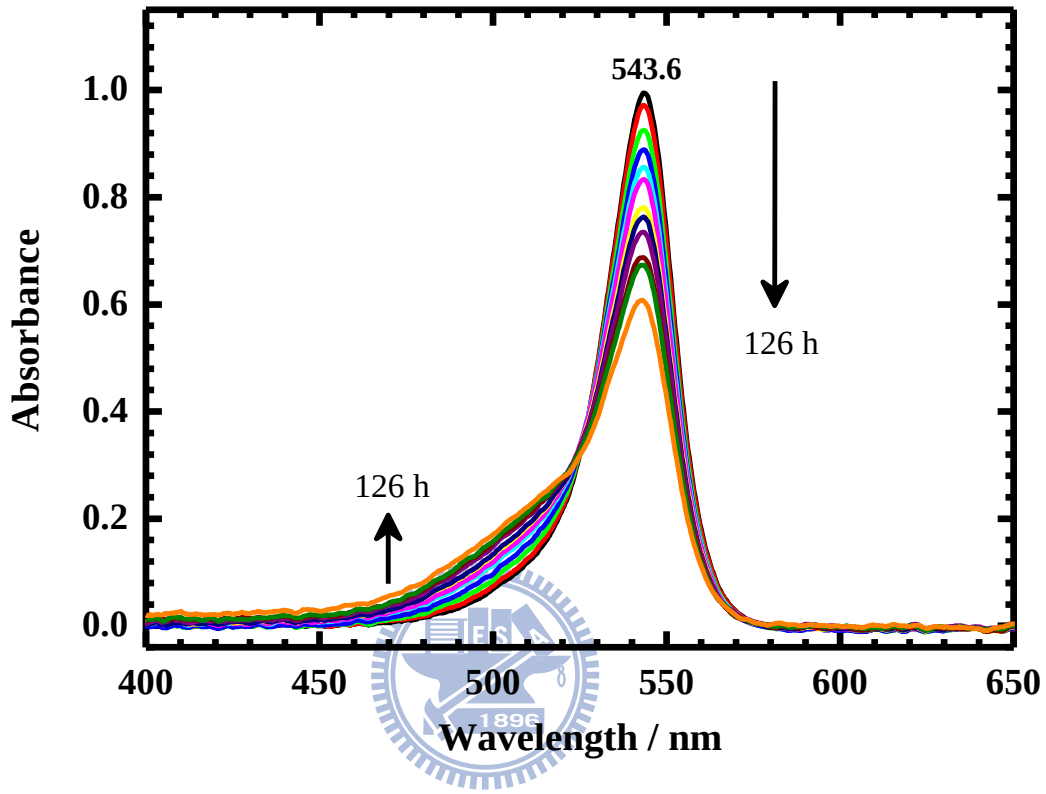

Figure 3-16. Temporal variation of visible absorption spectra of poly(3-octylpyrrole)squaraine in trichloromethane (3 mL) in a quartz cell (length 1 cm of optical path) to which was added a saturated solution (10 μL) of Ca^{2+} in trichloromethane: before addition (black curve), and after 0.5, 1, 2, 3, 7, 10, 19, 33, 46, 126 (blue curve) h. For this reaction we prepared a saturated solution of Ca^{2+} in trichloromethane over $Ca(ClO_4)_2 \cdot 4H_2O$.

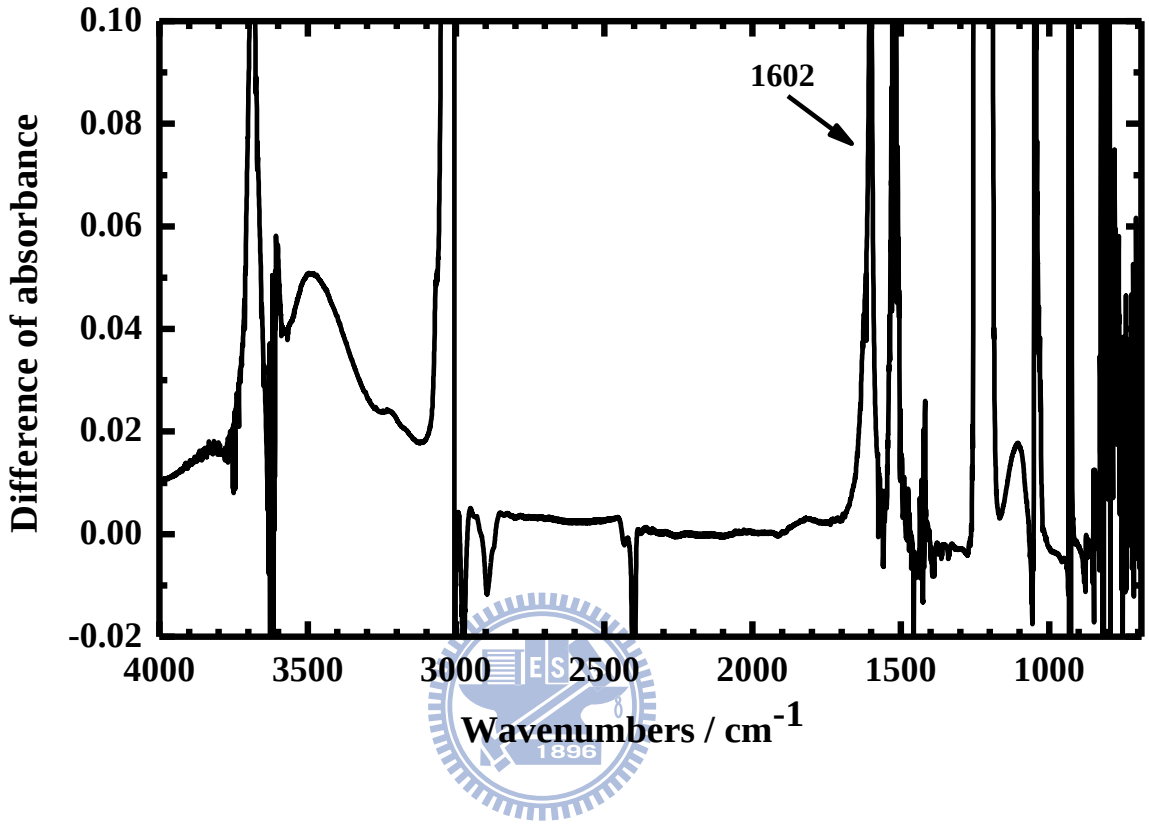

Figure 3-17. Differen Difference IR absorption spectrum of poly(3-octylpyrrole)squaraine in trichloromethane (optical path 1 mm) to which was added Cu^{2+} in solution.

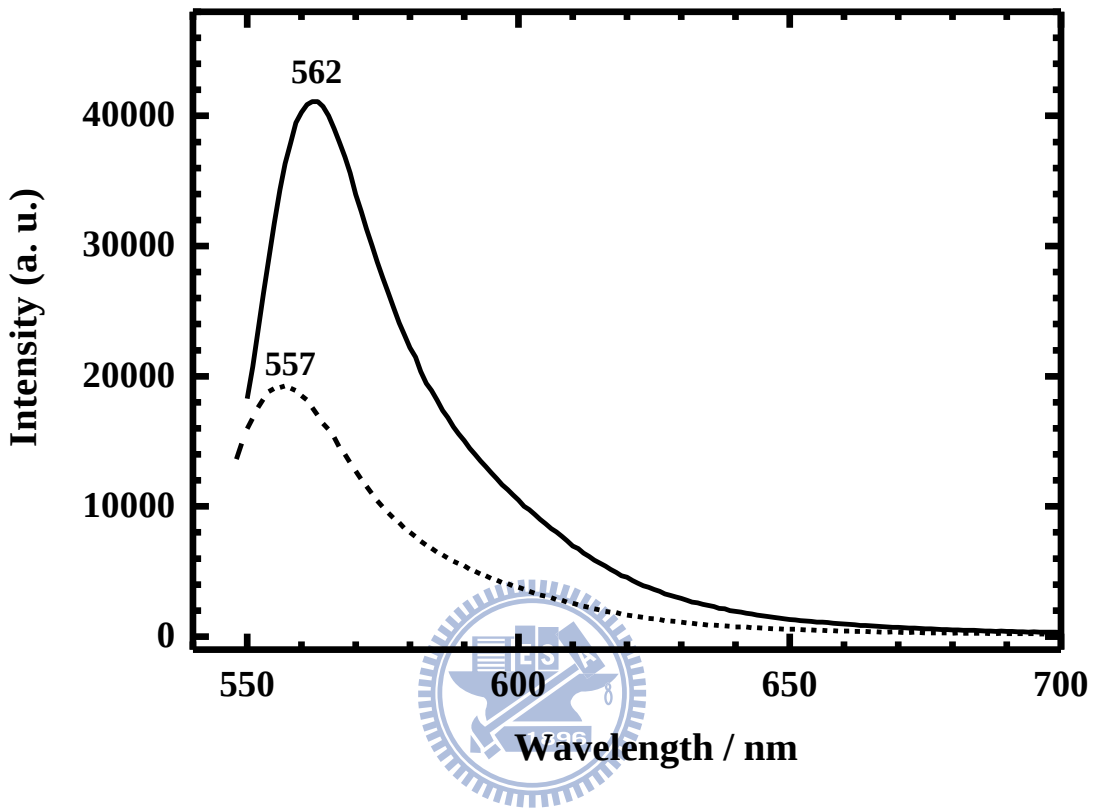

Figure 3-18. Photoluminescent spectra of poly(3-octylpyrrole)squaraine in trichloromethane solution: (solid line) no metal plate, (dashed line) with a Cu plate.

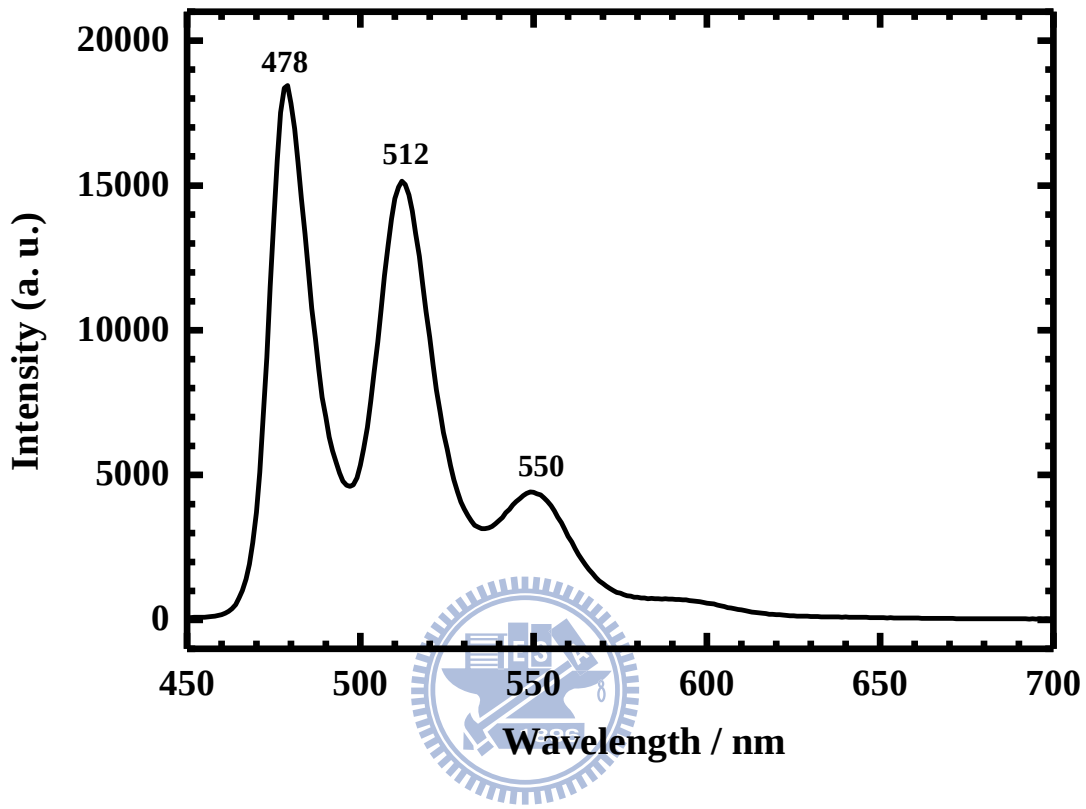

Figure 3-19. Photoluminescent spectrum of 2,3-benzanthracene under the same optical conditions; the spectrum was used as an external standard.

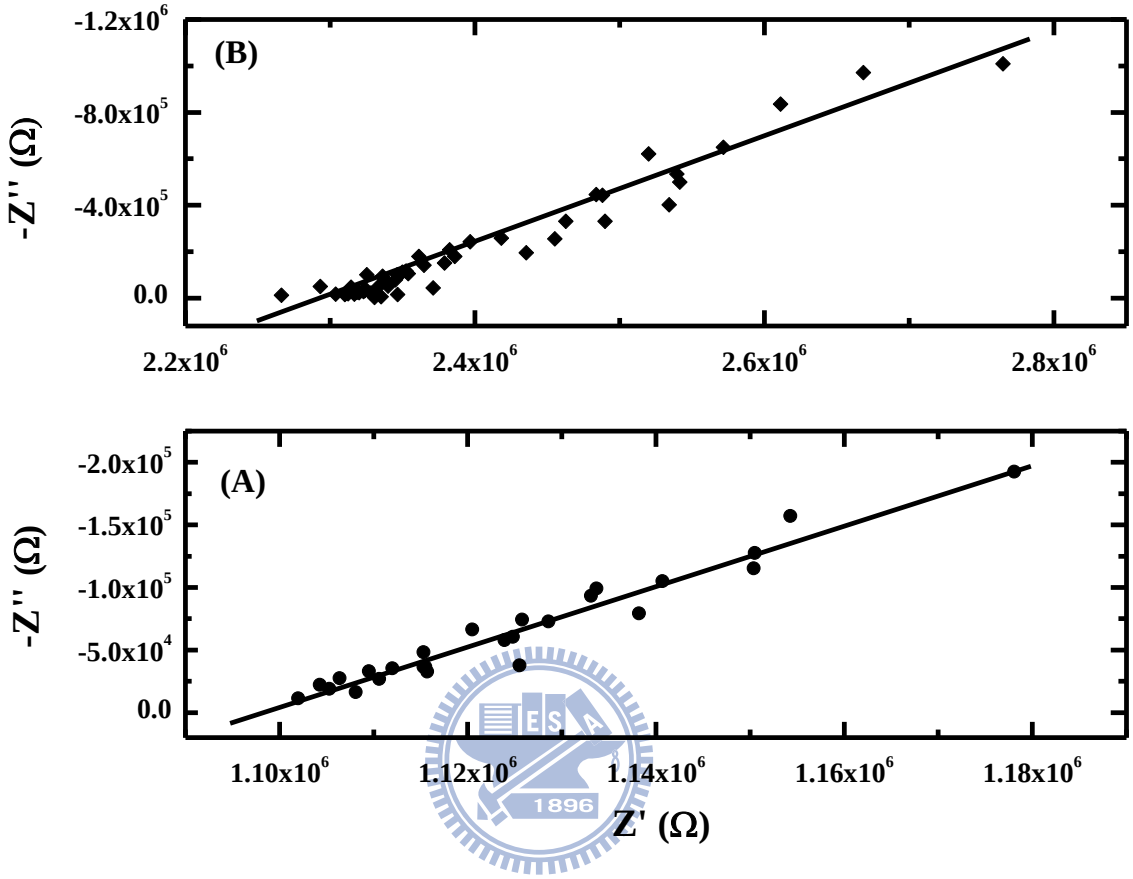

Figure 3-20. Impedance plots of poly(3-octylpyrrole)squaraine (3.5 mg/L) in solution: (A) the linear conformer and (B) the folded conformer.

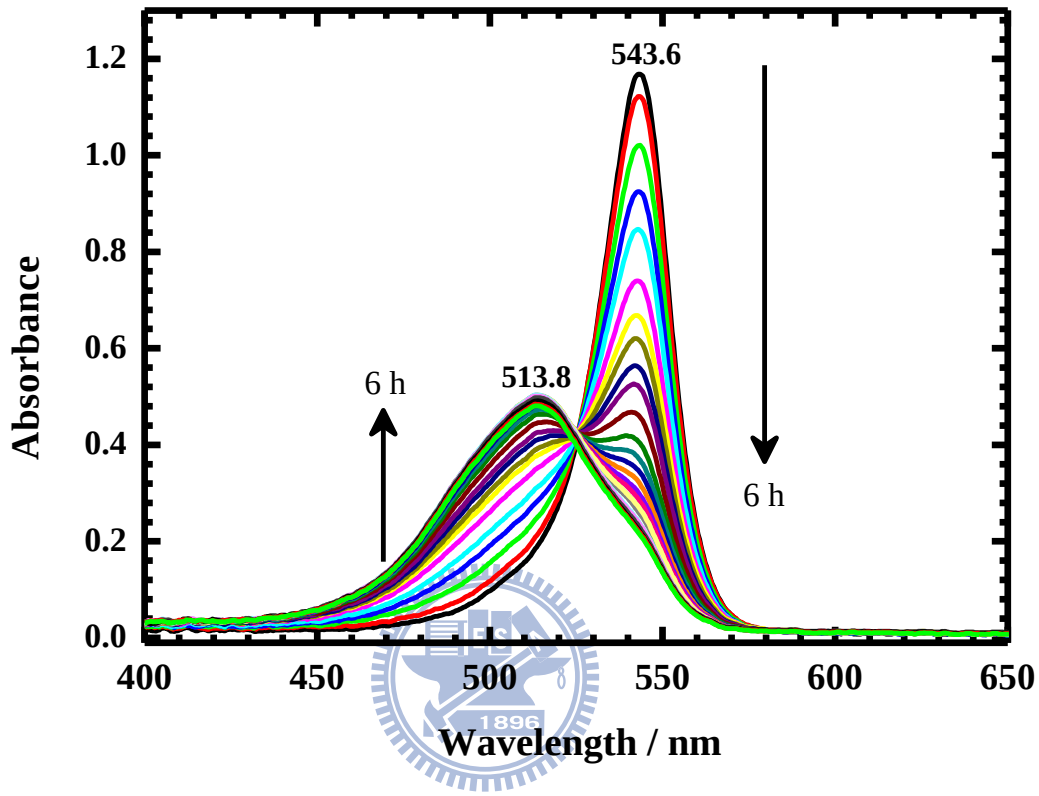

Figure 3-21. Temporal variation of the visible absorption spectra of poly(3-octylpyrrole)squaraine (3.5 mg/L) in trichloromethane solution (3.0 mL) in a silica cell (optical path 1 cm) into which was inserted a copper plate (surface area 1720 mm^2) at 296 K: before addition (black curve) and 6 h after addition (green curve).

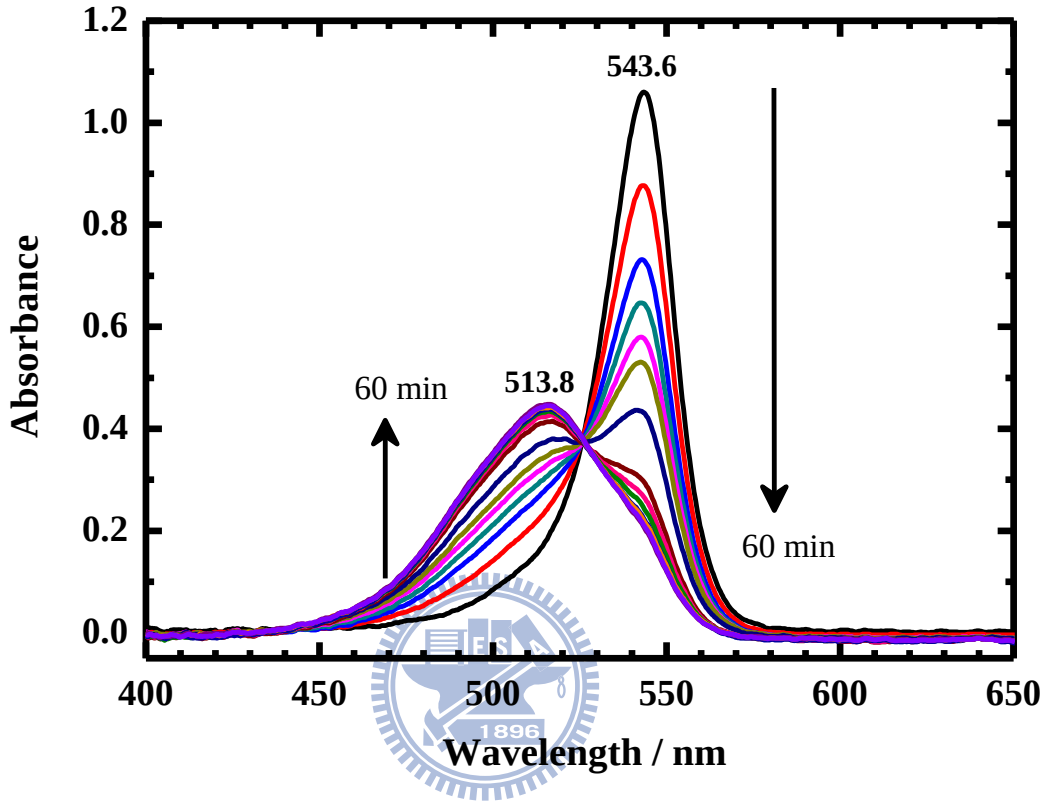

Figure 3-22. Temporal variation of the visible absorption spectrum of poly(3-octylpyrrole)squaraine in trichloromethane solution (conc. 3.5 mg/L) in a silica cell (optical path 1 cm) into which was inserted copper gauze was added to the solution at 296 K: before addition (black curve) and 60 min after addition (purple curve).

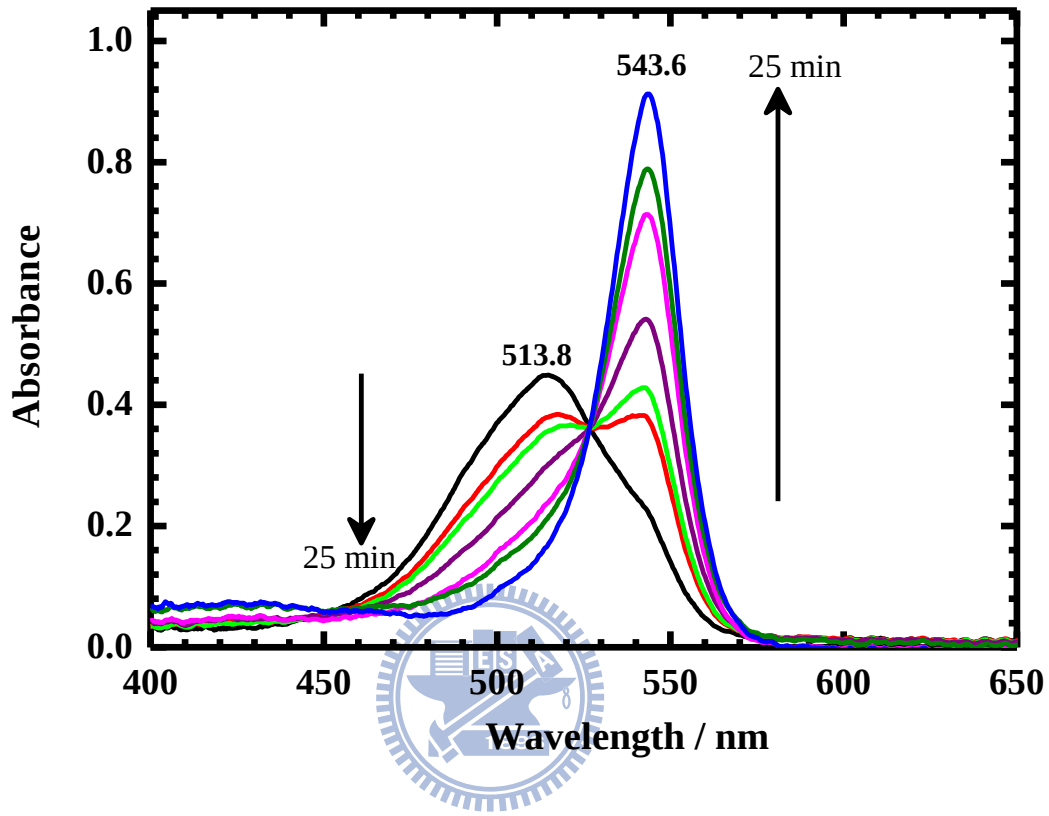

Figure 3-23. Temporal variation of the visible absorption spectrum of poly(3-octylpyrrole)squaraine in trichloromethane (conc. 3.5 mg/L) in a silica cell (optical path 1 cm) after removal of copper plates following ultrasonic agitation (40 kHz, 25 min): before agitation (black curve) and after agitation (blue curve).

Table 3-1. Relative rates of isomerization caused by active metals based on the decrease of absorption at 543.6 nm during 1 h.

Metal	Area / mm^2	Decrease / %	Relative rate[a]
Cu	860	22.3	1
Fe	593.2	5.66	0.37
Rh	371.6	2.05	0.21
Ag	907	2.0	0.09
Pt	545.7	1.1	0.08
Zn	430.6	0.57	0.06
Pb	381	0.3	0.03

[a]Relative rate is derived from the decrease of absorption and normalized with surface area.

3-6 Supporting Information

3-6.1 The beam line 23A of small and wide angle X-ray scattering (SWAXS) at NSRRC

Since May 2009, a dedicated small/wide angle X-ray scattering (SWAXS) end-station located at the BL23A beamline has been opened to all NSRRC users. The SWAXS instrument aims for structural characterization of air-liquid interfaces, thin films, and solution and bulk specimens, covering the length scale from ~0.1 nm to ~300 nm and the research fields in soft matter, nanomaterials, and alloy.

The optical layout of the beamline is shown in Figure 3-S1.

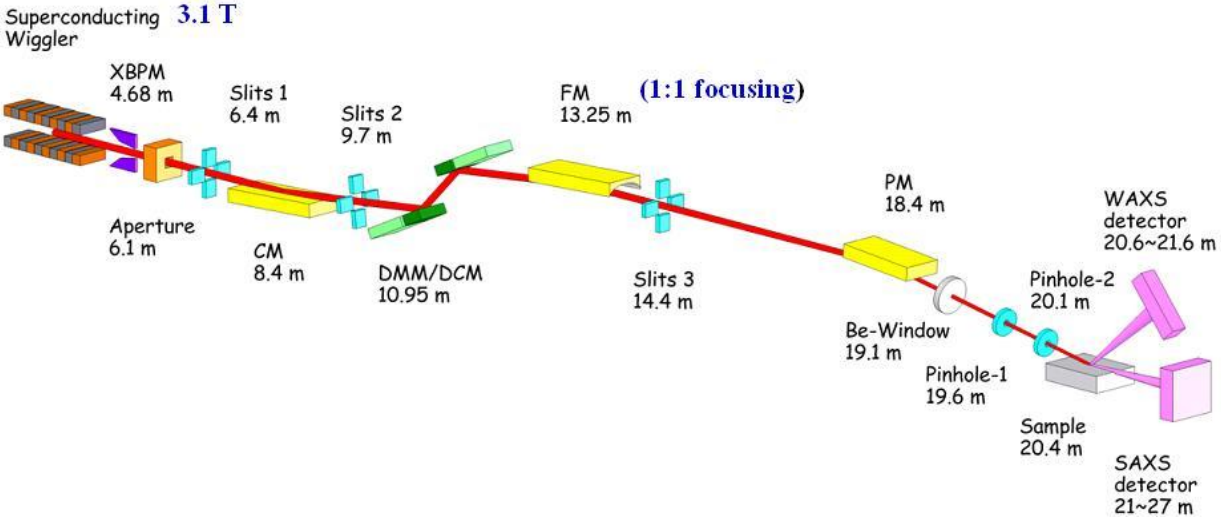

Figure 3-S1. The optical layout of the beamline BL23A for small/wide angle X-ray scattering (SWAXS) in National Synchrotron Radiation Center (NSRRC).

The technical data of BL23A beamline are listed in the following table.

Operational (general use)	Yes
%Time available (general use)	75 %
Experiments	SAXS/WAXS
Source	14 Poles, 6.1 cm Period Length, 3.1 Tesla Wiggler
Ring Current(mA)	300 mA
Average Beam Lifetime	Infinite Under NSRRC Top Up Conditions
Energy Range	5 ~ 23 keV (2.48 Å ~ 0.54 Å)
Energy Resolution	2.2 x 10E(-4) (DCM) or 1.2 x 10E(-2) (DMM)
Spot Size	FWHM: 0.8 mm (H) x 0.3 mm (V)
Optics	Vertically Collimating Mirror, Coupled Double Crystal Si(111)/Multilayer (Mo/B_4C) Monochromators, Toroidal Focusing Mirror
Flux	2 x 10E(10) (DCM) / 3 x 10E(11) (DMM)
Flux Detailed	Flux Measured Through a 0.5 mm Round Aperture @ 8 keV
Wavelength Min (Å)	0.54
Wavelength Max (Å)	2.48
Monochromator	Double Crystal/Multilayer Monochromators
Crystal Type	Si(111) or MoB_4C
Mirrors	Two strips: Rh/Pt double layers / bare Si surface
Mirror Cutoff	23 keV
Detectors	Linear Proportional Delayline Area Detector (180 mm by 180 mm); Linear detector: 180 mm; MARCCD165 (dia. 165 mm)
Lab Facilities	Heating Oven, Cooler, DSC, shear stage, stretching-heating device, stop-flow system
Software	Supersonic data collection acquisition system; MARCCD data acquisition system; NSRRC auto data collection kit; NSRRC SAXS Data Reduction Kit
Hardware	Linex & MS windows PC Control
Backup Devices	Windows PC; Data Analysis; Backup

3-6.2 A cell for measurement of small angle X-ray scattering

The drawing and the photo of the designed cell for measurement of small angle X-ray scattering are shown in Figure 3-S2 and Figure 3-S3, respectively.

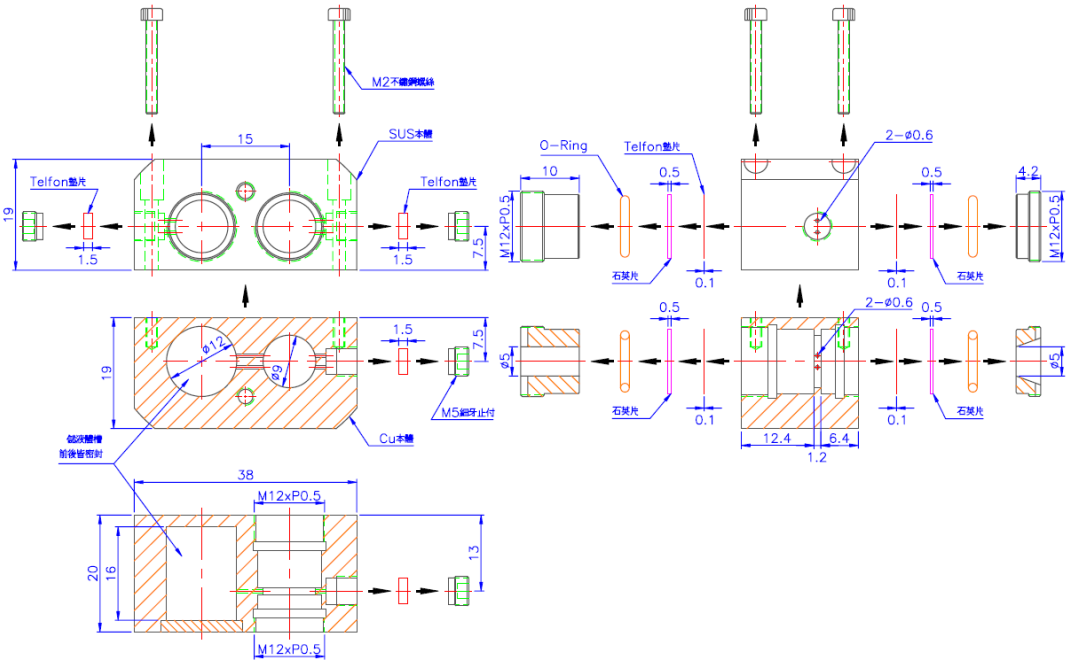

Figure 3-S2. The drawing of the liquid cell for measurement of small angle X-ray scattering at the beamline BL23A in National Synchrotron Radiation Center.

Figure 3-S3. The photo of the liquid cell for measurement of small angle X-ray scattering.

3-6.3 Temporal variation of visible absorption spectra of poly(3-octylpyrrole)squaraine in trichloromethane into which was inserted a Pb plate

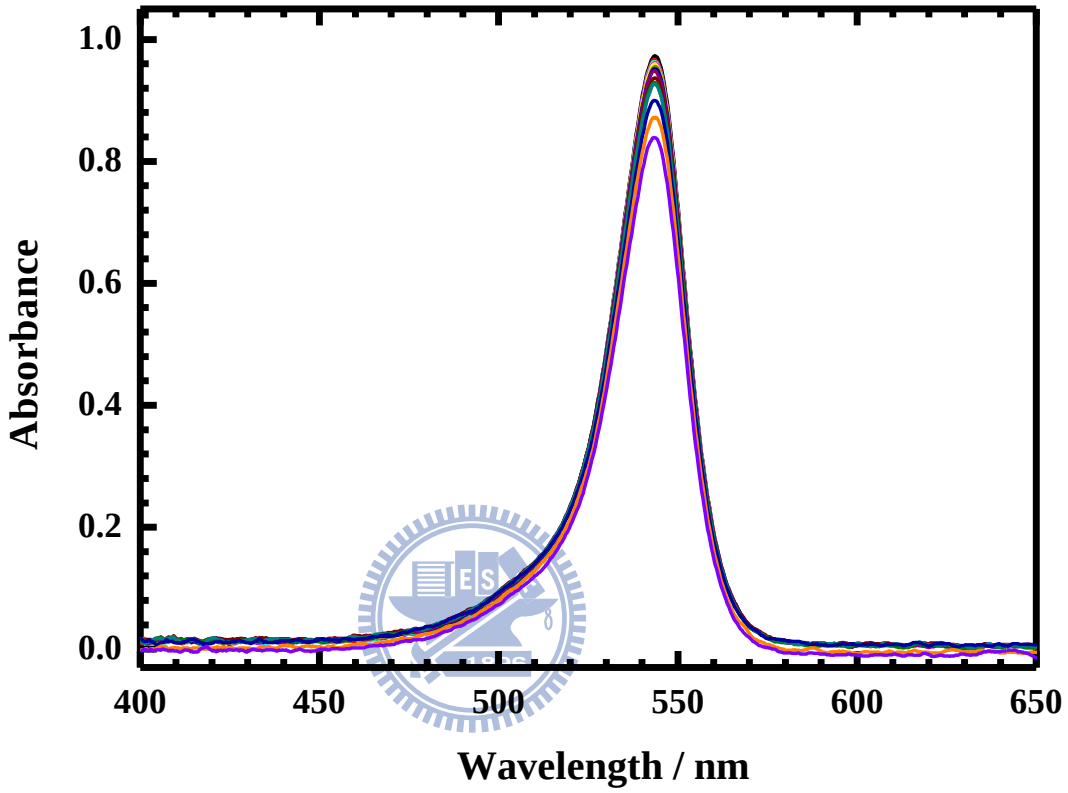

Figure 3-S4. Temporal variation over 384 h of visible absorption spectra of poly(3-octylpyrrole)squaraine (3.5 mg/L) in trichloromethane solution (3.0 mL) in a silica cell (optical path 1 cm) into which was inserted a Pb (surface area 381 mm^2) plate at 295 K.

3-6.4 Temporal variation of visible absorption spectra of poly(3-octylpyrrole)squaraine in trichloromethane into which was inserted a Zn plate

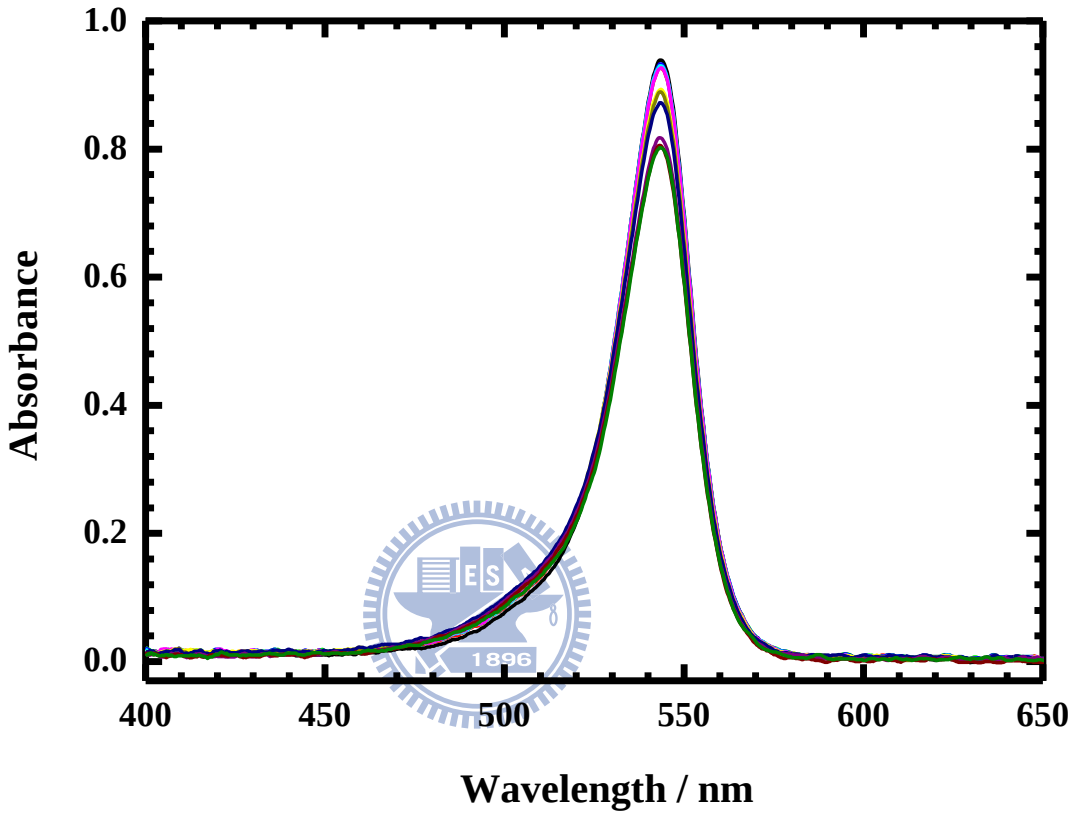

Figure 3-S5. Temporal variation over 280 h of visible absorption spectra of poly(3-octylpyrrole)squaraine (3.5 mg/L) in trichloromethane solution (3.0 mL) in a silica cell (optical path 1 cm) into which was inserted a Zn (surface area 431 mm^2) plate at 295 K.

3-6.5 Temporal variation of visible absorption spectra of poly(3-octylpyrrole)squaraine in trichloromethane into which was inserted a Pt plate

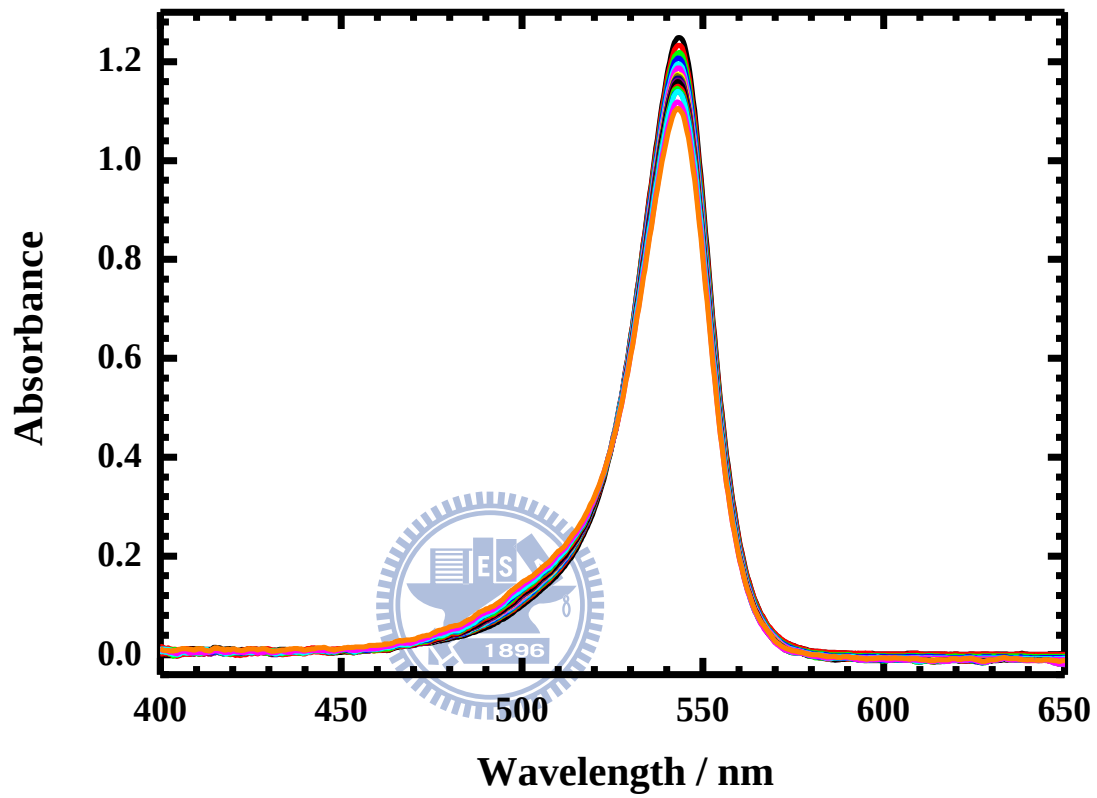

Figure 3-S6. Temporal variation over 58 h of visible absorption spectra of poly(3-octylpyrrole)squaraine (3.5 mg/L) in trichloromethane solution (3.0 mL) in a silica cell (optical path 1 cm) into which was inserted a Pt (surface area 363 mm^2) plate at 295 K.

Chapter 4 Conclusion

Polymers with extended π-electron conjugation have unique intrinsic conductivity and are classified as conjugated polymers or conducting polymers (CP). These materials attract increasing attention because of their novel electrical, optical and magnetic properties, which might be prospectively translated into diverse devices in optoelectronic, sensor, and biomedical applications.

Among these CP, polysquaraines are organic dyes containing squaraines and π-conjugated polymers; these compounds are suitable for the design of conducting polymers with small optical band gaps. This possession of unique optical, physical and chemical properties has made polysquaraines suitable materials for technical applications such as in solar cells, xerographic sensitizers, optical data storage, photodynamic therapeutics, and chemical sensors. In this thesis, we studied the synthesis and conformations of this new optoelectronic material of polysquaraine.

Considerable effort has been directed towards the synthesis of polysquaraines. As one polysquaraine, squaric acid reacts with pyrrole derivatives in condensation to form polymeric chains. In this condensation, the pyrrole derivative might react with the squaric acid with 1,2- or 1,3-addition and produce distinct backbone structures of poly(pyrrolyl)squaraines. In the first part of this work, we focused on investigation of influencing of the intrinsic nature of pyrrole derivatives in the condensation and impinging on the backbone structure of polysquaraine.

Condensation of squaric acid with pyrrole derivatives yields copolymers of the class of polysquaraines. In this condensation, the pyrrole derivative reacts with squaric acid

by 1,2- or 1,3-addition and generates covalent or zwitterionic backbones, respectively. The position of the alkyl group in the pyrrole derivative might affect this condensation and result in a distinctive backbone structure for the poly(pyrrolyl)squaraine.

We polymerized squaric acid with octyl linked to C- and N- positions in pyrrole derivatives, so effecting a synthesis of poly(1-octylpyrroyl)squaraine **P1** and poly(3-octylpyrroyl)squaraine **P3**, respectively. The backbone structures of the covalent and zwitterionic units in these polysquaraines are distinguished by their covalent and zwitterionic carbonyl functional groups having associated IR absorptions near 1750 cm^{-1} and 1600 cm^{-1}, respectively. By this means, we deduced that product **P3** from reagent 3-octylpyrrole possesses mostly zwitterionic repeating units (>97 %), whereas polymer **P1** from reagent 1-octylpyrrole was produced with backbone ratio 2:1 of zwitterionic repeating units to covalent ones. We hence conclude that the position of the alkyl group in the reagent of pyrrole derivative affects the construction in the condensation into poly(pyrrolyl)squaraine.

Also from the visible absorption, as shown in Figure 4-1, and photoluminescence spectra in varied solvents, TGA curves, and thermal IR measurements for these two polymers, the observations of these optical and thermal properties were reconciled to their structures.

The optical, physical and electronic properties of CP are affected strongly by a variation of the polymer conformation because of excitonic interaction among the constituent chromophores. To optimize the performance, controlling the conformation is a critical issue for applications based on these materials. Preceding workers have investigated the variation of the structural conformation for squaraine-based materials through solvent concentration, solvent polarity, temperature, metal ions and other

conditions. Besides induction by these external stimuli, we found that the conformation of polysquaraine can be controlled by active metals.

We synthesized the target CP poly(3-octylpyrrolyl)squaraine to possess mostly zwitterionic repeating units. Accompanied by color changes, the conformational structure of the carrier was altered on adding metal ions to solutions of the polymer and also induced by some active metals. Active metals induce a variation of the conformation of zwitterionic conducting polymer poly(3-octylpyrrole)squaraine in trichloromethane solution.

Evidence from infrared, visible and photoluminescent spectra and from small-angle X-ray scattering profiles unambiguously confirms the isomerization of this polysquaraine induced by the surfaces of active metals. Unlike the irreversible change induced by cations in solution, the folded conformation induced by active metals reverts to its original structure on eliminating contact between the metals and the solution.

Accompanied by altered optical properties, as displayed in Figure 4-2, this reversible structural modification of the zwitterionic polysquaraine induced by active metals represents a new chemical and physical process. The structure of the target polymer might switch from being linear to being folded. For a copper surface, the activation energy of isomerization between the two forms, whatever their nature, is 18.9±0.7 kJ mol-1, whereas for the reverse process the activation energy is 38±6 kJ mol-1. In a folding transformation, formation of intramolecular hydrogen bonds might play a key role.

This observation of a reversible structural modification, accompanying altered optical properties, for the zwitterionic polysquaraine induced by active metal plates is unprecedented; it represents a new chemical and physical process, and it has a potential to lead to the discovery of significant knowledge about the interactions of polymers with

metal surfaces, the dynamics and the energetics of polymer conformations. This observation of a reversible conformation for a zwitterionic polymer induced by a metallic surface provides an impetus to investigate both such a structural modification of other CP and applications of this phenomenon.

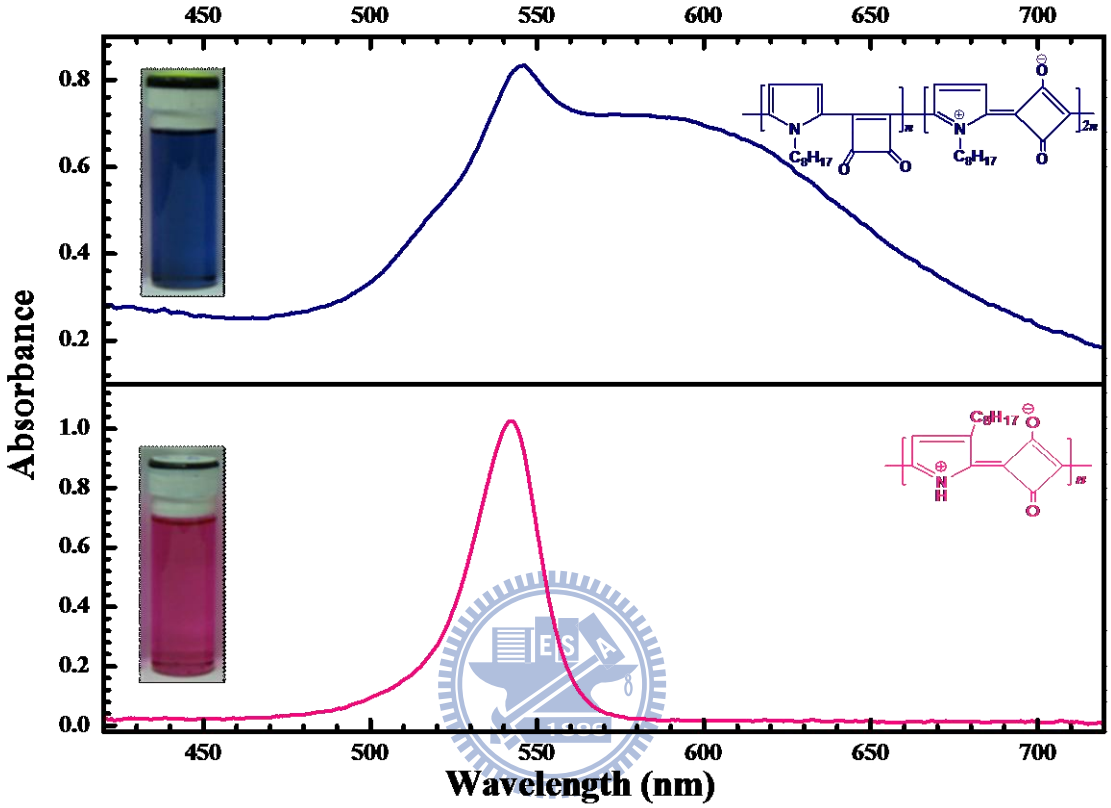

Figure 4-1. The position of the octyl group in the pyrrole derivative affects the construction of the polymer in poly(octylpyrrolyl)squaraine; as a result, visible absorption spectra are reconciled with the backbone structures of poly(octylpyrrolyl)squaraine as synthesized.

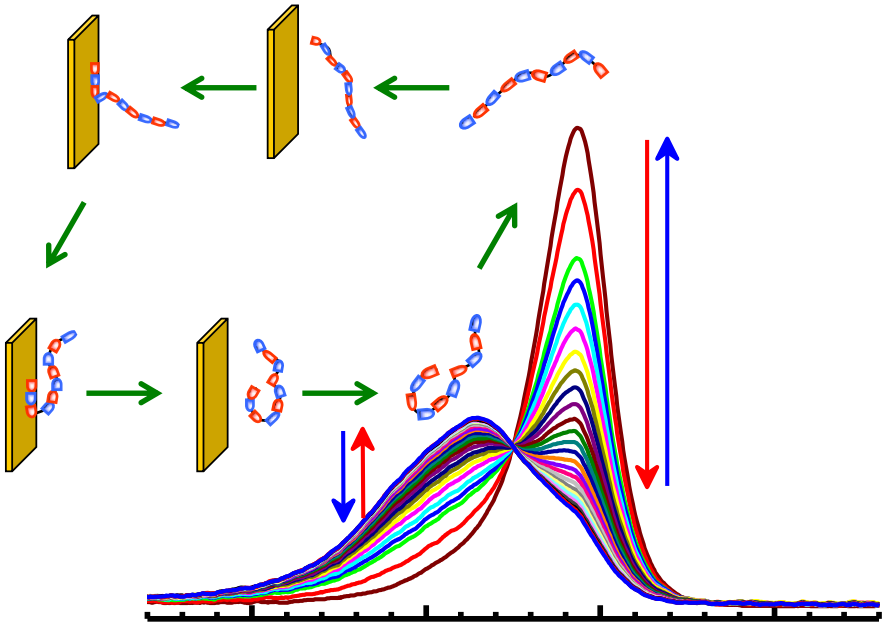

Figure 4-2. The visible absorption band of a zwitterionic conducting polymer poly(3-n-octylpyrrole)squaraine exhibits reversible color change on inserting and extracting active metal in trichloromethane solution. This color change implies a reversible variation of the conformation in solution; the folding conformer induced by active metal surface is re-converted to linear conformation on removing the metal plate.

References

[1] F. J. M. Hoeben, P. Jonkheijm, E. W. Meijer and A. P. H. J. Schenning, *Chem. Rev.* 2005, **105**, 1491.

[2] H. G. Kiess, (Ed.), "*Conjugated Conducting Polymers"* Springer, Berlin Germany, 1992.

[3] M. S. Freund and B. Deore, "*Self-Doped Conducting Polymers"* Wiley, New York USA, 2007.

[4] G. Zotti, B. Vercelli, A. Berlin, M. Pasini, T. L. Nelson, R. D. McCullough and T. Virgili, *Chem. Mater.* 2010, **22**, 1521.

[5] P. M. Beaujuge and J. R. Reynolds, *Chem. Rev.* 2010, **110**, 268.

[6] M. J. L. Santos, E. M. Girotto and A. G. Brolo, *Macromol. Rapid. Commun.* 2010, **31**, 289.

[7] N. B. Zhitenev, A. Sidorenko, D. M. Tennant and R. A. Cirelli, *Nature Nanotech.* 2007, **2**, 237.

[8] M. Helgesen, R. Søndergaard and F. C. Krebs, *J. Mater. Chem.* 2010, **20**, 36.

[9] P. Wagner, P. H. Aubert, L. Lutsen and D. Vanderzande, *Electrochem. Comm.* 2002, **4**, 912.

[10] A. Burke, L. Schmidt-Mende, S. Ito and M. Grätzel, *Chem. Commun.* 2007, 234.

[11] C. Mangeney, J. C. Lacroix, K. I. Chane-Ching, M. Jouini, F. Villain, S. Ammar, N. Jouini and P. C. Lacaze, *Chem. Eur. J.* 2001, **7**, 5029.

[12] Q. Wan, X. Wang, X. Wang and N. Yang, *Polymer* 2006, **47**, 7684.

[13] L. Beverina, M. Crippa, M. Landenna, R. Ruffo, P. Salice, F. Silvestri, S. Versari, A. Villa, L. Ciaffoni, E. Collini, C. Ferrante, S. Bradamante, C. M. Mari, R. Bozio and G. A. Pagani, *J. Am. Chem. Soc.* 2008, **130**, 1894.

[14] M. Gizdavic-Nikolaidis, J. Travas-Sejdic, G. A. Bowmaker, R. P. Cooney, C. Thompson and P. A. Kilmartin, *Cur. Appl. Phys.* 2004, **4**, 347.

[15] J. J. Gassensmith, E.Arunkumar, L. Barr, J. M. Baumes, K. M. DiVittorio, J. R. Johnson, B. C. Noll and B. D. Smith, *J. Am. Chem. Soc.* 2007, **129**, 15054.

[16] N. Gomez, J. Y. Lee, J. D. Nickels, C. E. Schmidt, *Adv. Funct. Mater.* 2007, **17**, 1645.

[17] V. V. J. Walatka, M. M. Labes and J. H. Perlstein, *Phys. Rev. Lett.* 1973, **31**, 1139.

[18] C. K. Chiang, C. R. J. Fincher, Jr., Y. W. Park, A. J. Heeger, H. Shirakawa, E. J. Louis, S. C. Gau and A. G. MacDiarmid, *Phys. Rev. Lett.* 1977, **39**, 1098.

[19] H. Shirakawa, E. J. Louis, A. G. MacDiarmid, C. K. Chiang and A. J. Heeger, *Chem. Commum.* 1977, 578.

[20] H. Shirakawa, *Angew. Chem. Int. Ed.* 2001, **40**, 2575.

[21] A. J. Heeger, *Angew. Chem. Int. Ed.* 2001, **40**, 2591.

[22] A. G. MacDiarmid, *Angew. Chem. Int. Ed.* 2001, **40**, 2581.

[23] K. Y. Law, F. C. Bailey and L. J. Bluett, *Can. J. Chem.* 1986, **64**, 1607.

[24] K. Y. Law and F. C. Bailey, *Can. J. Chem.* 1986, **64**, 2267.

[25] K. Y. Law, *J. Phys. Chem.* 1987, **91**, 5184.

[26] K. Y. Law, *J. Phys. Chem.* 1995, **99**, 9818.

[27] P. V. Kamat, S. Das, K. G. Thomas and M. V. George, *J. Phys. Chem.* 1992, **96**, 195.

[28] A. Treibs and K. Jacob, *Angew. Chem. Int. Ed.* 1965, **4**, 694.

[29] G. Maahs and P. Hegenberg, *Angew. Chem. Int. Ed.* 1966, **5**, 888.

[30] H.-E. Sprenger and W. Ziegenbein, *Angew. Chem. Int. Ed.* 1968, **7**, 530.

[31] W. Ziegenbein and H.-E. Sprenger, *Angew. Chem. Int. Ed.* 1966, **5**, 893.

[32] H.-E. Sprenger and W. Ziegenbein, *Angew. Chem. Int. Ed.* 1967, **6**, 553.

[33] H. A. Schmidt, *Synthesis* 1980, 961.

[34] E. E. Havinga, W. T. Hoeve and H. Wynberg, *Synth. Metals.* 1993, **55-57**, 299.

[35] E. E. Havinga, W. T. Hoeve and H. Wynberg, *Polymer Bull.* 1992, **29**, 119.

[36] H. A. M. V. Mullekom, J. A. J. M. Vekemams, E. E. Havinga and E. W. Meijer, M*ater. Sci. & Engi. R.* 2001, **32**, 1.

[37] G. Brocks and A. Tol, *J. Phys. Chem.* 1996, **100**, 1838.

[38] A. Ajayaghosh, Chem. Soc. Rev. 2003, 32, 181.

[39] A. Ajayaghosh and J. Eldo, Org. Lett. 2001, 3, 2595.

[40] J. Eldo and A. Ajayaghosh, Chem. Mater. 2002, 14, 410.

[41] F. Silvestri, M. D. Irwin, L. Beverina, A. Facchetti, G. A. Pagani and T. J. Marks, J. Am. *Chem. Soc.* 2008, **130**, 17640.

[42] W. Y. Wong, *Macromol. Chem. Phys.* 2008, **209**, 14.

[43] J. H. Yum, P. Walter, S. Huber, D. Rentsch, T. Geiger, F. Nüesch, F. D. Angelis, M. Grätzel and M. K. Nazeeruddin, *J. Am. Chem. Soc.* 2007, **129**, 10320.

[44] L. Beverina, R. Ruffo, C. M. Mari, G. A. Pagani, M. Sassi, F. D. Angelis, S. Fantacci, J. H. Yum, M. Grätzel and M. K. Nazeeruddin, *Chem. Sus. Chem.* 2009, **2**, 621.

[45] K. Y. Law, *Chem. Rev.* 1993, **93**, 449.

[46] S. Sreejith, P. Carol, P. Chithra and A. Ajayaghosh, *J. Mater. Chem.* 2008, **18**, 264.

[47] M. Emmelius, G. Pawlowski and H. W. Vollmann, *Angew. Chem. Int. Ed.* 1989, **28**, 1445.

[48] J. Fabian, H. Nakazumi and M. Matsuoka, *Chem. Rev.* 1992, **92**, 1197.

[49] M. A. B. Block and S. Hecht, *Macromolecules* 2004, **37**, 4761.

[50] J. J. Gassensmith, E. Arunkumar, L. Barr, J. M. Baumes, K. M. DiVittorio, J. R. Johnson, B. C. Noll and B. D. Smith, *J. Am. Chem. Soc.* 2007, **129**, 15054.

[51] A. Ajayaghosh, *Acc. Chem. Res.* 2005, **38**, 449.

[52] C. R. Chenthamarakshan and A. Ajayaghosh, *Tetrahed. Lett.* 1998, **39**, 1795.

[53] J. J. McEwen and K. J. Wallace, *Chem. Comm.* 2009, 6339.

[54] J. J. Gassensmith, J. M. Baumes and B. D. Smith, *Chem. Comm.* 2009, 6329.

[55] E. Arunkumar, A. Ajayaghosh and J. Daub, *J. Am. Chem. Soc.* 2005, **127**, 3156.

[56] C. R. Chenthamarakshan, J. Eldo and A. Ajayaghosh, *Macromolecules* 1999, **32**, 5846.

[57] Y. Chandrasekaran, G. K. Dutta, R. B. Kanth and S. Patil, *Dyes ans Pigments* 2009, **83**, 162

[58] K. Jyothish, M. Hariharan and D. Ramaiah, *Chem. Eur. J.* 2007, **13**, 5944.

[59] R. S.Grynyov, A. V. Sorokin, G. Y. Guralchuk, S. L. Yefimova, I. A. Borovoy and Y. V. Malyukin, *J. Phys. Chem. C* 2008, **112**, 20458.

[60] K. T. Arun, B. Epe and D. Ramaiah, *J. Phys. Chem. B* 2002, **106**, 11622.

[61] A. J. McKerrow, E. Buncel and P. M. Kazmaier, *Can. J. Chem.* 1995, **73**, 1605.

[62] K. Y. Law, *J. Phys. Chem.* 1989, **93**, 5925.

[63] R. S. Stoll, N. Severin, J. P. Rabe and S. Hecht, *Adv. Mater.* 2006, **18**, 1271.

[64] E. Arunkumar, P. Chuthra and A. Ajayaghosh, *J. Am. Chem. Soc.* 2004, **126**, 6590.

[65] E. Arunkumar, A. Ajayaghosh and J. Daub, *J. Am. Chem. Soc.* 2005, **127**, 3156.

[66] C. R. Chenthamarakshan, J. Eldo and A. Ajayaghosh, *Macromolecules* 1999, **32**, 251.

[67] L. P. Yu, M. Chen, L. R. Dalton, X. F. Cao, J. P. Jiang and R. W. Hellwarth, *Mat. Res. Soc. Symp. Proc.* 1990, **173**, 607.

[68] V. H.-E. Sprenger and W. Ziegenbein, *Angew. Chem.* 1968, **80**, 541.

[69] B. Stuart and D. Ando, "*Modern Infrared Spectroscopy*", 1st edition, John Wiley & Sons, Chichester 1996.

[70] B. C. Smith, "*Infrared Spectral Interpretation a Systematic Approach*", 1st edition, CRC Press LLC, 1998

[71] C. R. Chenthamarakshan and A. Ajayaghosh, *Chem. Mater.* 1998, **10**, 1657.

[72] A. C. Sant'Ana, L. J. A. D. Siqueira, P. S. Santos and M. L. A. Temperini, *J. Raman Spectroscopy*, 2006, **37**, 1346.

[73] G. J. Ashwell, A. N. Dyer and A. Green, *Langmuir* 1999, **15**, 3627.

[74] V. E. de Oliveira, G. S. de Carvalho, M. I. Yoshida, C. L. Donnici, N. L. Speziali, R. Diniz and L. F. C. de Oliveira, *J. Mol. Struct.* 2009, **936**, 239.

[75] G. J. Ashwell, G. Jefferies, A. Green, K. Skjonnemand, N. D. Rees, G. S. Bahra and C. R. Brown, *Thin Solid Films* 1998, **327-329**, 461.

[76] D. E. Lynch, U. Geissler and K. A. Byriel, *Synth. Metals.* 2001, **124**, 385.

[77] Y. Y. Chen and H. K. Hall, *Polymer Bull.* 1986, **16**, 419.

[78] D. E. Lynch, U. Geissler, J. Kwiatkowski and A. K. Whittaker, *Polymer Bull.* 1997, **38**, 493.

[79] D. E. Lynch, U. Geissler, I. R. Peterson, M. Floersheimer, R. Terbrack, L. F. Chi, H. Fuchs, N. J. Calos, B. Wood, C. H. L. Kennard and G. J. Langley, *J. Chem. Soc., Perkin Trans.* 1997, **2**, 827.

[80] D. E. Lynch, U. Geissler, N. J. Calos, B. Wood and N. N. Kinaev, *Polymer Bull.* 1998, **40**, 373.

[81] C. Reichardt, "*Solvent and Solvent Effects in Organic Chemistry*", 3rd edition, Wiley-VCH, Weinhein 2003.

[82] A. Masternak, G. Wenska, J. Milecki, B. Skalski and S. Franzen, *J. Phys. Chem. A.* 2005, **109**, 759.

[83] H. Meier, R. Petermann and J. Gerold, *Chem. Comm.* 1999, 977.

[84] G. Dufresne, J. Bouchard, M. Belletete, G. Durocher and Mario. Leclerc, *Macromolecules* 2000, **33**, 8252.

[85] J. Bouchard, M. Belletête, G. Durocher and Mario. Leclerc, *Macromolecules* 2003, **36**, 4624.

[86] S. Das, K. G. Thomas, R. Ramanathan and M. V. George, *J. Phys. Chem.* 1993, **97**, 13625.

[87] K. Umezawa, D. Citterio and K. Suzuki, *Chem. Lett.* 2007, **36**, 1424.

[88] C. Weder, *Chem. Comm.* 2005, 5378.

[89] M. J. Marsella, Z. Q. Wang and R. H. Mitchell, *Org. Lett.* 2000, **2**, 2979.

[90] M. Woodhouse, C. L. Perkins, M. T. Rawls, R. A. Cormier, Z. Liang, A. M. Nardes and B. A. Gregg, *J. Phys. Chem. C* 2010, **114**, 6784.

[91] M. R. Andersson, O. Thomas, W. Mammo, M. Svensson, M. Theander and O. Inganäs, *J. Mater. Chem.*1999, **9**, 1933.

[92] N. Rohde, M. Eh, U. Geiβler, M. L. Hallensleben, B. Voigt and M. Voigt, *Adv. Mater.* 1995, **7**, 401.

[93] F. Silvestri, I. López-Duarte, W. Seitz, L. Beverina, M. V. Martínez-Díaz, T. J. Marks, D. M. Guldi, G. A. Pagani and Tomás Torres, *Chem. Commum.* 2009, 4500.

[94] K. Lee, L. K. Povlich and Jinsang Kim, *Analyst* 2010, **135**, 2179.

[95] E. S. Forzani, H. Zhang, L. A. Nagahara, I. Amlani, R. Tsui and N. Tao, *Nano Lett.* 2004, **4**, 1785.

[96] W. Cheung, P. L. Chiu, R. R. Parajuli, Y. Ma, S. R. Ali and H. He, *J. Mater. Chem.*2009, **9**, 6465.

[97] R. Nagarajan, W. Liu, J. Kumar, S. K. Tripathy, F. F. Bruno and L. A. Samuelson, *Macromolecules* 2001, **34**, 3921.

[98] A. J. Moulé and K. Meerholz, *Adv. Funct. Mater.* 2009, **19**, 3028.

[99] M. Hallermann, I. Kriegel, E. D. Como, J. M. Berger, E. V. Hauff and J. Feldmann, *Adv. Funct. Mater.* 2009, **19**, 3662.

[100] S. De and S. Ramakrishnan, *Macromolecules* 2009, **42**, 8599.

[101] M. Binda, T. Agostinelli, M. Caironi, D. Natali, M. Sampietro, L. Beverina, R. Ruffo and F. Silvestri, *Org. Electron.* 2009, **10**, 1314.

[102] J. V. Ros-Lis, R. Martínez-Máñez, K. Rurack, F. Sancenón, J. Soto and M. Spieles, *Inorg. Chem.* 2004, **43**, 5183.

[103] A. Ajayaghosh, C. R. Chenthamarakshan, S. Das and M. V. George, *Chem. Mater.* 1997, **9**, 644.

[104] H.-C. Lu, W.-T. Whang and B.-M. Cheng, *Synth. Metals.* 2010, **160**, 1002.

[105] D. G. Liu, C. H. Chang, C. Y. Liu, S. H. Chang, J. M. Juang, Y. F. Song, K. L. Yu, K. F. Liao, C. S. Hwang, H. S. Fung, P. C. Tseng, C. Y. Huang, L. J. Huang, S. C. Chung, M. T. Tang, K. L. Tsang, Y. S. Huang,; C. K. Kuan, Y. C. Liu, K. S. Liang and U. S. Jeng, *J. Synchr. Rad.* 2009, **16**, 97.

[106] K. Liang, K. Y. Law and D. G. Whitten, *J. Phys. Chem.* 1994, **98**, 13379.

[107] H. Chen, K. Y. Law and D. G. Whitten, *J. Phys. Chem.* 1996, **100**, 5949.

[108] J. Wojtyk, A. McKerrow, P. Kazmaier and E. Buncel, *Can. J. Chem.* 1999, **77**, 903.

[109] F. J. Boerio and S. Wirasate, "Measurements of the Chemical Charateristics of Polymers and Rubbers by *Viberational Spectroscopy, in Vibrational Spectroscopy of Polymers: Principles and Practice*, N. J. Everall, J. M. Chalmers and P. R. Griffiths, (Eds), (Wiley, Chichester England, 2007, p.113-141.)

[110] K. R. Reddy, K.Tashiro, T. Sakurai, N. Yamaguchi, S. Sasaki, H. Masunaga, M. Takata, Macromolecules 2009, 42, 4191.

[111] K. Ishizu, N. Okamoto, T. Murakami, S. Uchida and S. Nojima, *Macromol. Chem. Phys.* 2009, **210**, 1717.

[112] R. L. Baldwin, *J. Biol. Chem.* 2003, **278**, 17581.

[113] N. Arora and B. Jayaram, *J. Computational Chem.* 1996, **18**, 1245.

[114] J. Emsley, *Chem. Soc. Rev.* 1980, **9**, 91.

[115] G. A. Jeffrey *An Introduction to Hydrogen Bonding* (Oxford, New York, USA, 1997).

[116] A. Lendlein and S. Kelch, *Angew. Chem. Int. Ed.* 2002, **41**, 2034.

[117] C. Liu, H. Qin and P. T. Mather, *J. Mater. Chem.* 2007, **17**, 1543.

[118] A. Lendlein, H. Jiang, O. Jünger and R. Langer, Nature 2005, **434**, 879.